Development of Lateralised Circuitry in the Zebrafish Brain

Isaac Henry Bianco

Department of Cell & Developmental Biology

University College London

2008

Thesis presented in partial fulfillment of the degree of

Doctor of Philosophy at the University of London

ProQuest LLC
789 East Eisenhower Parkway
P.O. Box 1346
Ann Arbor, MI 48106-1346

Declaration

I, Isaac Henry Bianco, confirm that the work presented in this thesis is my own. Where information has been derived from other sources, I confirm that this has been indicated in the thesis.

For my parents.

Acknowledgments

I am very fortunate to have had Steve Wilson as my PhD supervisor. Throughout my time in the lab, Steve has always been encouraging and enthusiastic about my work, suggested interesting and challenging experiments whilst giving me freedom to explore my own ideas. He has also given me several opportunities to teach and travel, and he's great fun.

I have also benefited from having Jon Clarke as my second supervisor. I have a learnt a great deal from him and thanks to his generosity have enjoyed several summers teaching (and learning) at Woods Hole.

I am extremely grateful to Claire Russell, who has been a friend and mentor throughout my time in the lab. Not only is Claire a brilliant teacher but she is also endowed with almost limitless patience, always prepared to answer my repetitive questions, lend a hand, or suggest a games evening or pub quiz.

I have made many friends in the lab and won't try to name them all. Hopefully it will suffice to say "thank you", especially for tolerating my musical taste and sharing more that a few pints in the JB. Our adventures to sunny beaches and up intrepid mountains have been a welcome relief from the hours on the confocal.

I am very grateful to David Attwell and the Wellcome 4 year PhD programme in Neuroscience for giving me this opportunity and it has been a pleasure getting through a PhD with the UCL8, all of whom have been great friends. In particular, living in London has been enhanced by sharing flats with Seb and Tiago. Seb has kindly hammered into me just how much fun a good knees-up at the Ceilidh can be on a friday night as well as the importance of correctly loading a washing machine and boiling pasta in sufficient hot water. Tiago and I have had many late-night chats about neuroscience in our inadequately-sized kitchen and enjoyed dozens of mini-beers in sunny Lisbon.

My parents have shown me love and support not only throughout my PhD, but my whole life. They are always there through thick and thin. I can't imagine how I could have better parents or how I can thank them enough. Mum and dad, I love you very much.

Abstract

Left–right asymmetry is a highly conserved feature of the nervous system. However, it is not known how functional lateralisation is represented at the level of lateral differences in circuit microarchitecture. In this study, I identify asymmetric neuronal connectivity in the larval zebrafish brain, resolve L–R differences in the morphology and connectivity of individual projection neurons and investigate the molecular and cellular mechanisms by which lateralisation develops.

The habenular nuclei form part of the highly conserved dorsal diencephalic conduction system. I find that the habenulae display *laterotopic* efferent connectivity, wherein left and right-sided axons are segregated along the dorso-ventral axis of their target, the interpeduncular nucleus (IPN). Habenular neurons elaborate remarkable "spiralling" terminal arbors within the IPN. I have identified two sub-types of habenular neuron, defined by axonal arbors with distinct morphology and targeting. Both sub-types are found in both the left and right habenula, but in substantially different ratios. Thus, the vast majority of left habenular neurons elaborate tall, crown-shaped arbors localised to the dorsal IPN, whereas almost all right-sided cells form flattened arbors restricted to the ventral IPN. This left–right asymmetry in cell-type composition, combined with the differential targeting of neuronal sub-types, underlies the *laterotopic* connectivity of the habenulae. This reveals a fundamental strategy that serves to differentiate functional circuitry on the two sides of the CNS: equivalent components are specified on both sides and lateralisation results from differences in the ratios of neuronal sub-types on the left and right.

Left-sided Nodal signalling is essential for controlling the orientation, or laterality, of *laterotopic* connectivity, but is not required for asymmetry *per se*. The left-sided parapineal nucleus is required for the development of normal asymmetric phenotypes, including the development of both left and right-sided axon arbors with appropriate morphology and targeting. However, following laser-ablation of the parapineal, left and right-sided neurons continue to elaborate arbors with distinct lateralised morphologies, indicating that additional developmental mechanisms act to convey left–right identity information to this highly conserved circuit.

Contents

List of Figures

Chapter 1

Introduction

1.1 Overview of brain lateralisation

Throughout the animal kingdom, the left and right sides of the brain display differences in neuroanatomy and physiology which are manifest in the form of lateralised cognitive functions and behavioural asymmetries. I will present a brief overview of CNS lateralisation, discuss the evidence supporting a link between structural and functional asymmetries, summarise our current understanding as to how asymmetries develop and the factors that modulate them and discuss theories as to why the left and right sides of the brain are different.

1.1.1 Functional lateralisation — cognitive and behavioural asymmetries

The most long recognised and extensively studied example of human cognitive lateralisation is the specialisation of the left cerebral hemisphere for language processing. This phenomenon was first proposed in the 19^{th} century by Broca and Wernicke, based on language deficits in patients with left hemisphere strokes or tumours and has subsequently been studied using a variety of techniques including Wada testing[1] and fMRI (reviewed in Toga & Thompson, 2003). A distributed network of left hemisphere cortical

[1]Wada Test: A surgical test used to assess hemispheric language dominance. Sodium amytal is injected into the carotid artery, causing a temporary anaesthesia of the ipsilateral hemisphere. If this hemisphere is dominant for language, the patient loses the ability to speak.

regions is implicated in various aspects of language processing; two key associative areas include the inferior frontal lobe (including Broca's area) which is involved in semantic processing and speech generation and the posterior superior temporal gyrus (including Wernicke's area and the planum temporale), involved in auditory and visual language perception. Most studies report a left hemisphere language dominance in approximately 93% of the population (*eg* Pujol et al., 1999). However, even in strongly lateralised individuals, the right hemisphere also performs specific language-associated functions, including aspects of semantic processing and word learning and retrieval (Jung-Beeman, 2005). The right hemisphere is thought to be particularly important for processing the contextual and non-literal meaning of language, allowing individuals to apply appropriate intonation and stress to spoken words, so as to convey emotions, as well as understanding high-level concepts such as metaphor and irony.

Lateralisation of the neural processors underlying the perception and production of communicative signals is also evident in other species. Japanese macaques show a right-ear advantage in the discrimination of species-specific vocalisations (Petersen et al., 1978) and zebra finches produce birdsong predominantly under right hemisphere control (Williams et al., 1992).

Functional studies in which humans perform the Shepard–Metzler 'mental rotation' task have indicated a rightwards lateralisation in visuospatial processing capacity. Subjects are shown pairs of 3D objects in different orientations and asked to decide if they are identical shapes or mirror images. Ditunno & Mann (1990) observed significantly better accuracy and faster response times when images were presented in the left visual field, indicating a right hemisphere processing advantage, possibly mediated by the parietal lobe.

In addition, several other cognitive functions have been suggested to show differences in lateral dominance in humans including emotional and attentional mechanisms and face perception (see Toga & Thompson, 2003).

Whilst the lateralisation of cognitive functions such as language and visuospatial reasoning does not translate into any overtly asymmetric behavioural outputs, many species do display lateralisation at the behavioural level. Approximately 90% of humans are more skilled with their right hand

than the left, implying a superior ability of the left hemisphere to orchestrate fine-scaled motor programmes. "Handedness" has also been recognised in other mammalian species; for example, non-human primates display hand preferences during gestural communication, tool-use and co-ordinated bi-manual tasks and paw-preference has been observed in rodents (Halpern et al., 2005).

Asymmetric use of the left and right eyes for particular viewing tasks has been described in several species (Vallortigara & Rogers, 2005) and the same basic pattern of lateralised eye use has been suggested to be conserved from fish to tetrapods (Miklosi et al., 1997). In both teleosts and chicks, the right eye system is used for assessing novel objects or environments and is thought to suppress behavioural responses until sufficient examination and cognitive analysis has been performed. By contrast, the left eye is used for monitoring familiar objects or empty scenes and may perform a "surveillance" role, where behavioural responses (*eg* escape) can be rapidly initiated by salient stimuli (*eg* appearance of a predator). Hence, zebrafish preferentially use their right eye for a controlled approach to targets to bite (Miklosi & Andrew, 1999) and chicks use their right eye to discriminate grain from a background of pebbles (Mench & Andrew, 1986; Rogers, 1990). By contrast, chicks use their left eye to watch out for predators and several teleosts preferentially use the left eye for sustained viewing of (familiar) conspecifics (Sorvano et al., 1999).

Functional lateralisation is not restricted to vertebrates. For example, Byrne et al. (2002) have reported lateralised eye use in *Octopus vulgaris*. Some species of spider show a left-leg preference for touching an opponent spider (in order to inspect it) and ants preferentially present their left side to nest-mates when resting (see commentary by Heuts & Brunt in Vallortigara & Rogers, 2005). In *C. elegans*, the left and right AWC olfactory neurons are molecularly and functionally asymmetric: only one neuron expresses the STR-2 G-protein coupled receptor, resulting in distinct odorant sensitivity profiles (Wes & Bargmann, 2001).

1.1.2 Neuroanatomical & neurophysiological asymmetries

What underlies functional lateralisation? Asymmetries in brain organisation have been identified from the level of the shape and size of large cortical

regions to the molecular composition of neurotransmitter receptors within discrete functional circuits.

Gross tissue morphology

Although the left and right hemispheres are similar in overall weight and volume, the human brain shows two stereotypical asymmetries at the level of its overall shape. The right frontal lobe is usually wider and protrudes anteriorly beyond the left frontal lobe whilst the left occipital lobe is wider and protrudes posteriorly. These asymmetric protrusions leave imprints upon the inner surface of the skull called *petalia*. Additionally, the brain hemispheres shows a counter-clockwise twisted appearance: The right sylvian fissure areas are "torqued" forward relative to their counterparts on the left side, whilst the left occipital lobe extends rightwards across the midline distorting the interhemispheric fissure towards the right. This phenomenon is known as Yakovlevian torque.

Asymmetries in the patterns of sulci and gyri have also been recognised; most prominent among these concerns the Sylvian fissure which, towards its posterior end, curves upwards more anteriorly and more steeply on the right side (Geschwind & Levitsky, 1968; Hochberg & Le May, 1975).

Whilst in humans, and other mammals, structural asymmetries comprise differences between homologous structures specified on both sides of the brain, in some species asymmetry is manifest in the form of nuclei that develop on only one side. For example, Pascual et al. (2004) identified such an "asymmetrical body", which is present on only the right side, in the brain of *Drosophila*. Moreover, in rare instances where flies show a symmetrical brain, with two such bodies, the flies are completely defective in long-term memory. Unilateral structural features have also been identified in lower vertebrates; in §1.2.5 I shall discuss examples in the dorsal diencephalon.

Tissue volume

The identification of differences in the quantity of neural tissue between equivalent regions on the left and right sides of the brain suggests that functional lateralisation might, at least in part, result from an asymmetrical distribution of neural substrate subserving a particular processing function.

Complementing the functional lateralisation described above, the most pronounced and consistent asymmetries in the human brain are to be found in cortical regions implicated in language processing. The planum temporale is a region of the posterior superior temporal gyrus which comprises the epicentre for left hemisphere language processing and contains Wernicke's posterior language comprehension area. In 65% of adults the left planum temporale has a larger volume than its right-hemisphere counterpart and in some cases may be up to ten times larger (Geschwind & Levitsky, 1968; Steinmetz, 1996). In anterior language regions, the pars triangularis and pars opercularis — located in the inferior frontal gyrus and which comprise Broca's speech area — display leftward asymmetries at the level of cortical surface area (Foundas et al., 1998).

By performing a voxel-based statistical analysis of grey matter volumes in a large sample of MRI scans, Watkins et al. (2001) reconfirmed previously reported rightward asymmetries in the cingulate sulcus and caudate nucleus as well as identifying a previously unreported rightward asymmetry in the anterior insular cortex.

Fibre tracts & neural connectivity

Recent studies employing diffusion tensor MRI (DT-MRI) tractography have added to the identification of asymmetries in fibre tracts and white matter, suggesting that differences in cortical and subcortical connectivity contribute to functional lateralisation.

Two recent studies using DT-MRI tractography identified pronounced leftward asymmetries in the relative fibre density of the arcuate fasciculus, a component of the perisylvian language network that directly interconnects Broca's territory in the left frontal lobe with Wernicke's territory in the left temporal lobe. Although there was variation in the extent of asymmetry, in many subjects this tract could only be detected in the left hemisphere (Catani et al., 2007; Nucifora et al., 2005).

Asymmetry has also been reported in the connectivity of the anterior temporal and inferior frontal lobes. The uncuate fasciculus interconnects these regions and is 27% larger and contains 33% more fibres in the right hemisphere (Highley et al., 2002).

As discussed in §1.1.5, the chick visual system becomes functionally lat-

eralised in response to light. This functional asymmetry is associated with a left–right difference in the size of the thalamofugal tract; in normally lateralised chicks there are more fibres from the left thalamus, which is fed by the light-stimulated right eye (Rogers & Deng, 1999).

Cytoarchitecture

In addition to the macrostructural asymmetries described above, left–right differences in neuroanatomy have also been identified at the microscopic level of the sizes and organisation of cellular fields. For instance, Galaburda et al. (1978) found a strong positive correlation between the gross asymmetry of the planum temporale and the cytoarchitectonic asymmetry of the area of cellular field Tpt, a region of auditory association cortex located on and around the planum temporale.

Are asymmetries in the overall sizes of equivalent regions on the left and right sides of the brain due to differences in the total number of neurons or do they result from differences in cell packing density (or a combination of both)? In support of the second possibility, Amunts et al. (1999) described a higher neuronal density in Brodman area 44 (the posterior part of Broca's area in the inferior frontal lobe) on the left. However, studies in the rat cortex have found that asymmetries in the primary visual cortex are due to left–right differences in the total number of neurons, rather than in cell packing density (Rosen, 1996). Moreover, in both the primary visual cortex and somatosensory/somatomotor area (SM-I) of the rat, as well as in the planum temporale of humans, the degree of asymmetry shows a negative correlation with total (left+right) size. Furthermore, for the planum temporale it is the size of the smaller (but not larger) side that predicts the magnitude of asymmetry. These results are interesting because they show that rather than asymmetry arising as a result of enlargement of one side of the brain, instead it results from the production of a "small" side and consequently, more asymmetric brains contain a lower total number of neurons as compared to symmetric brains (Rosen, 1996).

Examination of microscopic anatomy has also uncovered asymmetries that suggest differences in the organisation of functional circuits. In posterior language-associated cortical regions there are differences in micro- and macro-columnar architecture that have led to the suggestion that the left

hemisphere has the capacity to perform more refined computational analyses. At the microcolumnar level, the widths of cell columns and spacing between them is greater on the left with the consequence that left-sided pyramidal neurons contact fewer adjacent cells (despite them having broader basilar dendritic trees, see below). This might result in a less redundant and more specialised circuit architecture, with improved separation of processing streams capable of analysing auditory inputs in greater detail. Additionally, the left hemisphere contains a greater number of selectively interconnected functional macrocolumns. It has been speculated that this too could enable the analysis and evaluation of more discrete aspects of the incoming auditory information, resulting in a more detailed and comprehensive analysis on the left (see Hutsler & Galuske, 2003, and references therein).

Single-cell morphology

Although there are very few reports of neuroanatomical asymmetries at the level of individual neurons, left–right differences in dendritic morphology and cell size have been described. In regions of the frontal cortex involved in speech production (including Broca's area and precentral motor cortex) left-sided neurons show a greater extent of high-order dendritic branching than right-sided cells. However, the length of lower-order branches is greater on the right (Scheibel et al., 1985). In the posterior superior temporal lobe, small pyramidal cells on the left side have longer dendritic processes with a greater degree of branching and more dendritic spines than cells in the right hemisphere (Anderson et al., 1999).

In several cortical regions, asymmetries in the size of pyramidal neurons have been described. For example, a subpopulation of layer III magnopyramidal neurons have been identified in Broca's area, which are significantly larger on the left side than on the right (Hayes & Lewis, 1995).

A microstructural study of the posterior superior temporal lobe found that white matter volume was greater on the left and this was associated with left-sided axons having significantly thicker myelin sheaths, as determined by electron microscopy (Anderson et al., 1999). These thicker sheaths are likely to result in faster conduction velocities in left-sided axons, which might account for the left dominance in certain aspects of language processing.

Synaptic properties

CNS asymmetry extends to the molecular organisation of neural circuits. In the mouse hippocampus, GluRϵ2 subunits are asymmetrically allocated between NMDA receptors on the left *versus* right sides and between the apical *versus* basal dendrites of individual pyramidal neurons (Kawakami et al., 2003).

1.1.3 Association between structural and functional asymmetries

The various anatomical and neurophysiological asymmetries described above are expected to result in different processing architectures and computational properties on the left and right sides of the brain, which would be expected to underlie functional lateralisation. However, establishing clear relationships between structural and functional asymmetries as well as between different lateralised functions has not been straightforward, especially in humans.

Whilst some studies have described reversals of cerebral language dominance accompanied by structural reversals, for example in the planum temporale (Foundas et al., 1994) and pars triangularis (Foundas et al., 1996), other researchers have reported right-hemisphere language dominance in the absence of clear structural asymmetries in the planum temporale (Moffat et al., 1998), questioning the dependence of functional lateralisation upon structural asymmetries in language-associated cortical regions. Because recently reported asymmetries in language-associated fibre tracts (see above) show a frequency of left lateralisation (~83%, Catani et al., 2007) that is similar to the usual values reported for left-sided language dominance (>90%) (whereas the planum temporale shows leftward asymmetry in only 65% of individuals), it has been suggested that it may be these asymmetries in language *pathways* that represent the substrate for functional lateralisation. However, a recent study using fMRI and DT-tractography found leftward asymmetry in the arcuate fasciculus irrespective of whether the left or right hemisphere displayed functional language dominance (Figure 1.1 and Vernooij et al., 2007).

Similarly, in a study of epilepsy patients with either right or left-sided

Figure 1.1: **Structural and functional language-associated asymmetries in right and left-handers.**
Language-related fMRI activation in the superior and middle temporal gyrus (orange-yellow) and DT-tractography revealing the arcuate fasciculus on the left (green) and right (red) sides. (A) A right-handed subject showing left hemisphere dominance for both language processing and connectivity. (B) A left-handed subject showing an "atypical" rightwards asymmetry for language processing, but a leftwards asymmetry in the size of the arcuate fasciculus. Thus, structural and functional asymmetries are not tightly coupled in the language pathway. Note also that the magnitude of both the functional and structural asymmetry is greater in the right-hander. Adapted from Vernooij et al. (2007).

language function, Dorsaint-Pierre et al. (2006) found that leftward asymmetry of the planum was retained regardless of the directionality of the functional asymmetry. Notably, however, a grey-matter concentration asymmetry of the pars opercularis *did* reverse in patients with right-hemisphere language localisation. Furthermore, a study by Tzourio-Mazoyer et al. (2004) identified an atypical individual where language comprehension and language production were represented in opposite hemispheres. These observations indicate that different anatomical and functional asymmetries can show discordant laterality, suggesting they might arise via distinct developmental mechanisms.

This idea is supported by a study of three people with *situs inversus totalis*, a condition in which the left–right situs of the heart and visceral organs are reversed. Kennedy et al. (1999) found that whilst the frontal and occipital petalia were reversed in these patients, concordant with the reversals in visceral anatomy, two patients retained a leftward dominance in the volume of the planum temporale and all three showed classical leftward asymmetry in fMRI signals during a language processing task. Thus, there

may be at least two independent pathways specifying the orientation of CNS asymmetries, only one of which is concordant with the pathway determining heart/visceral laterality.

Although handedness represents the most conspicuous behavioural asymmetry in humans, very few studies have described corresponding anatomical asymmetries which might be expected to lie in the hand representation area of the motor cortex. One exception is a report by Amunts et al. (1996), which showed that the depth of the central sulcus is greater in the left hemisphere in right-handers and *vice versa* in left-handers. Furthermore, this macroanatomical asymmetry was associated with a left–right difference in neuropil volume in Brodmann's area 4 (the primary motor cortex), suggesting greater neural connectivity on the side controlling the preferred hand.

With respect to language-associated asymmetries, left-handers do not necessarily show a mirror-reversal in structure or function but rather they display a modest increase in the frequency of rightwards asymmetry and a general reduction in the magnitude of both structural and functional asymmetries. Whilst 96% of right-handers show left-hemisphere language dominance, this falls to 76% for left-handers, with the remaining 24% showing rightwards or bilateral language representation (Pujol et al., 1999). Moreover, the strength of functional lateralisation (Tzourio et al., 1998) and the magnitude of structural asymmetries, such as the volume of the planum temporale (Steinmetz, 1996) and relative fibre density in the arcuate fasciculus (Hagmann et al., 2006; Vernooij et al., 2007), are reduced in left-handers, indicating a more symmetrical — although still on average leftwards — representation between the two sides of the brain (Figure 1.1).

In contrast to studies of human brain asymmetry, clear links between anatomical and behavioural lateralisation have been established in some other species, notably chickens. As mentioned above, asymmetric light stimulation in the egg lateralises the chick visual system, resulting in asymmetric visual object discrimination behaviour after hatching. Removing the head of the developing chick from the egg, occluding the normally light-stimulated right eye with a patch and exposing the normally concealed left eye to light, results in concordant reversal of both anatomical and behavioural asymmetry (Rogers & Sink, 1988; Rogers, 1990). This demonstrates a clear structure–function relationship within the context of CNS lateralisation.

1.1.4 Advantages of CNS lateralisation

The widespread occurrence of CNS asymmetries in many diverse animal species is strongly indicative that this feature of nervous system organisation confers a survival advantage. Certainly, there are several theoretical reasons that cerebral lateralisation might be beneficial (for review see Vallortigara & Rogers, 2005). Lateralisation has been suggested to increase *neural capacity* by specialising neural substrate on the left and right sides for distinct computational roles, thereby avoiding wasteful duplication of the same circuits in the two hemispheres. By separating specialised circuits, lateralisation is also thought to *reduce interference* and incompatibility of function between different cognitive processors, thereby allowing efficient, simultaneous *parallel processing* on the two sides. An additional advantage is that the localisation of a specific cognitive function to one or other hemisphere confers the same advantages as other forms of *compartmentalisation*: it allows for more rapid and efficient processing.

This latter factor has been suggested to be particularly relevant to language cognition and may have been the evolutionary driving force behind its lateralisation (Toga & Thompson, 2003). It is believed that language processing requires detailed temporal analyses of streams of auditory inputs (Hutsler & Galuske, 2003). Models of interhemispheric *versus* intrahemispheric processing suggest that the time delay associated with the transcallosal transfer of information between the left and right hemispheres would be incompatible with high resolution, time-critical computations. Rather than transferring information back and forth via the corpus callosum between circuits in the the left and right hemispheres, it may be more efficient to utilise specialised unilateral networks where information is sent short distances between focal areas (Ringo et al., 1994). This requirement for finely detailed temporal analysis may have resulted in hemispheric specialisation for language and other cognitive processing functions. Notably, the midsagittal area of the corpus callosum is smaller in right-handers than in non-right-handed individuals (Witelson, 1985) and the latter group display reduced cerebral lateralisation (see §1.1.3).

In support of an association between neural lateralisation and auditory processing ability, the asymmetry coefficient of the planum temporale is

almost twice as great in musicians with perfect pitch as compared to non-musicians (Steinmetz, 1996). Furthermore, dyslexic individuals with deficits in phonological processing show greatly reduced asymmetry of the planum temporale. However, the association between human brain lateralisation and cognitive ability is not as straightforward as these examples suggest. Firstly, individuals with "atypical" reversed or bilateral functional language representation show intellectual and language skills similar those with normal leftwards lateralisation (Knecht et al., 2001). Furthermore, in a recent study examining asymmetry of the arcuate fasciculus by DT-MRI, Catani et al. (2007) observed better performances at remembering words by semantic association in individuals with more bilaterally *symmetric* fibre tracts[2].

There are, however, numerous examples in different species that support the postulate that CNS lateralisation increases neural performance. For instance, cats displaying strongly lateralised paw use show shorter reaction times in visuomotor tasks than non-lateralised cats (Fabre-Thorpe et al., 1993), compatible with the idea that unilateral networks can process information faster. McGrew et al. (1999) observed wild chimpanzees in Gombe National Park, Tanzania and reported that lateralised animals that consistently use the same hand for probing for termites were more successful in catching them than ambidextrous individuals and Sovrano et al. (2005) found that fish from lines selected for a high degree of behavioural lateralisation were better at spatial reorientation than non-lateralised fish.

CNS asymmetries are also associated with enhanced neural capacity in invertebrates. As discussed in §1.1.2, a structural asymmetry has been identified in *Drosophila* which is essential for flies to form long-term memory (Pascual et al., 2004). In *C. elegans*, molecular asymmetry of the AWC olfactory neurons mediates a left–right segregation of odorant sensitivity, which is necessary for accurate odor discrimination (Wes & Bargmann, 2001).

Behavioural studies of chicks support the hypothesis that brain asymmetry facilitates parallel processing, which results in superior behavioural performance under conditions of high cognitive load. Rogers et al. (2004) tested chicks on the dual task of discriminating grain from a distracting background

[2]Note that the California Verbal Learning Test used in this study is a complex cognitive task thought to involve interaction between verbal memory and conceptual ability and is known to engage the right hemisphere.

of small pebbles whilst simultaneously being vigilant for a model predator. Lateralised chicks (hatched from eggs exposed to light) were able to engage their left hemisphere (right eye) for grain discrimination whilst using their right hemisphere (left eye) to monitor overhead for the predator and showed better performance on both tasks than non-lateralised chicks (hatched from dark-incubated eggs). The non-lateralised chicks were so disturbed by the dual task that their performance actually deteriorated as they continued to search for food. However, when the model predator was removed, both lateralised and non-lateralised chicks did equally well and showed improvement during the task of pecking at grain alone. These results suggest that when the brain needs to perform qualitatively different tasks simultaneously, lateralisation improves behavioural performance by enabling the left and right hemispheres to be separately engaged on different processing functions with reduced interference between those functions.

Population laterality

A feature of CNS asymmetries in several species is that they show a consistent directional bias within the population, known as "population laterality" or "directional asymmetry". For instance, in species showing asymmetric eye useage, rather than half of the population preferentially using their left eye for a particular viewing task and the other half using their right eye, there is typically a majority of 65–90% of individuals lateralised in the same direction. But is there a selective advantage to such directional asymmetry? The proposed advantages of CNS lateralisation, outlined above, only require asymmetry at the level of the individual (a condition also known as "anti-symmetry") with no requirement for a particular direction, or *laterality*, of that asymmetry. This question is all the more relevant because some clear disadvantages seem inevitable: When perceptional or behavioural asymmetries show a population bias, the resultant *predictability of behaviour* could be learnt and exploited by predators and by prey. For example, toads, which show a left-eye dominance in predator vigilance, would be expected to be more vulnerable to attack from their right side.

Vallortigara & Rogers (2005) have proposed that population laterality is important for maintaining coordination between lateralised individuals in the context of "social" or group behaviours. In their model, they suggest

directional asymmetry arises as an "evolutionarily stable strategy" wherein it is advantageous for an individual to align the direction of their asymmetric behaviour with the majority of other individuals so as to gain a survival advantage by virtue of being part of a group. Some support for this hypothesis derives from a study of shoaling in fish, a behaviour which confers protection from predators. Bisazza et al. (2000) found that in sixteen species of fish, six displayed shoaling behaviour, and in all of those species population laterality for turning bias was observed. Of the species that did not shoal, six did not display population laterality but the remaining four did. A second study offering support for the hypothesis that population laterality facilitates social cohesion found that groups of lateralised chicks form more stable social hierarchies than non-lateralised chicks (Rogers & Workman, 1989). However, a recent study challenges the idea that population lateralisation mediates social behaviour as a result of the coordination of asymmetric behaviours among individuals. Bisazza & Dadda (2005) found that pairs of *Girardinus falcatus* selected for a high degree of lateralisation (as assessed by turning preference) performed better at shoaling than non-lateralised fish. However, shoaling was just as good in "mixed" pairs of fish that were strongly lateralised, but in *opposite* directions (*ie* one left-turning fish and one right-turning fish). This was interpreted as suggesting that perhaps the computational advantages associated with cerebral asymmetry are the driving force behind shoaling, rather than a simple alignment of (turning) behaviour. Finally, a study of predator–prey interactions demonstrates that population lateralisation is relevant to interactions between different species. Hori (1993) studied scale-eating cichlid fish in Lake Tanganyika. These fish have an asymmetric mouth that opens on either the left or right, enabling them to bite scales from the flanks of other fish. The direction of mouth opening shows population lateralisation that fluctuates with $\sim$5 year periodicity, alternately favouring the left or right side. This is because the laterality of mouth opening is under genetic control and frequency-dependent selection is exerted by the prey's alertness, such that scale-eater fish that attack from the unexpected side, at any one time, are at an advantage.

1.1.5 Development of neural asymmetry

Despite extensive accounts of neural lateralisation in various regions of the CNS in many animal species, relatively little is understood of the development of brain asymmetry. Whilst the extent to which variation in neural lateralisation is under genetic control is unclear, several other influences, including the prenatal environment, hormone levels and behavioural experience have been suggested to modulate the direction and/or degree of neural asymmetry. Work in *C. elegans* and zebrafish is also shedding light on the molecular mechanisms that underlie the development of left–right differences in the nervous system.

Genetic models

Two similar genetic models, both based upon the Mendelian inheritance of a single gene, have been proposed to explain the variation in human cerebral dominance and handedness (Annett, 1972, 1998; McManus, 1985)[3]. In the "Right Shift" model, Annett suggests that unknown environmental factors result in the development of asymmetric hand skill, which follows a Gaussian distribution in the population. By promoting left hemisphere dominance, a "right-shift" (RS+) allele shifts this distribution in favour of the right hand. By contrast, the RS– allele does not influence hemispheric asymmetry and therefore does not shift the distribution of relative hand skill. Genetic variation is maintained by heterozygous advantage and in more recent revisions of the model the alleles act additively. The majority of the population are either RS+/+ or RS+/– and consequently right-handed with leftwards hemispheric language dominance. A minority are RS–/–; these individuals do not show strong cerebral lateralisation and are equally likely to be either left or right-handed. This is compatible with the observations that CNS asymmetries are weaker and frequently reversed in left-handers (see §1.1.3).

Studies of handedness and cortical anatomical asymmetries in twins have attempted to unravel the relative contributions of genetic and environmen-

[3]The McManus model proposes two alleles control handedness, "Dextral", *D*, (analogous to the RS+ allele) and "Chance", *C*. As in the recent Right Shift model, neither allele is dominant but rather they act additively. *DD* homozygotes are always right-handed, *CC* homozygotes are equally likely to be right-handed or left-handed and 75% of *DC* heterozygotes are right-handed, with 25% left-handed (McManus, 1985).

tal influences to neural lateralisation and provide some support for genetic heredity of brain asymmetry[4]. Thompson et al. (2001) created genetic brain-maps using MRI scan data from identical and fraternal twins and found that grey matter volumes show considerable genetic heritability in a broad region of the cortex. Moreover, they observed significantly greater genetic control over left hemisphere language territories (including Broca's and Wernicke's areas) than their right hemisphere counterparts.

An MRI study by Geschwind et al. (2002) examined lobar brain volumes in twin-pairs and provides some support for the right-shift theory. Pairs of monozygotic (MZ) twins concordant for right handedness ("RR-pairs", assumed to carry the RS+ allele) showed greater similarity in the volumes of both left and right-sided cortical regions compared to pairs of MZ twins where at least one twin was left-handed ("non-RR" pairs, presumed to be RS−/−). This was interpreted as indicating greater genetic control over the size of left and right brain regions in the presence of the hypothetical right-shift gene. Moreover, twins from non-RR pairs failed to display significant asymmetries in the frontal and temporal cortex (whether they were left *or* right-handed), supporting the notion that left handedness is associated with a genotype that results in reduced cerebral lateralisation.

By contrast, a study using structural equation modelling to analyse variation in handedness concluded that genetic factors have only a modest influence (genetic heredity accounts for only about 16% of variation) and that non-shared environmental factors are considerably more important, accounting for approximately 84% of individual variation (Su et al., 2005). One explanation that may reconcile these apparently incompatible conclusions is that adaptive evolution might have occurred whereby selective pressures have led to the right-shift gene being carried by the majority of the population (genetic homogeneity); consequently, environmental influences are left as the major source of variation in handedness (Su et al., 2005).

Provins (1997) has also argued that environmental interactions and motor learning, but not an innate genetic factor, are the main determinant

[4]A potential concern with these studies has been that twin-specific developmental factors such as inter-uterine crowding, birth order and mirror imaging might affect handedness and mean twins are not representative of the general population. However, recent studies suggest that none of these factors influence handedness and twins are no more likely than singletons to be left-handed (Su et al., 2005; Medland et al., 2003).

of lateral asymmetry in hand use and Laland et al. (1995) has proposed a combined gene–culture model that suggests parental influences modulate a genetic predisposition towards right-handedness (approximately 78% probability) but that no genetic variation underlies variation in hand preference.

A major challenge to the genetic models is that the hypothesised gene has not been identified. However, a recent genome-wide linkage study has identified the leucine rich repeat trans-membrane neuronal 1 (LRRTM1) gene, which is expressed during the development of forebrain structures, as the first potential genetic influence on human handedness and cerebral asymmetries (Francks et al., 2007).

In other model species, however, there is good evidence for genetic control over variation in brain asymmetry and/or laterality. In food reaching tasks, different strains of mice differ in the magnitude of individual paw preference (degree of asymmetry) but contain approximately equal numbers of left-pawed and right-pawed individuals (*ie* there is no population laterality) (Biddle et al., 1993). Furthermore, selective breeding can select for both strongly and weakly lateralised mice, but not for a particular direction of paw preference (Collins, 1991). These observations suggest that in mice genetic factors influence the *degree* of neural asymmetry, but do not control its *direction* (laterality). By contrast, the goldbelly topminnow *Girardinus falcatus* has been selectively bred for both the direction and strength of turning preference (Bisazza et al., 2007), suggesting genetic variation underlies both magnitude *and* direction of cerebral lateralisation in this species.

Prenatal environment

Both anatomical and functional asymmetries appear early in human development. For example, Chi et al. (1977) have described anatomical asymmetries in the language-associated temporal cortex as early as 31 weeks' gestation and ultrasound observations of fetuses from 15 weeks old show a preference for sucking the right thumb, suggesting that at least some degree of handedness develops prior to birth (Hepper et al., 1991). This early presentation suggests that genetic variation and/or prenatal environmental conditions are responsible for the observed variation in asymmetry phenotypes between individuals. Whilst some studies indicate that heritable genetic factors only have a modest effect on *variation* in cerebral lateralisation (see above), there

is evidence that prenatal environmental factors constitute an important variable influencing the early development of neural lateralisation.

For example, two-thirds of human fetuses develop with their right side facing outwards and Previc (1991) has argued that asymmetries in the intrauterine environment, including fetal posture, contribute to the development of perceptual and motor asymmetries. During later stages of chick development, the head is rotated such that the right eye is exposed to light, entering through the egg shell and air sac membranes, whereas the left eye is shielded by the body. The resultant asymmetric light exposure is essential for the development of visual system asymmetry; if eggs are incubated in the dark, chicks fail to develop both anatomical and eye-usage asymmetries and if light-stimulation is artificially reversed, so to is the direction of lateralisation (Rogers, 1990, and see §1.1.3).

Gender & hormones

At both anatomical and functional levels, cerebral lateralisation is more pronounced in men than women. Men show stronger left hemisphere dominance for language processing (Shaywitz et al., 1995) as well as a greater degree of asymmetry in language associated fibre tracts, whereas women display a more bihemispherically distributed language network (Hagmann et al., 2006; Catani et al., 2007).

Gender differences in brain asymmetries have been shown to be influenced by hormonal signalling in rats; sex-specific asymmetries in neocortical thickness are dependent on pre- and post-natal androgenic and ovarian sex steroids (Diamond et al., 1981). Similarly, Geschwind & Galaburda have suggested that *in utero* testosterone levels influence the development of brain asymmetries in humans (discussed in Toga & Thompson, 2003).

Functional adaptation & experience

Evidence from several species suggest that brain asymmetries are sufficiently plastic as to be modified by an animal's behaviour and its environmental experience.

Collins (1975) has demonstrated experience-dependent plasticity of lateralised behaviour in mice. He showed that a large group of inbred mice that

were initially equally divided among those favouring the left or right paw became predominantly right-pawed if exposed to a "biased world" in which it was easier to obtain food with the right paw. Furthermore, asymmetric paw use in rats has been shown to cause lateralisation of brain anatomy, namely an increase in neuropil volume and reduction in cell packing density in the contralateral motor cortex (Diaz et al., 1994).

There is some evidence that asymmetries in sensory input pathways could influence behavioural asymmetries in mice. In mouse strains that were selectively bred for asymmetric whisker pads, mice which displayed supernumerary right whiskers were more likely to develop a preference for left paw use and *vice versa* (Barneoud & Van der Loos, 1993). A proposed neurological mechanism posits that the enlargement of the barrel field in the somatosensory cortex contralateral to the enlarged whisker pad reduces the availability of cortical territory and encourages motor dominance to develop in the opposite hemisphere.

In lobsters, sensory experience, during a critical sensitivity period, is essential for lateralising the nervous system and consequently for the development of morphologically and functionally asymmetric claws (Govind, 1992). Stochastic differences in mechanosensory inputs lateralise the claw ganglion into distinct "crusher" and "cutter" sides. If lobsters are reared in smooth plastic trays with no objects to manipulate, they develop two small, fast-closing cutter claws, rather than a single cutter and a massive crusher claw.

As a further example of environmental influences, predator stress leads to changes in anxiety behaviour in rats as a result of long term potentiation of limbic pathways in the right hemisphere (Adamec et al., 2005).

Molecular–genetic mechanisms

Recent work, principally in two models of developmental genetics, *C. elegans* and zebrafish, is helping to uncover the developmental mechanisms that break symmetry in the nervous system and specify the direction (laterality) of asymmetry (for recent reviews see Sagasti, 2007; Halpern et al., 2005; Concha, 2004).

Studies of two pairs of sensory neurons in *C. elegans* have produced models both for the development of neural asymmetry without a directional bias

in the population (antisymmetry) and for the development of asymmetry with invariant laterality (directional asymmetry/population laterality) (see review in Sagasti, 2007, and references therein).

Asymmetry with randomised laterality The *C. elegans* AWC olfactory neurons display antisymmetry. Within a population, half of the animals express the G-protein-coupled olfactory receptor STR-2 exclusively in the left neuron, AWCL, whereas the other 50% of animals show asymmetric expression only in the right neuron, AWCR. This molecular asymmetry results in different odorant sensitivity profiles for the two neurons and consequently enhances odorant detection and discrimination (Wes & Bargmann, 2001).

A conceptual model for the development of asymmetry proposes that the two AWC neurons, which are unrelated by lineage and born on opposite sides of the animal, communicate with one another so as to ensure a coordinated decision wherein only one neuron expresses *str-2* and the other does not (Figure 1.2 and Sagasti, 2007). In this model, initially small, stochastic differences in signalling between the neurons are amplified by positive and negative feedback mechanisms such that the two neurons achieve mutually exclusive stable states that are translated into unique cell fates[5]. Reciprocal communication is possible because the neurons project axons across the midline to contact one another and consequently, axon pathfinding mutations that disrupt these contacts abrogate asymmetry.

Through the identification of neuronal symmetry (nsy) mutants, it has been determined that left–right differences in calcium signalling act cell-autonomously to control the molecular phenotype of the AWC neurons: Calcium entry through voltage gated calcium channels activates the calcium/calmodulin-dependent protein kinase CaMKII, which in turn activates MAP kinase signalling that leads to repression of *str-2* expression. In one neuron, calcium signalling is low and in the other it is high, such that one cell expresses *str-2* and the other does not.

Although it is presently unknown how interactions between the two AWC neurons establish this asymmetry in calcium signalling, a clue has come from the *nsy5* mutant. *nsy5* encodes an innexin protein that forms gap junction

[5]Whilst this model bears similarities to lateral signalling mediated by the Notch pathway, Notch signalling is not involved in establishing AWC asymmetry.

Figure 1.2: **Models for the development of nervous system asymmetries in *C. elegans*.** *Left*: AWC olfactory neurons develop asymmetry without directional bias. *Right*: ASE gustatory neurons develop asymmetry with invariant laterality. Modified after Sagasti (2007).

channels and mosaic analyses indicate that the gene acts not only in the AWC cells, but also in other bilaterally symmetric neurons. This has led to the hypothesis that gap-junction mediated signalling between networks of cells underlies communication between the left and right sides involved in breaking symmetry.

Asymmetry with consistent laterality In contrast to the AWC neurons, asymmetry between the ASE gustatory neurons shows the same laterality in every worm. Among a number of genes that show lateralised expression, the guanalyl cyclase gene *gcy5* is always expressed in ASER, whereas *gcy7* is consistently expressed in ASEL.

Although ASEL and ASER initially both express left *and* right-characteristic genes, signalling pathways act soon after the cells are born to resolve this initial equivalency and establish left–right specificity in gene expression. In contrast to the AWC model, no interactions are required between the ASE cells and there is no overlap in the molecular–genetic pathways that mediate asymmetry in the AWC and ASE pairs.

The ASE neurons utilise a genetic feedback circuit containing both transcription factors and micro RNAs (miRNAs) which repress one another so as to achieve one of two mutually exclusive stable outcomes (Figure 1.2). This bistable genetic switch adopts opposite states in ASEL and ASER and downstream transcriptional pathways translate this difference into cell-specific molecular phenotypes. But what signalling mechanism establishes asymmetry and results in opposite halves of the transcription factor/miRNA feedback loop being activated in the two cells? ASEL and ASER descend from different embryonic lineages and Poole & Hobert (2006) have suggested that a very early molecular asymmetry, acting along the *anterior-posterior* (AP) axis at the four-cell stage, establishes different identities within these lineages. This information is retained through ten further cell divisions to eventually influence the fate of the ASE neurons. The nature of the AP-orientated asymmetric factor, how it is retained, and how it influences the bistable genetic loop are yet to be resolved.

Neural asymmetry in vertebrates Until recently, very little was known about the molecular–genetic pathways that establish brain asymmetries in

vertebrates. However, progress has been made as a result of cellular and genetic analyses of the development of directional asymmetries in the larval zebrafish brain. In contrast to the directional asymmetry of ASE neurons in *C. elegans*, where the same developmental event both generates asymmetry and specifies its laterality, in the zebrafish dorsal diencephalon, symmetry breaking and the control of laterality appear to be mediated by independent pathways. As is the case for AWC neurons, communication between the two sides of the brain is likely to be important to ensure a coordinated decision that results in unique lateral identities on the left and right. I present a review of the zebrafish data in §1.3.

Whilst zebrafish is the only vertebrate species in which direct links have been established between asymmetric gene expression and the development of neural asymmetry, a recent study by Sun et al. (2005) identified 27 genes that are asymmetrically expressed in the human brain at fetal stages. One example is the transcription factor Lim domain only 4 (LMO4), which is consistently expressed more strongly in the right perisylvian cortex from 12 to 14 weeks gestation. Asymmetric expression is conserved in mice, albeit with randomised laterality. Sun & Walsh (2006) have speculated that asymmetries in the secretion of morphogens from the dorsal or ventral midlines of the neural tube or from the anterior neural ridge could translate into left–right differences in induction of transcription factors such as LMO4 and so bring about asymmetric cortical patterning.

1.2 The dorsal diencephalic conduction system

1.2.1 Overview

The dorsal diencephalon, or epithalamus, contains the bilaterally paired habenular nuclei and the pineal complex. As I shall discuss in §1.3, this region has been the focus of recent studies in zebrafish into the molecular, genetic and cellular mechanisms by which neural asymmetries develop.

The habenulae form part of the dorsal diencephalic conduction system (DDC), a pathway which is very highly conserved and indeed, found in all vertebrates. In this section, I shall briefly review the neuroanatomy of the DDC, consider its physiological and behavioural importance and discuss current examples of neural asymmetries within the epithalamus. For a more

extensive review of the anatomy and functions of the DDC, the reader is referred to Sutherland (1982); Lecourtier & Kelly (2007).

The DDC is one of two major pathways which interconnect the limbic forebrain and sites in the midbrain and hindbrain, the other pathway being the medial forebrain bundle (MFB). These two pathways appear to represent parallel neural circuits; they share sources of afferent inputs as well as efferent targets and the DDC originates from the anterior MFB. This parallelism is also represented at the functional level as there is similarity and overlap in the physiological and behavioural involvement of these pathways.

The DDC comprises three components: The habenular nuclei, the stria medullaris (SM), which is the fibre tract through which inputs from the forebrain arrive at the habenulae, and the fasciculus retroflexus (FR), a prominent fibre tract that predominantly carries efferent axons from the habenulae towards targets in the midbrain/hindbrain.

1.2.2 Habenula

Along with the pineal complex, the bilaterally-paired habenulae (Hb) are the only nuclei in the epithalamus. They are located adjacent to the third ventricle and rostral to the posterior commissure and the habenular commissure runs between them.

In mammals, the habenular complex comprises two separate nuclei on each side — the "medial" (MHb) and "lateral" (LHb) habenulae. The lateral habenula is further subdivided into principal medial and lateral subdivisions. These different components of the habenular complex receive different afferent inputs and project to largely distinct efferent targets such that in terms of patterns of connectivity, the DDC comprises three partially overlapping sub-circuits (Herkenham & Nauta, 1977, 1979; Kim & Chang, 2005). In outlining the anatomy of the DDC, I shall focus primarily on patterns of connectivity described in the rat, which have been well studied. Some species differences will also be mentioned, where relevant, but I will not attempt a description of the comparative neuroanatomy of the DDC in any detail.

Medial habenula

Medial habenular circuitry is highly conserved (Sutherland, 1982). The medial habenula primarily receives inputs from the septum and projects to the interpeduncular nucleus (IPN) of the ventral midbrain. This basic pattern of connectivity comprises the "core" of the DDC and appears to be conserved in all vertebrate species that have been examined.

Afferent connectivity The major source of afferent innervation of the MHb derives from the supracommissural septum, with axons coursing in the stria medullaris (Herkenham & Nauta, 1977). Septal sites themselves receive inputs from the hippocampus and subiculum. Axons from the two most significant septal nuclei also terminate in different sub-domains of the medial habenula — the septofimbrial nucleus innervates the rostral MHb whilst the nucleus triangularis innervates the caudal MHb. In the rat, almost every neuron in these two septal nuclei is likely to project to the MHb. More minor inputs derive from the nucleus accumbens and the nucleus of the diagonal band.

The MHb also receives minor ascending inputs, principally derived from monoaminergic nuclei, which are also targets of both medial and lateral habenular efferent axons. Thus, axons from the median raphé ascend through the fasciculus retroflexus and provide serotonergic inputs to the MHb. Dopaminergic inputs derive from the interfascicular nucleus of the ventral tegmental area (VTA) and noradrenergic inputs from the locus coeruleus. These latter axons reach the MHb by coursing anteriorly in the MFB and then joining the SM.

Efferent connectivity The main target of MHb axons is the IPN (Herkenham & Nauta, 1979). The MHb contains both cholinergic neurons (in its ventral two-thirds) and dorsally-located substance P-containing neurons (Contestabile et al., 1987). Both types are contacted by the major afferent axons from the septofimbrial nucleus and nucleus triangularis, and both project down the core of the FR to innervate the IPN. MHb axons terminate in a topographic manner wherein neurons of the dorsal MHb innervate the lateral IPN, those of the medial MHb innervate the ventral IPN and lateral MHb neurons project to the dorsal IPN (Herkenham & Nauta,

1979; Contestabile & Flumerfelt, 1981).

Minor efferent projections of the MHb have been suggested to the VTA and median raphé.

Although little is known about intrinsic habenular circuitry and the extent to which communication exists between the MHb and LHb, two observations provide evidence for a medial to lateral connection. A subset of MHb axons project through the LHb and in so doing display *en passant* boutons that might represent presynaptic terminals (Kim & Chang, 2005) and sectioning of MHb efferent axons has been reported to reduce substance P levels in the LHb (see Sutherland, 1982).

Lateral habenula

The lateral habenula is thought to be involved in the motor–limbic interface as it receives inputs from pallidal, limbic and hypothalamic sources and projects to the ventral midbrain tegmentum (Sutherland, 1982).

Afferent connectivity An important feature of the lateral habenula is that it represents a point of convergence for neural information from the basal ganglia and the limbic forebrain (Herkenham & Nauta, 1977).

A major source of innervation of the LHb in the rat derives from the entopeduncular nucleus (EP, which is the non-primate equivalent if the internal segment of the globus pallidus). In the rat, virtually every entopeduncular neuron appears to project to the LHb, suggesting the axons are collaterals of the pallido–thalamic pathway. This pallido–habenular pathway also exists in cats and monkeys. However, in the monkey it appears that whilst the LHb receives substantial innervation from the internal segment of the globus pallidus, this innervation derives from a different group of pallidal neurons to those that innervate premotor neurons in the thalamus and brainstem (Parent et al., 2001).

Limbic regions of the forebrain constitute the second major source of afferent innervation of the LHb. A continuous band of cells, stretching from the anterior lateral preoptic area, through the lateral hypothalamus to the mid-hypothalamus projects to the LHb. Afferent inputs from the medial frontal cortex have been reported. Additionally, the suprachiasmatic nucleus, which is concerned with the generation of circadian rhythms in

mammals, projects vasopressin-containing axons to the LHb (Buijs, 1978). A second source of circadian information is suggested by the finding that in mouse melanopsin-expressing retinal ganglion cells project to the LHb (Hattar et al., 2006).

Although the MHb and LHb receive most of their afferent inputs from different sources, there is some degree of overlap. Thus, the LHb receives a small descending input from septal regions, including the nucleus of the diagonal band, nucleus accumbens and lateral septal nucleus. Additionally, the LHb receives ascending innervation from monoaminergic nuclei, at least some of which overlap with sources innervating the MHb. Thus, axons from the median raphé and ventral central grey provide serotonergic and noradrenergic inputs. Midline neurons of the ventral tegmental area (interfascicular and para-nigral nuclei) provide dopaminergic inputs to the medial part of the LHb, probably via the FR. Notably, this region of the VTA contains many neurons belonging to the A10 region, which gives rise to the mesolimbic "reward" pathway.

In summary, the afferent connectivity of the LHb may enable motivational/emotional states (encoded by limbic inputs) to modulate motor behaviours (orchestrated by the striatum and represented by pallidal efferents).

Efferent connectivity The LHb contains predominantly glutamatergic neurons as well as some GABAergic and cholinergic cells and establishes efferent connectivity with a wide range of targets. Many of these targets are themselves sources of afferent inputs to the LHb (Herkenham & Nauta, 1979; Lecourtier & Kelly, 2007).

For example, the LHb projects to the limbic forebrain, including the lateral hypothalamic area, lateral preoptic area and ventrolateral septum.

The LHb establishes descending connectivity with numerous monoaminergic nuclei in the midbrain and hindbrain. A major projection, especially from the medial LHb, innervates the median and dorsal raphé; LHb activity inhibits the raphé, probably as a result of activation of GABAergic interneurons in the nucleus. The LHb innervates and inhibits the dopaminergic VTA and the substantia nigra *pars compacta* (SNc), which has significance for reward prediction mechanisms (see §1.2.4). This efferent connection establishes a feedback circuit as dopaminergic neurons of the substantia nigra

project to the dorsal striatum (caudato–putamen), which in turn connects to the pallidum, a major source of afferent innervation of the LHb. There are many other efferent targets of the LHb including several thalamic nuclei, the superior colliculus, dorsal and ventral tegmental nuclei, nucleus accumbens and noradrenergic locus coeruleus.

In summary, LHb circuitry provides a feedback circuit connecting limbic and striatal nuclei in the forebrain to the sources of their monoaminergic afferents in the midbrain and hindbrain.

1.2.3 Interpeduncular nucleus

The IPN receives most of the efferent axons from the MHb, and therefore is central to medial habenular control over downstream circuitry.

The IPN is a singular, unpaired structure, located at the ventral midline of the posterior midbrain/anterior hindbrain. It comprises a number of morphologically defined subnuclei. In the rat, Lenn & Hamill (1984) have identified seven subnuclei, including three that are described as unpaired, being located at the midline and which are flanked laterally by four bilaterally-paired subnuclei. A large number of neurotransmitters are expressed in a spatially-organised manner within the IPN and it establishes connectivity with an array of nuclei; this has led to the suggestion that it is an important integrative centre (reviewed in Morley, 1986).

Afferent connectivity A major source of innervation of the IPN is from the MHb. Other afferent inputs to the IPN derive from the nucleus of the diagonal band (NDB), dorsal tegmental nucleus (DTN), raphé, central grey, supramammillary nucleus and locus coeruleus (Contestabile & Flumerfelt, 1981; Shibata et al., 1986).

Biochemical studies have identified extremely high levels of acetylcholine, choline acetyltransferase, acetylcholine esterase and high-affinity choline uptake within the IPN and the habenulo-interpeduncular pathway is considered one of the major cholinergic pathways in the brain (*eg* Contestabile & Fonnum, 1983). Cholinergic innervation is likely to derive from both the MHb as well as from the DTN and neurons in the basal forebrain (septum and preoptic area); the latter are thought to project axons that extend, uninterrupted, through the habenula and FR to reach the IPN (Contestabile

& Fonnum, 1983; Woolf & Butcher, 1985). There is evidence that a wide range of additional neurotransmitters are present in the IPN, including γ-aminobutyric acid (GABA, probably deriving from the NDB), substance P (from the MHb) and various monoamines (noradrenaline, dopamine and serotonin) and neuropeptides (including cholecystokinin, leucine-encephalin, methionine-encephalin, vasointestinal peptide and somatostatin) (see Morley, 1986).

As mentioned above, MHb axons terminate in a topographic manner within the IPN and accordingly, Contestabile et al. (1987) and Eckenrode et al. (1987) have shown that cholinergic and substance P-containing inputs are largely segregated within the IPN. Cholinergic fibres are confined in the unpaired midline core of the IPN, whereas substance P signalling shows greater localisation to the peripheral subnuclei.

Efferent connectivity The dorsal tegmental nucleus (DTN) is the major target of IPN efferent connectivity. The IPN also innervates the ventral tegmental nucleus and the raphé. In addition, the IPN makes ascending projections to various neuronal nuclei, several of which are sources of afferent inputs to both the medial and lateral habenulae, thus establishing further feedback circuits within the DDC. Thus, efferent targets include the nucleus of the diagonal band, preoptic area, dorsolateral hypothalamus, septum, mediodorsal nucleus of the thalamus, hippocampus and entorhinal cortex and the lateral habenula (Shibata & Suzuki, 1984; Morley, 1986).

1.2.4 Physiological & behavioural functions

In accordance with the diversity of its afferent inputs and efferent targets, the DDC is involved in a diverse range of cerebral functions (reviewed in Sutherland, 1982; Lecourtier & Kelly, 2007). One central theme is the importance of the DDC in regulating the activity of monoaminergic nuclei in the ventral midbrain. I discuss some of its many behavioural and physiological functions below.

Control of dopaminergic circuitry: motor activity & reward prediction Habenular lesions may result in increased locomotor activity in rats, especially in response to novel environmental stimuli (Lee & Huang,

1988). This effect is likely to be mediated by midbrain dopaminergic (DA) neurons, which are innervated by the LHb. Electrical stimulation of the LHb inhibits the activity of DA neurons in the VTA and SNc (Christoph et al., 1986), probably as a result of activation of GABAergic interneurons (see Lecourtier & Kelly, 2007) and conversely, habenular lesions result in increased dopaminergic transmission (Lisoprawski et al., 1980; Nishikawa et al., 1986), suggesting that habenular efferent circuitry exerts a tonic inhibitory effect upon DA neurons. The SNc modulates motor programmes orchestrated by basal ganglia circuitry through nigrostriatal innervation of the caudato-putamen. As the LHb receives substantial inputs from the basal ganglia (globus pallidus/entopeduncular nucleus, see §1.2.2), the DDC provides a feedback circuit where basal ganglia circuitry can modulate its dopaminergic afferents in the midbrain; Sasaki et al. (1990) have provided functional data supporting a role for the entopeduncular nucleus, stria medullaris and habenula in negative feedback control over the SNc.

Midbrain dopaminergic neurons are also centrally involved in appetitive learning of new behavioural responses to positive reinforcers ("rewards"). The LHb is one of the few regions of the brain to be inhibited by hedonic stimuli and recently, Matsumoto & Hikosaka (2007) have shown that the LHb instructs midbrain DA neurons as to the absence of a reward. In monkeys performing a visually-guided saccade task, LHb neurons are activated by visual targets that signify the absence of a reward and inhibited by targets that predict forthcoming reward (whereas DA neurons of the SNc show the opposite responsiveness). In unrewarded trials, the activation of LHb neurons preceded the inhibition of SNc neurons and mild electrical stimulation of the LHb inhibits the SNc. Therefore, it appears that the LHb provides information regarding the nature of salient environmental stimuli to midbrain reward circuits in the form of negative reward-related signals. Thus, it is likely to be involved in the adjustment of behavioural strategies.

Cognition The DDC has been implicated in cognitive processes, in particular relating to spatial learning and attention.

An involvement of the habenular complex in spatial learning has come from studies in rats using the classical Morris water-maze test. Villarreal et al. (2002) found that after training in the water-maze, aged, memory-

impaired rats showed reduced cytochrome oxidase activity (a read-out of neuronal activity) in the LHb as compared to young unimpaired rats. The LHb was one of only a few brain regions to show this change and it was not observed after control swimming in the absence of learning, suggesting that LHb metabolic activity is correlated with spatial memory performance. Supporting a functional role for the habenula in spatial reference memory, Lecourtier et al. (2004) showed that Hb lesions impaired memory acquisition and retrieval in the Morris water-maze. Spatial memory is known to involve the hippocampus, which also contributes the major afferent input to the septofimbrial nucleus and nucleus triangularis. These septal nuclei in turn provide the major input to the MHb (§1.2.2). This has led to the suggestion that the habenula might be involved in learning via the integration of hippocampal signals, relating to memory formation or retrieval, with activity of the nucleus accumbens, relating to whether a behavioural strategy was rewarded (Lecourtier & Kelly, 2007). Moreover, it has recently been shown that habenular lesions alter synaptic plasticity between the hippocampus and nucleus accumbens (Lecourtier et al., 2006).

Lecourtier & Kelly (2005) investigated a role for the habenular complex in attentional mechanisms using a specific behavioural test of attention in rats, the 5-Choice Serial Reaction Time Test. Habenular lesions resulted in an increase in premature responding, which might represent the emergence of an impulsive mode of behaviour. This effect was blocked by haloperidol, suggesting it is caused by increased dopaminergic transmission from midbrain DA neurons, which are inhibited by descending habenular efferents (above). A second effect was that rats displayed a progressive deterioration in choice accuracy, which was probably not due to dysregulation of DA signalling. Whilst the mechanism of this defect is unclear, it might involve changes in noradrenergic or cholinergic transmission, both of which are affected by DDC circuitry (discussed in Lecourtier & Kelly, 2007). The observation that choice accuracy was not impaired immediately after surgery but then subsequently showed a progressive decline, is an unusual feature and Lecourtier & Kelly (2007) draw attention to the progressive alterations in serotonergic and GABAergic function within the IPN that have been seen after habenular lesions.

Aversive responses The LHb is responsive to various noxious stimuli in the rat (Benabid & Jeaugey, 1989) and the activation of LHb neurons by nociceptive inputs has been suggested to be responsible for inhibition of DA neurons of the SNc (Gao et al., 1996). In addition, induction of Fos immunoreactivity, which is indicative of neuronal activation, occurs in the LHb in response to stress (Smith et al., 1997) and both electrical stimulation or morphine injections into the habenula produces analgesia in a rat model of tonic pain (Cohen & Melzack, 1985, 1986).

Several studies indicate that the DDC is involved in learning conditional avoidance responses (behavioural responses to avoid aversive stimuli). Habenular lesions appear to inhibit learning by reducing behavioural flexibility, especially under stressful conditions. For instance, in an operant one-way active avoidance task, Thornton & Bradbury (1989) found that habenular lesioned rats were able to learn an escape response when the aversive stimulus (electroshock) was mild and the inter-stimulus time was long, but were defective, as compared to control animals, under more stressful conditions (higher stimulus intensities and shorter intervals between shocks). Furthermore, in a pre-pulse inhibition (PPI) task, designed to assess sensory gating and information filtering, mice with habenular lesions failed to show an increase in PPI after exposure to a fear-conditioning paradigm (Heldt & Ressler, 2006). One explanation is that stress associated with fear conditioning causes an increase in PPI in wild-type mice, mediated by habenular effects on monoamine systems. Further support for a role of the DDC in adaptation to stress derives from the observation that plasma corticosterone levels are chronically elevated in FR lesioned rats (Murphy et al., 1996).

Circadian rhythms The nuclei comprising the dorsal diencephalon are involved in regulating circadian rhythms. In addition to the habenulae, the epithalamus contains the pineal complex, and the pineal has a conserved role in the generation and/or regulation of circadian rhythms (Falcon, 1999). In lower vertebrates, the pineal is directly photoreceptive, enabling its circadian activity to be entrained to the 24 hour day–night cycle. In non-mammalian vertebrates it comprises the clock, or pacemaker, of the circadian system and in all vertebrates is involved in the regulation of rhythmic behaviours and physiological responses through the secretion of melatonin (Falcon, 1999). In

mammals, the suprachiasmatic nuclei (SCN) of the hypothalamus act as the major pacemaker and receive light information via the retino-hypothalamic pathway. The SCN clock controls rhythmic activity of the pineal (Klein & Moore, 1979) via the sympathetic nervous system and the pineal continues to modulate circadian rhythms through release of melatonin.

In addition to the pineal, the habenular complex appears to be involved in circadian functions. The LHb expresses melatonin receptors (Weaver et al., 1989) and in some species habenular cells synthesise melatonin (Sato et al., 1991). Additionally, the LHb is innervated by SCN neurons (Buijs, 1978) as well as by melanopsin-expressing RGCs (Hattar et al., 2006). Zhao & Rusak (2005) have shown that Hb neurons, especially in the LHb, respond to retinal illumination and show higher baseline firing *in vivo* during the day than the night. Moreover, LHb cells maintain this rhythmicity *in vitro* for at least 48 hours. Whilst the functions of these oscillations and retinal illumination responses are unclear, accumulating evidence suggests the habenular complex might form part of the output pathway regulating circadian rhythms that are generated in the SCN. Certainly, many of the behaviours influenced by the DDC show circadian variations, including sleep (below). Intriguingly, the LHb response to stress (assessed by c-Fos immunoreactivity) has been reported to be greater during the night than the day (Chastrette et al., 1991).

Sleep Evidence suggests that both the habenula and IPN are involved in regulating aspects of sleep. Lydic et al. (1991) observed a significant increase in glucose utilisation in the habenula during rapid-eye movement (REM) sleep in cats and electrical stimulation of the LHb was reported to cause a decrease in REM sleep and an increase in non-REM sleep (Goldstein, 1983).

Both the FR and IPN appear to be important regulators of normal sleep patterns and duration. Haun et al. (1992) found that transecting the FR disrupted both the REM and non-REM component of sleep and more recently, Valjakka et al. (1998) demonstrated that FR lesions disrupt REM sleep and hippocampal theta rhythms. Eckenrode et al. (1992) showed that transplants of a suspension of fetal habenular cells near the denervated IPN of FR-lesioned rats can restore normal patterns of substance P and/or ChAT

innervation. When substance P innervation of the IPN was restored there was recovery of the integrity of REM sleep, whereas transplants that reestablished cholinergic innervation restored the non-REM component (resulting in recovery of sleep duration) (Haun et al., 1992). Moreover, the extent of recovery was correlated with the number of transplanted cells. It was proposed that the function of the IPN in REM sleep might be mediated by its projection to the dorsal tegmentum, which in turn innervates the "REM sleep induction zone" of the dorsomedial pons.

Reproductive and maternal behaviour DDC circuitry appears to be involved in female-specific sexual behaviour (Modianos et al., 1974). However, lesions studies have produced inconsistent results, showing either an increase or decrease in the receptivity of female rats after habenular lesions (discussed in Sutherland, 1982). Intriguingly, Kemali et al. (1990) observed that in the frog, the habenulae are larger in spring than in winter and this seasonal change in habenular size was most noticeable in females. As frogs are sexually active in spring, they hypothesised that hormonal signals initiating reproduction might mediate this effect on the habenula.

Maternal behaviour is a second social behaviour influenced by the DDC. Matthews-Felton et al. (1995) found that LHb lesions caused substantial disruptions to maternal behaviour in rats.

Involvement in psychosis DDC circuitry has been implicated in a number of psychological conditions including depression, anxiety, schizophrenia and neuropathological responses to addictive drugs.

In three animals models of depression, Caldecott-Hazard et al. (1988) observed that metabolic activity in the LHb is specifically increased and that administration of the anti-depressant drug tranylcypromine inhibited the elevation of metabolic rate in the LHb as well as the depressive behaviours. Furthermore, Thornton et al. (1985) found that habenular lesions blocked the effect of an anti-depressant drug in reversing depressed behaviours that were induced in rats by forced swimming. The habenular complex provides the main forebrain projection to the raphé and exerts control over the activity of raphé neurons (Wang & Aghajanian, 1977). LHb activity appears to inhibit raphé neurons as a result of activation of GABAergic

interneurons (see Lecourtier & Kelly, 2007). The midbrain raphé are the major source of cerebral serotonin and clinically effective anti-depressants are thought to work by facilitating serotonergic signalling, suggesting that serotonin deficiency may underlie depression. Morris et al. (1999) observed that in human patients where depressive relapses were triggered by rapid depletion of blood tryptophan (the precursor to serotonin), positron emission tomography (PET) signals displayed correlated increases in the habenula and dorsal raphé as patients' rating of their depressed mood worsened. Recently, Yang et al. (2008) reported that in two rat models of depression (where serotonin levels in the dorsal raphé are depleted), LHb lesions improved the behavioural responses of the rats and this was accompanied by an increase in dorsal raphé serotonin levels. It was therefore hypothesised that overactivity of the LHb contributes to the pathogenesis of depression by inhibiting the raphé.

It has also been suggested that pathology of the habenula may contribute to schizophrenia (*eg* Lecourtier et al., 2004). In a human fMRI study, where subjects had to perform a difficult mental task and therefore made numerous errors, the habenular complex was activated when informative feedback was given about errors. Such activation did not occur in schizophrenic patients, who were also impaired in the task (Shepard et al., 2006). This result indicates that impaired activity of DDC circuitry is correlated with impaired cognitive performance in schizophrenia. Shepard et al. (2006) suggest that LHb dysfunction would limit a person's ability to learn from errors, which is one of the most characteristic cognitive deficits associated with schizophrenia. Although the cause and effects of the observed habenular dysfunction are unknown, there are some clues regarding potential pathological mechanisms. Firstly, an elevated incidence of habenular and pineal calcification has been observed in schizophrenic patients (Sandyk, 1992; Caputo et al., 1998). Secondly, influenza A virus, which increases the risk of schizophrenia if experienced prenatally, selectively attacks the habenula, paraventricular thalamic and brain stem monoaminergic areas when introduced into the mouse brain via the olfactory bulb (Mori et al., 1999).

DDC circuitry appears to be specifically vulnerable to the neurotoxic effects of addictive drugs (reviewed in Ellison, 2002). Continuous administration of drugs that potentiate dopamine signalling, including cocaine,

D-amphetamine and methamphetamine, causes degeneration of axons in the sheath of the FR deriving from LHb neurons, whereas continuous nicotine causes a remarkably specific degeneration of axons from MHb neurons, which descend in the core of the FR. Ellison (2002) has suggested the FR represents a "weak link" that may mediate the progressive effects of drug taking such as addiction and relapse and FR pathology may be involved in various psychoses.

1.2.5 Asymmetry within the epithalamus & DDC

The dorsal diencephalon displays neural asymmetry in many animal species. Indeed, structural asymmetries in this region have been described in virtually all classes of vertebrates (reviewed in detail in Concha & Wilson, 2001). Asymmetries are most conspicuous in fish, amphibians and reptiles, whilst birds and mammals show more subtle lateralisation.

The two components of the epithalamus — the habenulae and pineal complex — show left–right differences in size, cytoarchitectonic organisation, neurochemistry and connectivity.

Habenular asymmetry

Size The left and right habenulae show conspicuous differences in size in many species. For instance, in the lamprey, the right nucleus is considerably larger than the left (Yanez & Anadon, 1994). This mode of lateralisation is common in fish; most actinopterygii (ray-finned bony fishes), with the exception of the teleosts, show rightwards asymmetries in habenular size (see Concha & Wilson, 2001).

In amphibians, the habenulae are divided into major dorsal and ventral subdivisions, which are analogous to the medial and lateral habenulae of mammals, respectively. Asymmetries have been described between the dorsal nuclei; the frog *Rana esculenta* shows a number of pronounced epithalamic asymmetries, including a larger dorsal nucleus on the left (Braitenberg & Kemali, 1970; Kemali et al., 1990).

Habenular size asymmetries are considerably more subtle in birds and mammals. However, quantitative volumetric analyses have uncovered left–right differences. Thus, in the albino rat, the left medial habenula is slightly

(5%) larger than the right (Wree et al., 1981), whereas in the albino mouse rightwards lateralisation is apparent in the lateral habenula during development and adulthood (Zilles et al., 1976).

Cytoarchitecture and cell morphology Amphibians and reptiles show asymmetries in the subnuclear organisation of the habenulae. Such asymmetries are also apparent in fish species, but are less conspicuous than left–right differences in size.

In the enlarged right habenula of the lamprey, neurons are organised into three major layers, which are arranged dorsoventrally and separated by areas of neuropil, whereas only a single domain of periventricular neurons is seen on the left (Yanez & Anadon, 1994).

In *Rana esculenta* the larger left dorsal habenula is subdivided into quite distinct medial and lateral subnuclei, whereas only a single nucleus comprises the right dorsal habenula (Gugliemotti & Fiorino, 1998; Guglielmotti & Fiorino, 1999). In terms of both cytoarchitecture and cell morphology, the lateral subnucleus on the left is similar to the single right-sided nucleus. The left medial subnucleus possesses distinctive features and can be further subdivided into medial and lateral neuropils. It contains a unique population of large and ramified projection neurons that are absent from both the left lateral subnucleus and the right dorsal habenula.

Neurochemistry Habenular lateralisation is also manifest in terms of molecular differences between the left and right sides, including asymmetries in the distribution of neurotransmitters. For example, Ekstrom & Ebbesson (1988) have identified a discrete serotonin-immunoreactive subnucleus, exclusively within the left dorsal habenula of the coho salmon.

The unique character of the medial subnucleus of the left dorsal habenula of the frog is further evidenced by its distinctive neurochemical properties. For instance, this subnucleus alone displays high levels of melatonin binding (Wiechmann & Wirsig-Wiechmann, 1993) and calretinin immunoreactivity (Guglielmotti et al., 2004). Furthermore, Guglielmotti & Fiorino (1999) found that NADPH-diaphorase histochemistry (which reports the presence of nitric oxide synthase in neural tissue, Hope et al., 1991), is exclusively localised within the lateral neuropil of the left medial subnucleus, but is not

detected in the left lateral subnucleus nor the right dorsal habenula.

Fibre tracts Left–right differences between the habenulae are associated with asymmetries in the major efferent pathway from the dorsal diencephalon, the fasciculus retroflexus. Thus, in both the lamprey and the Siberian sturgeon, the larger right habenula is associated with a thicker right FR and in the sturgeon, right-sided axons are larger in calibre than those on the left (Adrio et al., 2000).

Asymmetries in myelination have also been described. For instance, in the cartilaginous fish *Scyllium stellare*, only the larger left habenula contains neurons extending myelinated axons (Miralto & Kemali, 1980; Kemali et al., 1980).

In addition to the asymmetrical subnuclear organisation of the dorsal habenula in *Rana esculenta*, Gugliemotti & Fiorino (1998) have described asymmetry in the routing of axons towards the IPN. On the left side, the lateral subnucleus of the dorsal habenula gives rise to a tract that follows a peripheral route through the thalamus, whereas neurons of the medial subnucleus project axons along a more medial trajectory, bordering the third ventricle. These two contingents of the FR merge before innervating the IPN. On the right side, medial and lateral tracts are also formed, but they both derive from the single dorsal subnucleus of the right habenula.

Pineal complex asymmetry

The pineal complex comprises the pineal, or epiphysis, and in some species a second nucleus, the parapineal. The pineal is likely to be present in all vertebrates and serves a neuroendocrine role, producing the hormone melatonin; in lower vertebrates it is a photoreceptive structure (Falcon, 1999; Concha & Wilson, 2001). The pineal does not display overt asymmetry, being located at the dorsal midline of the epithalamus (although subtle asymmetries have been described in the location of the pineal stalk, Liang et al., 2000).

A second photoreceptive structure, the parapineal, or parietal eye, may also evaginate from the diencephalic roof plate. A parapineal has been described in lampreys, teleosts and certain species of lizard, but has not been detected in amphibians, birds or mammals. The parapineal consistently displays asymmetric connectivity within the epithalamus, projecting efferent

axons that exclusively innervate the left habenula. In species of lizards possessing a parietal eye[6], efferent axons innervate a restricted region of the left medial habenula (pars dorsolateralis, Engbretson et al., 1981). In teleosts, parapineal axons terminate in a defined rostro-dorsal region of the left habenula; in the coho salmon, this terminal field may be coincident with the unilateral serotonergic subnucleus that is exclusively found in the left habenula (Ekstrom & Ebbesson, 1988; Concha & Wilson, 2001).

In lampreys and lizards the parapineal/parietal eye is located at the dorsal midline, but in teleosts it is asymmetric both in its connectivity and location, moving laterally to occupy a position adjacent to the left habenula on the left side of the midline.

It has been suggested that the presence of a parapineal nucleus and the development of habenular lateralisation might be causally associated (discussed in Engbretson et al., 1981; Harris et al., 1996; Concha & Wilson, 2001; Guglielmotti & Cristino, 2006). In species of lizard which possess a parietal eye, more pronounced asymmetries in habenular subnuclear organisation are apparent than in species of reptiles lacking a parietal eye. However, in the lamprey, although the parapineal innervates the left habenula, it is the right nucleus that is enlarged. Moreover, striking habenular asymmetries have been described in vertebrates which appear not to possess a parapineal (*eg* amphibians), questioning any link between asymmetry in the habenulae and pineal complex. As discussed is §1.3, recent work in zebrafish is helping to examine this relationship.

In summary, the epithalamus constitutes the epicentre of the dorsal diencephalic conduction system. This highly conserved circuit is involved in a diverse range of behaviours, which we are still only beginning to understand. Neural asymmetries are present in the epithalamus in many species and range from left–right differences in size to asymmetries in neurotransmitter expression and descending circuitry. Notably, in many cases lateralisation involves the specification of a unique feature on either the left or right side (*eg* the serotonergic subnucleus of the left habenula in the coho salmon, or

[6]The parietal eye is considered an equivalent of the parapineal but forms a more sophisticated photoreceptive organ than is found in lampreys and teleosts. Its structure resembles the lateral eyes and electrophysiological studies show it to be a fully functional photoreceptive organ; it emerges from a foramen in the skull.

the left-sided parapineal). This stands in contrast to lateralisation in some other regions of the brain, such as the cortex, where asymmetry appears to involve differences between comparable structures that are present bilaterally.

1.3 Zebrafish as a model for the development of brain asymmetry

In this section, I will review recent work in zebrafish which has provided the first insights into the genetic pathways and tissue interactions which mediate the development of brain asymmetry in vertebrates.

1.3.1 Directional asymmetry in the zebrafish dorsal diencephalon

The zebrafish dorsal diencephalon presents an excellent model for the study of neural lateralisation. Several prominent asymmetric phenotypes develop with high consistency and reliability during embryonic and larval stages, suggesting that they are under substantial genetic control. Moreover, because these phenotypes show population laterality, the zebrafish dorsal diencephalon provides an opportunity to determine whether, in the vertebrate CNS, the same molecular-genetic mechanism(s) both establish asymmetry and determine its laterality, or whether there are independent pathways for these two aspects of lateralisation.

Pineal complex As in other teleosts, the zebrafish possesses two photoreceptive nuclei in the epithalamus, the pineal and parapineal, both of which derive from the same embryonic anlage in the dorsalmost region of the dorsal diencephalon (Concha et al., 2003). The pineal evaginates from the dorsal midline to form a photoreceptive vesicle connected to the brain by the pineal stalk. Although the pineal is largely symmetric, subtle asymmetry has been described in the location of the base of the stalk, which shows a modest bias towards the left side of the midline (Liang et al., 2000). By contrast, the parapineal displays conspicuous asymmetry, being exclusively located on the left (Concha et al., 2000). However, fate mapping experiments have

revealed that the parapineal has a bilateral origin (Concha et al., 2003). Parapineal precursors derive from the rostral end of the pineal/parapineal anlage on both left and right sides of the midline. At around 24–28 hpf they condense to form a morphologically distinct nucleus which then commences leftwards migration from approximately 30 hpf. The parapineal proceeds in an arc, initially migrating laterally, away from the midline, but at later stages returning medially, such that by 4 dpf it comes to rest on the left side of the pineal stalk (Concha et al., 2003). During the course of migration, the parapineal contemporaneously extends efferent axons, beginning at around 50 hpf, which innervate a restricted dorsomedial subregion of the left habenula. Thus, both in its location and connectivity, the parapineal is asymmetric.

Habenulae The habenulae display both neuroanatomical and molecular lateralisation. Although the left habenula is only modestly larger (~15–20% at 4 dpf, Halpern et al., 2003) in overall size than the right nucleus, it displays a greater density of neuropil, predominantly in the same dorsomedial region that receives parapineal innervation (Concha et al., 2000, 2003). This asymmetry in neuropil organisation is first evident at around 70 hpf and increases in magnitude until around 4 dpf.

In addition, several molecular asymmetries differentiate the left and right habenulae. Especially notable are the related genes *leftover (lov)*, *right-on (ron)* and *dexter (dex)* which are members of the potassium channel tetramerisation domain containing (KCTD) family. Whilst *lov* is expressed at higher levels and in more cells in the left habenula (Figure 2.1B), *ron* and *dex* are expressed more broadly on the right (Gamse et al., 2005). Molecular asymmetry emerges before the development of neuroanatomical lateralisation. Expression of *lov* begins in the left habenula at around 38 hpf, in very close proximity to the migrating parapineal, before spreading through a larger domain on the left; asymmetric expression is retained into adult stages (Gamse et al., 2003). *ron* and *dex* expression begins later, at around 2 dpf and is also lateralised from the outset.

In summary, the zebrafish dorsal diencephalon displays a number of morphological and molecular asymmetries by larval stages. These asymmetries

display very strong population laterality: in over 95% of fry the parapineal migrates to the left and the left habenula displays a greater density of neuropil and elevated expression of *lov*; the laterality of these asymmetries is reversed in only 5% or less of wild-type (WT) embryos/larvae (Concha et al., 2000; Gamse et al., 2003).

1.3.2 Specification of laterality by Nodal signalling

The observation that genes encoding components of the Nodal signalling pathway (summarised in Figure 1.3) are expressed asymmetrically in the dorsal diencephalon during embryogenesis led to the finding that this signalling pathway specifies the laterality of neural asymmetries.

The secreted transforming growth factor-β family member Nodal plays an evolutionarily conserved role in the development of asymmetries in the viscera (reviewed in Raya & Belmonte, 2006). Although the details of the initial symmetry breaking event may vary in different species, there appears to be a conserved role for the embryonic node, the midline and left-sided activation of the Nodal pathway in the establishment of left–right identity in the body. Indeed, the Nodal pathway is activated unilaterally in the left lateral plate mesoderm (LPM) in all vertebrates. In the predominant model, after specification of the AP and dorso-ventral (DV) axes, chiral rotation of monocilia in the node in mouse (or Kuppfer's vesicle in zebrafish) establishes a "nodal flow" that is transduced into asymmetric induction of *nodal* expression on the left. Expression of *nodal* spreads rapidly throughout the left LPM by a reaction–diffusion mechanism and is prevented from spreading to the right side of the body by midline barriers (see Tabin, 2006). Transient Nodal signalling induces more long-lived left-sided expression of the homeodomain transcription factor-encoding gene *pitx2*, which influences the asymmetric positioning and morphogenesis of the heart and visceral organs.

Nodal-related genes are expressed asymmetrically in the zebrafish dorsal diencephalon during midsomitogenesis (Sampath et al., 1998; Concha et al., 2000; Liang et al., 2000). Between 18 and 22 hpf, the Nodal-related gene *cyclops (cyc)*, the Nodal antagonist-encoding gene *lefty1* and *pitx2*, which encodes a downstream transcriptional effector of Nodal signalling, are expressed exclusively on the left side of the epithalamus in a region that is likely to contain precursors of both the pineal complex and left habenula (Concha

Figure 1.3: **The Nodal signalling pathway.** Nodal ligands operate through an Activin-like pathway wherein they bind to Type II Ser/Thr kinase receptors which activate Type I Activin-like receptors which in turn phosphorylate Smad2. Smad2 forms a nuclear complex with Smad4 and members of the FAST family of forkhead domain transcription factors to regulate expression of downstream genes such as *pitx2*. EGF-CFC proteins, including zebrafish One-eyed pinhead, are membrane-tethered cofactors that are essential for cells to respond to Nodal signals. By contrast, Lefty TGF-β molecules act as antagonists of Nodal signalling, possibly by competing for binding to Type II Activin-like receptors. Nodal signalling induces *lefty* expression, establishing a negative feedback loop that attenuates Nodal signalling and renders it transient.
Adapted from Schier & Shen (2000). Names of Nodal pathway components expressed in the zebrafish epithalamus are shown in italics.

et al., 2003). The essential EGF-CFC signalling cofactor One-eyed pinhead and the Fast1 forkhead transcription factor and effector of Nodal signalling, Schmalspur, are expressed bilaterally. Hence, during a brief temporal window that precedes the development of asymmetric phenotypes, the Nodal signalling pathway is activated unilaterally in the left dorsal diencephalon.

The functional importance of the Nodal pathway was assessed in mutant and morphant[7] embryos with disrupted Nodal signalling (Figure 1.4). Injection of wild-type *oep* RNA into maternal–zygotic *oep*$^{-/-}$ embryos at the one-cell stage, provides sufficient Oep protein to rescue early, but not late Nodal signalling. The resultant late-zygotic *oep*$^{-/-}$ (LZ*oep*$^{-/-}$) embryos show normal midline development and are viable, but because they lack later Oep activity, Nodal signalling is absent from the epithalamus. Despite the loss of asymmetric Nodal pathway activity, LZ*oep*$^{-/-}$ larvae establish epithalamic asymmetries, including unilateral migration of the parapineal and asymmetric development of habenular neuropil and expression of *lov*. However, the laterality of these asymmetries is randomised (Concha et al., 2000; Gamse et al., 2003). Whilst in 50% of LZ*oep*$^{-/-}$ larvae asymmetries develop with normal leftwards laterality, in the other 50% of larvae, the parapineal migrates to the right along with a corresponding reversal in habenular asymmetries. *No tail* (*ntl*)[8] mutant and morphant larvae present the opposite scenario; the Nodal pathway genes *cyc* and *pitx2* are induced on both sides of the epithalamus, probably due to disrupted development of the midline, which is required to restrict the expression of Nodal pathway genes to the left diencephalon (Concha et al., 2000). However, as in LZ*oep*$^{-/-}$ larvae, heterotaxic randomisation is observed: apparently normal left and right-characteristic identities develop, but with randomised laterality. These results indicate that left-sided Nodal signalling is neither necessary nor sufficient to direct the development of left identity and it is also not necessary for epithalamic asymmetry. Rather, the function of unilateral Nodal activity appears to be to bias the direction, or *laterality*, of neural asymmetries consistently in one direction.

[7]Morphant embryos/larvae are generated by injecting early stage embryos with morpholino-modified antisense oligonucleotides, which abrogate the expression of selected genes by pairing to complementary sequences in transcripts and so blocking their translation or splicing.

[8]*no tail* is the zebrafish homologue of the mouse *T (Brachyury)* gene (Schulte-Merker et al., 1994)

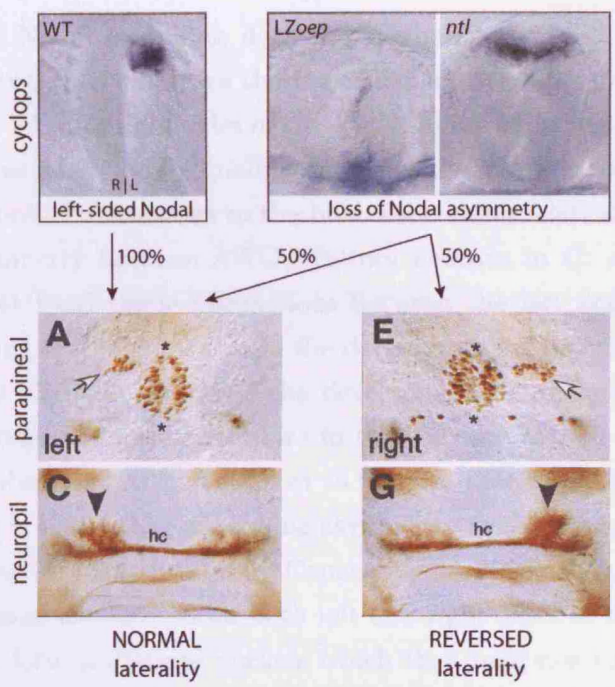

Figure 1.4: **Nodal signalling specifies the laterality of epithalamic asymmetries.** *Top*: Transverse frontal views showing *cyc* expression in the dorsal diencephalon of 22 hpf wild-type and mutant embryos. Nodal signalling is activated unilaterally, on the left side in WT embryos, but is absent in LZ*oep*$^{-/-}$ mutants and bilaterally symmetric in *ntl*$^{-/-}$ mutants (or morphants). *Bottom*: Dorsal views of the epithalamus labelled with anti-Islet antibody to visualise pineal and parapineal cells (white arrows) or anti-acetylated α tubulin antibody to visualise habenular neuropil. WT embryos almost always show leftwards migration of the parapineal and develop increased neuropil density in the left habenula (indicated by black arrowhead). In both LZ*oep*$^{-/-}$ and *ntl*$^{-/-}$ mutants, where lateralised Nodal signalling is absent, asymmetry continues to develop in the dorsal diencephalon, but with randomised laterality. Thus, ~50% of embryos develop with normal laterality (left panels), whereas parapineal position and habenular neuroanatomy are concordantly reversed in the other ~50% (right panels). Data adapted from Concha et al. (2000).

In summary, leftwards population laterality in the dorsal diencephalon is dependent upon asymmetric activation of the Nodal signalling pathway.

1.3.3 Symmetry breaking in the dorsal diencephalon

If unilateral Nodal signalling does not mediate the development of neural asymmetry, then what are the molecular and cellular mechanisms that result in the left and right sides of the epithalamus adopting distinct phenotypes and how does Nodal signalling influence the laterality of the symmetry breaking process? Analogous to the bilateral communication thought to establish asymmetry between AWC olfactory neurons in *C. elegans*, there is evidence that local tissue interactions between the left and right sides of the developing epithalamus ensure the development of asymmetry and that bidirectional signalling between the developing habenulae and parapineal act to coordinate laterality decisions in these structures.

Several observations lend support to the idea that migration of the parapineal organ is central to establishing asymmetry in the dorsal diencephalon. Firstly, lineage tracing studies by Concha et al. (2003) showed that parapineal precursors are located on both left and right sides of the midline and condense to form a discrete nucleus which then migrates towards the left. However, in situations where Nodal signalling is disrupted, we have seen that the parapineal migrates to either the left or right sides with equal tendency. Because splitting of the parapineal is almost never observed (~0.3% of wild-type embryos, Gamse et al., 2003), the bilateral origin and subsequent unilateral migration will, by definition, break symmetry in the dorsal diencephalon. Secondly, parapineal migration precedes the development of lateralised characteristics of the habenulae. *lov* expression begins at around 38 hpf and is initially induced in close proximity to the migrating parapineal (Gamse et al., 2003) and elaboration of parapineal efferent axons within the left habenula is synchronised in time and space with the development of asymmetric habenular neuropil (Concha et al., 2003). These observations have led to the suggestion that the parapineal might instruct the development of left habenular identity.

However, experimental studies in which parapineal precursors are eliminated by laser-ablation, have led to conflicting conclusions regarding the functional importance of the parapineal. Gamse et al. (2003) claim that

parapineal-ablation abolishes habenular asymmetry and both left and right nuclei show the reduced levels of neuropil and *lov* expression characteristic of the right habenula. These authors have suggested that asymmetry arises as a step-wise process in the epithalamus: first the parapineal migrates unilaterally and secondly, it signals to the adjacent habenular nucleus to promote the development of left identity. In this model, right-sided characteristics develop as a default state in the habenular not associated with the parapineal. However, in a separate study, Concha et al. (2003) have reported that although the magnitude of the asymmetries is reduced following parapineal ablation, left–right differences in gene expression and neuropil organisation are still apparent. Thus, these authors suggest the parapineal is not involved in the initial establishment of left–right identity but rather acts to reinforce lateralised phenotypes.

Laser-ablation experiments have demonstrated a role for habenular precursors in establishing the laterality of both parapineal and habenular asymmetries (Concha et al., 2003). Habenular precursors are located in the ventral epithalamus, directly adjacent to the developing pineal complex in the dorsal epithalamus, and ablation of these ventral cells (at 22–24 hpf) affects both migration/connectivity of the parapineal as well as habenular lateralisation. Thus, ablation of left habenular precursors in wild-type embryos frequently results in rightwards migration and connectivity of the parapineal (~40%) and the right habenula developing patterns of gene expression and neuropil density characteristic of the left nucleus. Moreover, such ablations can impose laterality in LZ*oep*$^{-/-}$ and *ntl*-morphant (*ntl*-MO) embryos, which usually display heterotaxic randomisation (see §1.3.2). For instance, ablation of right-sided ventral epithalamic cells in LZ*oep*$^{-/-}$ embryos results in leftwards migration of the parapineal and the left habenula developing left-characteristics (74%).

On the basis of these results and the fact that experimentally manipulated and mutant embryos almost never display symmetry in the epithalamus, Concha et al. (2003) have proposed a mutual inhibition model for the development of asymmetry in the dorsal diencephalon (see Figure 1.5). In this model, the left and right sides "compete" for left identity by producing signals which inhibit the ability of the contralateral side to assume left-sided character. Although the molecular or cellular nature of this communication

Figure 1.5: **Development of asymmetry in the dorsal diencephalon.**
(A) Schematic illustrating the development of concordant epithalamic asymmetries. The earliest known asymmetry is the activation of Nodal signalling on the left side of the brain (*cyc*, crosshatching), encompassing both parapineal (yellow) and habenular (pink) precursors. Subsequently, parapineal cells aggregate and migrate leftwards, dependent upon left-sided habenular precursors. At later stages the parapineal innervates the left habenula and influences its gene expression. These reciprocal interactions ensure concordance of lateralised phenotypes between the habenulae and parapineal.
(B) Mutual inhibition model for symmetry breaking in the CNS. The left and right epithalamus are thought to produce antagonistic signals that inhibit the contralateral side from acquiring left identity. (B*i*) In WT embryos, left sided Nodal biases the competition such that the left side consistently "wins". (B*ii*) In LZ*oep*$^{-/-}$ mutants, an absence of Nodal signalling means the competition is initially equal and the outcome is stochastic. (B*iii*) A similar stochastic outcome occurs in *ntl*-MO embryos where Nodal provides an equal boost to both sides. (B*iv*) Ablation of left habenular precursors in WT embryos abrogates the advantage of the left side and results in a high frequency of laterality reversals. (B*v*) Ablation of right-sided ventral epithalamic cells in LZ*oep*$^{-/-}$ restores a leftwards advantage to the competition and consequently the left side consistently wins. (B*vi*) In embryos with bilateral Nodal activity, either ablation of right habenular precursors or inhibition of Nodal signalling by exogenous Lefty1 on the right, restores the advantage to the left epithalamus resulting in consistent leftwards laterality.
Adapted from Concha et al. (2003).

is unknown, it has been suggested that these inhibitory signals act across the dorsal midline. This mechanism ensures a coordinated decision whereby only one side can develop as "left" and the other is prevented from doing so. The function of left-sided Nodal signalling is to bias this competition from the start, so that in wild-type embryos, the left side consistently "wins", resulting in leftwards population laterality. In LZ*oep*$^{-/-}$ and *ntl*-MO embryos, the asymmetric Nodal bias is lost; consequently, the outcome of the competition is stochastic and in half of the embryos the right side will "win" resulting in the reversal of asymmetry phenotypes. Strong evidence for a direct role of epithalamic Nodal signalling in the development of neural lateralisation comes from an experiment in which plasmid DNA encoding the the Nodal antagonist Lefty1 was introduced into the right epithalamus of *ntl*-MO embryos by focal electroporation. The parapineal consistently migrated to the contralateral (left) side, demonstrating that the *local* inhibition of Nodal signalling inhibits the acquisition of left identity (Concha et al., 2003).

Overall, the ablation data suggest that the initial symmetry breaking event involves mutual inhibition mediated by habenular precursors. The side which is successful in acquiring left identity would then attract the parapineal and bidirectional signalling between the parapineal and the adjacent habenula appears to stabilise and strengthen left-sided character.

In summary, current data suggest that asymmetry is established in the zebrafish dorsal diencephalon as a result of competitive interactions between the left and right sides and reciprocal signalling between the developing habenulae and parapineal ensures coordination and robustness of different lateralised phenotypes.

1.3.4 Behavioural asymmetry in zebrafish

In addition to providing a model for the molecular and cellular mechanisms underlying the development of brain lateralisation, zebrafish provides an opportunity to correlate anatomical asymmetries in the CNS with animal behaviour.

Zebrafish display behavioural asymmetries in the form of biased turning direction and differential eye use for particular viewing tasks. This visual system lateralisation takes a similar form to that in tetrapods where the

right eye is used for examining complex or novel scenes and the left eye is used for viewing familiar objects (Miklosi et al., 1997; Miklosi & Andrew, 1999). Moreover, a number of behavioural asymmetries are already apparent at larval stages (Watkins et al., 2004; Barth et al., 2005).

Barth et al. (2005) examined both lateralised and non-lateralised behaviours in larvae and adults of the *frequent situs inversus (fsi)* line, in which a high frequency of fish show concordant reversals in the laterality of both visceral (heart, pancreas, gut) and epithalamic asymmetries. Whilst some asymmetric behaviours, including the pattern of left and right eye use in a mirror viewing task, are reversed in *fsi* fish with anatomical reversals, other lateralised behaviours do not reverse. Moreover, a novel, non-lateralised behaviour was observed in anatomically reversed larvae that is not apparent in normally lateralised *fsi* fish or wild-types. These results suggest there are multiple pathways specifying brain laterality, at least one of which is not concordant with visceral laterality and not affected in *fsi*. The emergence of novel behaviours might be a consequence of the erroneous superposition (or separation) of neural processing functions arising from reversals of a sub-set of neural asymmetries.

Whilst the function of epithalamic asymmetry is unknown (in any species), because the laterality of certain asymmetric behaviours correlates with epithalamic laterality, these behaviours may be regulated by the asymmetric circuitry of the dorsal diencephalon. Alternatively, they might be under the control of other asymmetric neural substrate, the laterality of which is coupled to the laterality of the epithalamus.

In summary, behavioural studies in zebrafish are starting to reveal a new level of complexity in the regulation of neural asymmetries and suggest that multiple, independent pathways are likely to determine laterality. Zebrafish present an attractive model in which to identify these pathways and experimentally manipulate lateralised circuits to directly assess their functional relevance.

1.4 Aims and scope of this thesis

To understand the basis for functional lateralisation of the brain, it is necessary to relate neural asymmetry at different levels of brain organisation

and function. The aim of such an integrative approach is to combine cognitive and behavioural analysis, physiological studies of network activity, cell–anatomical descriptions of cytoarchitecture and circuit organisation and finally the morphological and molecular–genetic phenotypes of individual neurons. As discussed in this Chapter, progress has been made in describing neural lateralisation at each of these levels, but few studies have attempted to elucidate causative relationships that span across the different levels in this hierarchy.

Because zebrafish is amenable to a wide variety of experimental approaches, it represents an excellent model in which to study the nervous system at these different levels (Concha, 2004). As described in §1.3, recent work in zebrafish has identified neural asymmetry at the level of cellular and genetic phenotypes, begun to uncover the developmental mechanisms by which such asymmetries arise and demonstrated the potential to associate structural asymmetries with lateralised behaviours.

Three major areas have yet to be addressed. The first challenge is to identify neural lateralisation in the architecture of functional circuits, secondly, physiological analyses are required to identify asymmetries in neural processing activity and finally, the organisation and function of these circuits must be experimentally manipulated to establish causal relationships with behavioural outputs.

In this thesis I attempt to address the first of these aims. I identify lateralisation in the efferent circuitry of the dorsal diencephalon and show that the laterality of this connectional asymmetry is controlled by Nodal signalling. By examining the morphology and connectivity of individual projection neurons I identify a strategy used to achieve lateralisation in this circuit wherein the same neuronal sub-types are produced on both sides of the brain, but in different ratios. Finally, I extend our understanding of the role of the parapineal in controlling asymmetry phenotypes in the habenulo-interpeduncular system.

Chapter 2

Laterotopic Habenular Efferent Circuitry

2.1 Lateralisation of the larval zebrafish dorsal diencephalon

By larval stages, both molecular and neuroanatomical asymmetries are evident in the zebrafish epithalamus (Figure 2.1 and Gamse et al., 2005, 2003; Concha et al., 2003, 2000; Liang et al., 2000). The most conspicuous neuroanatomical asymmetry is the migration of the parapineal nucleus to the left side of the brain. Not only are parapineal neurons unilaterally located but they also establish efferent connectivity exclusively with the left habenula. The habenulae are asymmetric with respect to the organisation of their neuropil and the expression of several genes, including *lov*.

2.2 Labelling the habenulo-interpeduncular projection using lipophilic tracer dyes

The molecular and neuroanatomical differences between the left and right habenulae suggest they have distinct neural functions. However, both nuclei project to the IPN, an unpaired midline nucleus in the ventral midbrain. How is left and right information handled at the target? One possibility is that the circuit becomes symmetric, wherein the IPN integrates afferent inputs from the two sides and there is no further lateralisation in down-

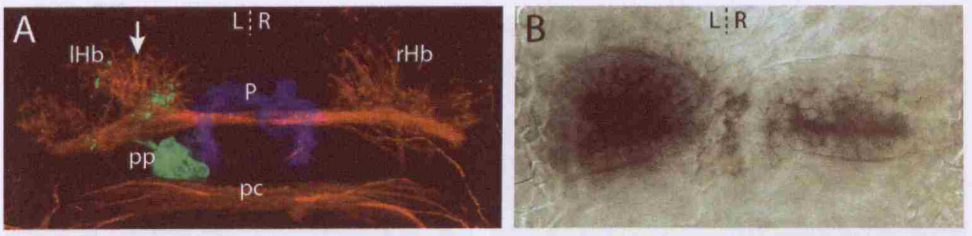

Figure 2.1: **Asymmetries in the larval zebrafish epithalamus**
(A) Confocal projection of the dorsal diencephalon of a 4 dpf Tg(*foxD3*:GFP) transgenic zebrafish. GFP expression labels the pineal complex (parapineal in green and pineal in blue) and neuropil is visualised by anti-acetylated α tubulin immunostaining (red). The left habenula possesses a dorsomedial domain of dense neuropil (arrow) not visible on the right. This neuropil domain is predominantly innervated by efferent axons from the left-sided parapineal. (B) *Leftover* expression in the dorsal diencephalon of a 4 dpf larva reveals more extensive and stronger expression on the left. Images are dorsal views, anterior top. Abbreviations: Hb, habenula; pp, parapineal; P, pineal; pc, posterior commissure; l, left; r, right.

stream processing. Alternatively, the habenulae might differ in their target connectivity such that distinct circuits, with different left–right origins are maintained, despite convergence upon a unilateral nucleus.

To investigate this question, I used lipophilic dye tracing to differentially label left and right habenular efferent axons in intact larval brains and subsequently examined the pattern of axonal connectivity by confocal microscopy.

Lipophilic carbocyanine dyes efficiently labelled the habenulo-interpeduncular projection (Figure 2.2). Habenular axons descend in the fasciculus retroflexus (FR) which follows a caudal and medial trajectory towards the ventral midline of the posterior mesencephalon/anterior hindbrain. At the level of the oculomotor nucleus, the tract splits into two contingents. The majority of axons continue medially to innervate the IPN, terminating on both sides of the midline with a doughnut-shaped innervation pattern. The second contingent of axons passes around the IPN and terminates just caudal to it, again on both sides of the midline, in a ladder-shaped pattern. Anti-5HT immunostaining indicated that this latter termination site coincides with the rostral subdivision of the serotonergic raphé nucleus (Figure 2.2C and Teraoka et al., 2004).

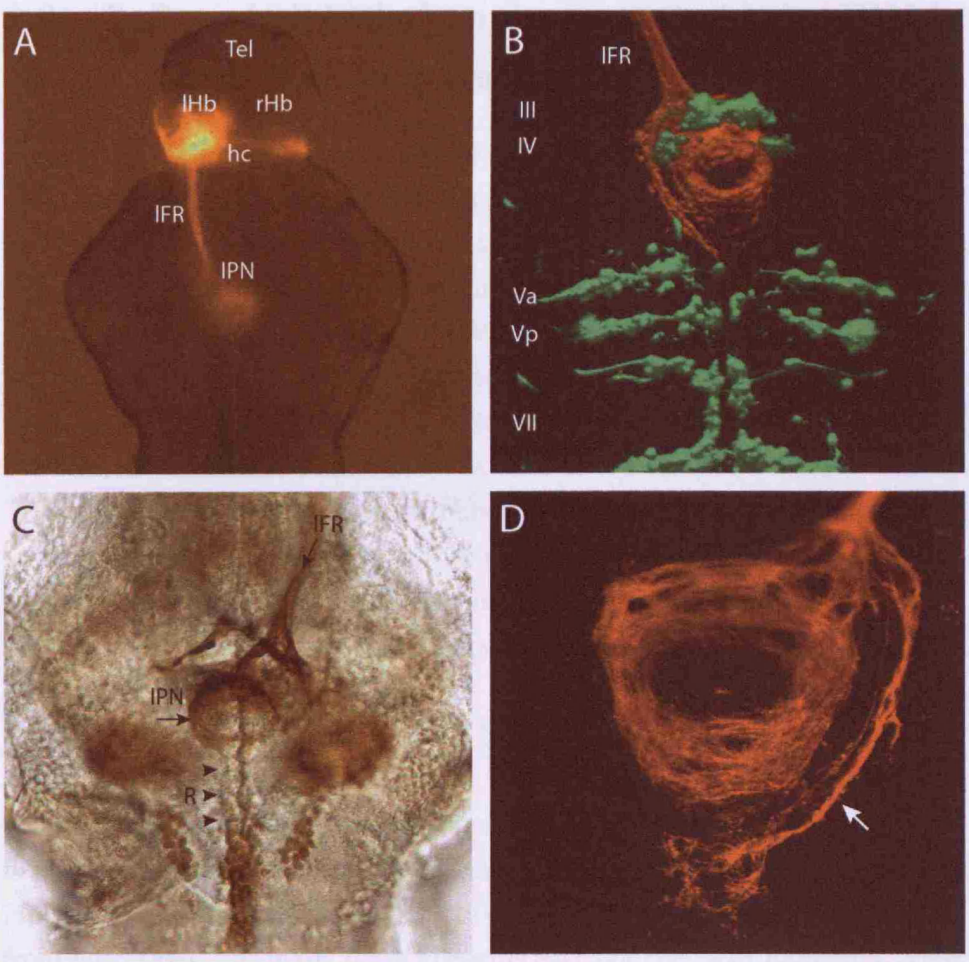

Figure 2.2: **Labelling the habenulo-interpeduncular projection using carbocyanine dyes.**
(A) Epifluorescence image of a dissected 4 dpf larval brain in which the left habenulo-interpeduncular tract has been labelled by application of DiI to the left habenula. Axons traversing the habenular commissure have also been labelled, some of which terminate in the right habenula (Hendricks & Jesuthasan, 2007). However, no labelling of the contralateral FR is observed. (B) 3D confocal reconstruction of the posterior midbrain/anterior hindbrain of a 4 dpf Tg(*islet1*:GFP) larva. Left habenular axons have been labelled using DiI (red) and GFP labels the cranial motor nuclei (green). The IPN lies caudal to the oculomotor nucleus (III) and anterior to the trigeminal motor nucleus (V). (C) Ventral view of a 4 dpf larval brain in which left habenular axons are labelled with photoconverted DiI (arrows) and the serotonergic raphé has been labelled using an anti-5HT polyclonal antibody (brown, arrowheads). (D) Confocal projection showing right habenular axon terminals labelled with DiI. The contingent of habenular axons which pass around the IPN (arrow) terminate with a ladder-shaped pattern in a midline location that is coincident with the anterior region of the raphé. All panels except (C) are dorsal views, anterior top. Abbreviations: R, raphé.

2.3 Left and right habenulae innervate the IPN in a *laterotopic* manner

The use of different coloured dyes to explicitly and differentially label left and right habenular axons revealed a striking asymmetry in the pattern of innervation of the IPN. Left and right-sided axons are segregated along the DV axis of the IPN such that the majority of left-sided axons terminate in a dorsal subdomain whereas almost all right-sided axons target the ventral IPN (Figure 2.3). Because axons from the left and right sides of the brain show topographic mapping onto the IPN target, we have described the habenular efferent connectivity pattern as *laterotopic*.

To determine the location of habenular axon terminals in the IPN, I unilaterally labelled either the left *or* right habenula and subsequently photoconverted the fluorescent tract tracing and performed histological sectioning (Figure 2.4A,B). In a second experiment, both left *and* right habenular axons were labelled with different coloured dyes in the Tg(*h2afz*–GFP) transgenic line in which all cells can be visualised by nuclear expression of a histone–GFP fusion protein (Figure 2.4C). These analyses reveal the IPN contains morphologically distinct dorsal and ventral subdomains and confirm that the dorsal IPN (dIPN) receives almost exclusively left habenular innervation whereas the ventral IPN (vIPN) receives significant innervation from both sides, but many more fibres derive from the right habenula. Most IPN cell bodies are located within a midline "core" of the nucleus and are surrounded by the afferent axon terminals. In the ventral region, the axons surround the central core, in an arrangement reminiscent of an electromagnetic coil. In the dorsal arborisation territory, left-sided axons surround and cover the dIPN neurons like a hat.

2.4 Developmental timecourse of *laterotopic* connectivity

To examine the development of asymmetric habenulo-interpeduncular connectivity, I performed dye tracing in embryos and larvae that were fixed at 2 h intervals between 48 and 72 hpf.

At 48 hpf, no innervation of the IPN is apparent. However, by this stage

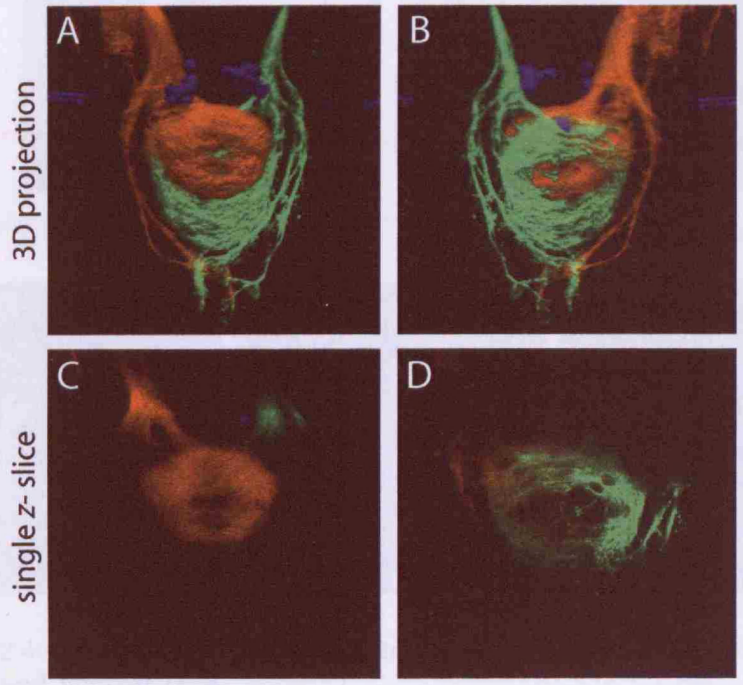

Figure 2.3: ***Laterotopic* habenulo-interpeduncular connectivity.**
(A-D) Confocal images of the ventral midbrain of a 4 dpf Tg(*foxD3*:GFP) larva in which left habenular axons have been labelled with DiD (red) and right habenular axons with DiI (green). The oculomotor nucleus is labelled by GFP expression (blue) in this transgenic line. (A,B) 3D reconstructions from either the dorsal (A), or ventral (B) aspect. (C,D) Single confocal z-slices through either the dorsal (C), or ventral (D) IPN. Left-sided axons preferentially terminate in the dorsal IPN whereas almost all right-sided axons target the ventral IPN. All images: anterior top.

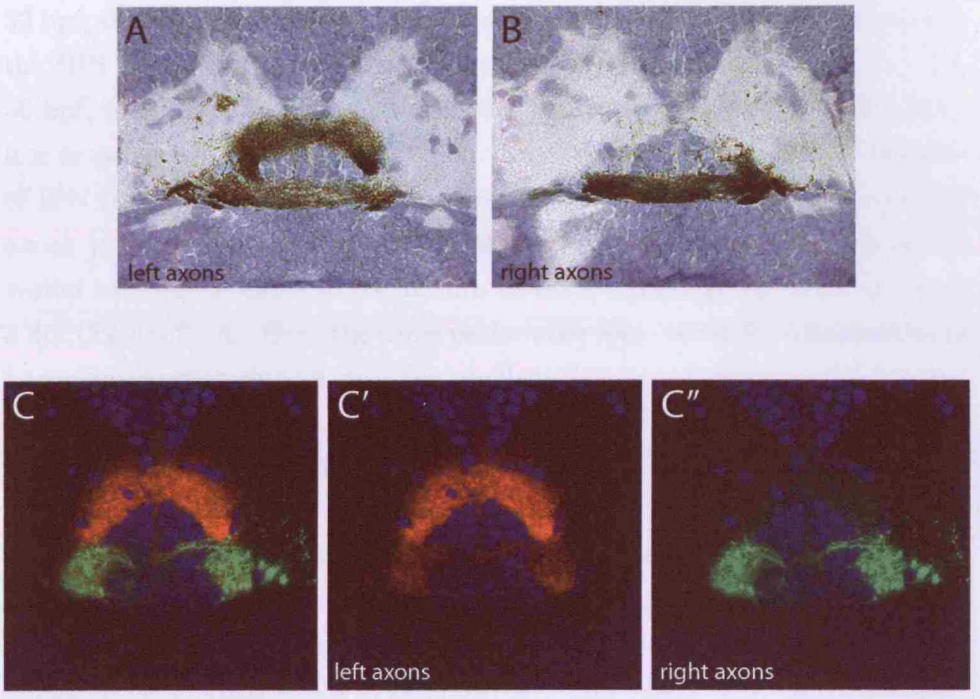

Figure 2.4: **Localisation of left and right habenular axon terminals to the dorsal and ventral IPN.**
(A,B) Transverse histological sections through the brains of 4 dpf larvae in which either the left (A) or right (B) habenulo-interpeduncular tract was labelled with photoconverted DiI. (C–C") A single confocal *z*-slice, in transverse orientation, through the IPN of a 4 dpf Tg(*h2afz*–GFP) larva in which all cell nuclei are labelled by GFP expression (blue). The IPN displays clear dorsal and ventral as well as left and right subdivisions. Left habenular axons are labelled with DiD (red) and right-sided axons with DiI (green). (C') shows only left-sided axons (red and blue channels only) whereas (C") shows only right-sided axon terminals (green and blue channels only). Left habenular axons predominantly innervate the dIPN and make less substantial projections to the ventral target. These axons surround and cover the dIPN like a hat. Almost all right-sided axons innervate the vIPN where they surround the centrally-located cell bodies in a manner reminiscent of an electromagnetic coil. All images: dorsal, top.

habenular axons have already extended a considerable distance past the target, well into the ventral hindbrain. Both left and right-sided tracts bifurcate and cross the ventral midline at a location anterior to the IPN, before continuing caudally on both ipsilateral and contralateral sides of the brain. From 52 hpf, short axonal processes can be observed, which are orientated towards the IPN region and derive from the major caudally-directed fascicles. By 56 hpf, these processes have reached the IPN and established the first midline crossing within the target region. Over the next few hours the density of IPN innervation gradually increases: from 62 hpf, I consistently observe axons to have surrounded the central "core" and subsequently the innervation pattern develops to its mature larval morphology by approximately 3 dpf (Figure 2.5A). Over the same period, the long, caudally-directed tracts become progressively less strongly labelled; they are scarcely visible beyond 70 hpf.

Do left and right axons show differential connectivity from the outset, or do they initially show symmetric targeting with a subsequent phase of remodelling? To answer this question, I examined the relative DV locations of axon terminals in confocal z-stacks and 3D reconstructions. At 60 hpf, when axons first arborise within the IPN, left habenular arbors are already located dorsal to right-sided axons (7/9 embryos). Moreover, there is consistently more left-derived innervation apparent at these early stages (Figure 2.5B). Therefore, the left habenula appears to innervate the target earlier than the right nucleus and asymmetric DV targeting is evident from the the earliest stages of IPN connectivity. I did not observe any asymmetries in the caudally-directed tracts that extend into the hindbrain at early stages and axons from the left and right sides appear to cross the midline at the same DV level within the decussation anterior to the IPN.

2.5 *Laterotopic* habenular efferent connectivity is conserved in two other teleost species

Is *laterotopic* habenulo-interpeduncular connectivity unique to zebrafish, or is it conserved in other species?

I have begun to address this question by examining the pattern of habenular efferent circuitry in two other teleosts species, *Astyanax* and medaka,

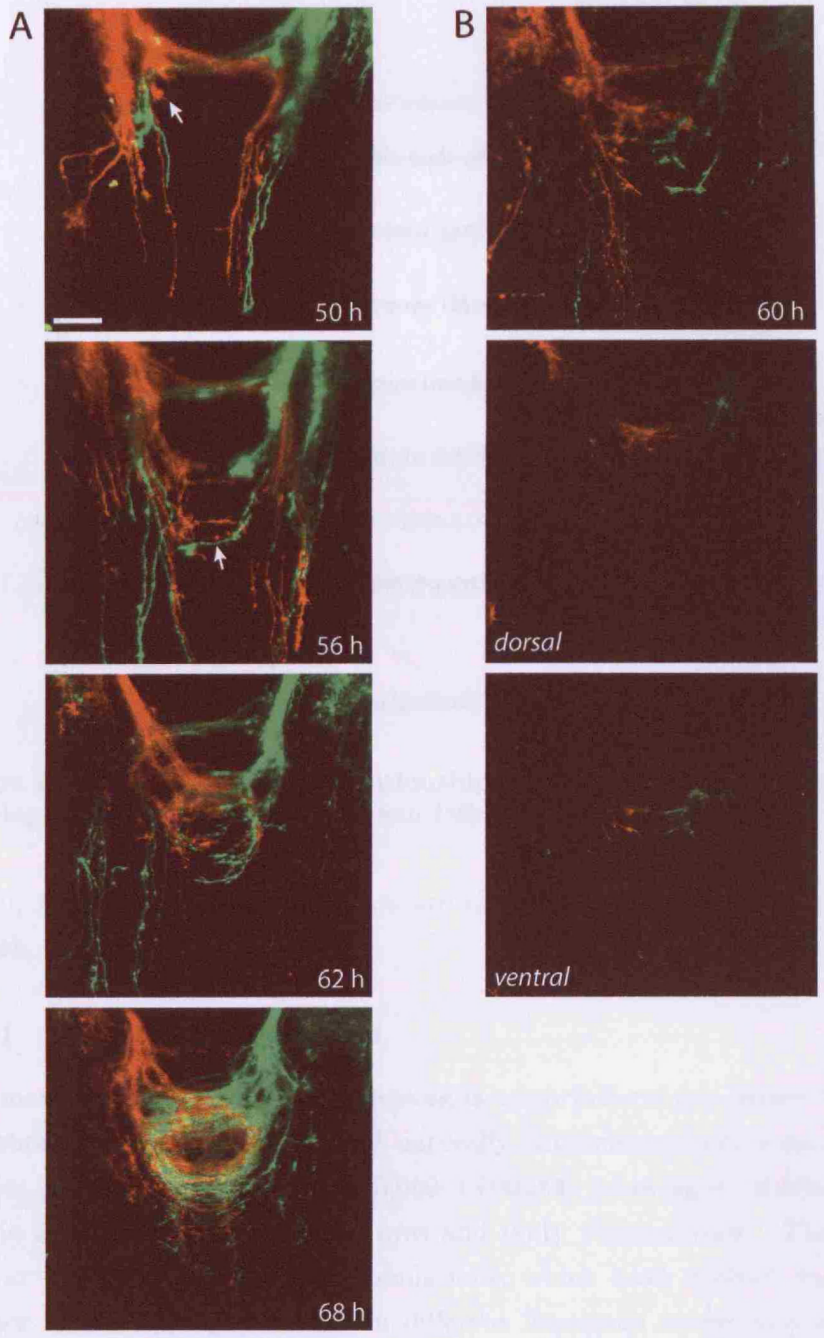

Figure 2.5: **Developmental timecourse of habenulo-interpeduncular connectivity** (A) Confocal maximum-intensity projections at the indicated timepoints between 50 and 68 hpf, showing left (red) and right (green) habenular axons in and around the IPN. The arrow at 50 hpf indicates an axonal process orientated towards the IPN target. The arrow at 56 hpf shows an early example of habenular axons crossing the midline at the IPN. (B) IPN innervation at 60 hpf. Confocal maximum-intensity projection (top) and single z-slices at a dorsal (middle) or ventral (bottom) level. At this early stage of IPN innervation, left-sided axons terminate dorsal to right-sided axons. Scale bar: 30 μm.

Figure 2.6: **The phylogenetic relationships of teleosts commonly used in developmental biology.** Adapted from Jeffery (2001).

which, within the teleost infraclass are closely or distantly related to zebrafish, respectively.

2.5.1 *Astyanax mexicanus*

The mexican tetra, *Astyanax mexicanus*, is a cypriniform fish closely related to zebrafish (Figure 2.6). Several naturally occurring populations of this species have diverged recently (10,000–1,000,000 years ago). Surface fish live in surface streams and have eyes and body pigmentation. There are also at least 29 blind cavefish populations, which have evolved from the surface fish and adapted to life in different limestone caves; they display various degrees of eye degeneration and loss of body pigmentation as well as a variety of other regressive and constructive adaptive changes (Jeffery, 2001).

I have examined habenular neuropil density and efferent connectivity in larvae from surface fish as well as from blind cavefish derived from the "Tinaja" cave. Whilst habenular neuropil appears bilaterally symmetric in *Astyanax* (5.5–6.5 dpf, n=8, Figure 2.7C), I find that both surface fish

(5–6.5 dpf, n=10) and Tinaja cavefish (5 dpf, n=8) possess *laterotopic* habenular efferent circuitry. Left and right-sided axons are segregated along the DV axis of the IPN and moreover, the laterality is the same as I observed in larval zebrafish (Figure 2.7D,E): Left-sided axons terminate predominantly in the dIPN with lesser innervation of the vIPN, whereas right-sided axons almost exclusively project ventrally.

2.5.2 Medaka

Medaka, *Oryzias latipes*, is a teleost more distantly related to zebrafish, as these species separated from their last common ancestor ~110 million years ago (Figure 2.6).

In two strains of medaka, Cab (a northern strain) and Kaga (a southern strain), I have observed very striking *laterotopic* habenular efferent connectivity (Cab: 7 dpf, n=6; Kaga: 8 dpf, n=5; Figure 2.8). Left and right-sided habenular axons display *complete* DV segregation within the IPN: Left-sided axons are exclusively localised to the dIPN with no innervation of the ventral target, which is exclusively occupied by right-sided axons.

2.6 Discussion

2.6.1 The left and right habenulae display asymmetric efferent circuitry

My results reveal that within the habenulo-interpeduncular tract there is prominent and stereotypical connectional asymmetry whereby left and right-sided inputs are mapped in a *laterotopic* manner along the DV axis of the IPN. This finding represents one of the first descriptions of asymmetry at the level of axonal connectivity in the vertebrate brain.

In terms of neural processing, the segregation of habenular inputs at their midline target provides a simple and elegant way for circuits on the left and right sides of the brain to differentially control bilaterally symmetric downstream pathways. Therefore, although each habenula nucleus appears to innervate both sides of the target, the transformation of left–right segregation to dorso–ventral segregation potentially allows for distinct "left-derived" and "right-derived" circuits to be maintained downstream of the

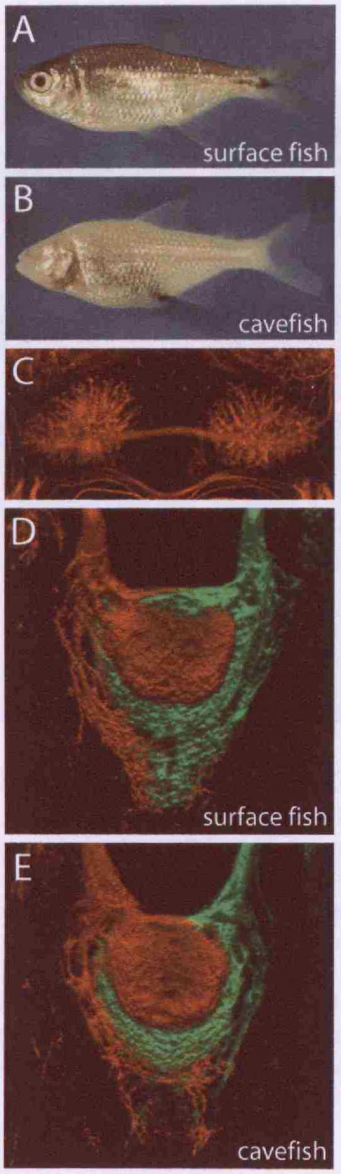

Figure 2.7: ***Laterotopic* connectivity in *Astyanax*.** (A,B) Adult surface fish (A) and cavefish (B). Amongst other adaptive changes, cavefish have lost eyes and body pigmentation. Images: Yoshiyuki Yamamoto and Bill Jeffery. (C) Confocal maximum-intensity projection of the epithalamus of a 6.5 dpf surface fish larva showing habenular neuropil visualised by anti-acetylated α tubulin immunostaining. In contrast to zebrafish, habenular neuropil appears largely bilaterally symmetric. Dorsal view, anterior top. (D,E) 3D confocal reconstructions of left (red) and right (green) habenular axon terminals innervating the IPN in a 5 dpf surface fish (D) and a 5 dpf Tinaja cavefish (E). A similar innervation pattern is seen in both cases, wherein left-sided axons predominantly innervate the dIPN and right-sided axons are confined to the vIPN. Dorsal views, anterior top.

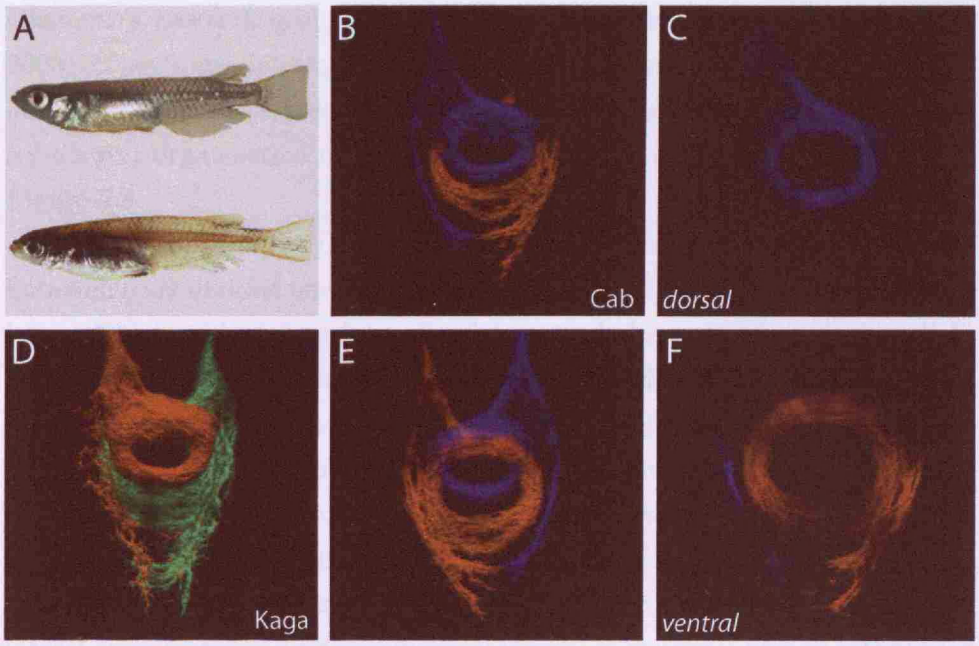

Figure 2.8: ***Laterotopic* habenulo-interpeduncular connectivity in medaka.** (A) Adult male medaka fish of the northern Cab (top) and southern Kaga (bottom) strains. Adapted from Wittbrodt et al. (2002). (B-F) Confocal imaging of dye tracing in a representative Kaga (D) and Cab (B,C,E,F) larva. (D) 3D reconstruction of left (red) and right (green) habenular axons terminals in the IPN of a Kaga larva, 8 dpf, dorsal view. (B,E) 3D reconstruction of left (blue) and right (red) habenular axons terminals in the IPN of a Cab larva, 7 dpf. (B) shows a dorsal view and (E) shows a ventral view of the 3D reconstruction. (C,F) Single confocal z-slices through the dorsal (C) or ventral (F) IPN show the complete DV segregation of left and right axons.

dorsal and ventral IPN. Additionally, the IPN could perform comparative analyses or integration of left and right inputs, which may converge into a common output pathway. I return to these questions in §3.8.4, below.

2.6.2 *Laterotopic* circuitry in adult zebrafish

To study these lateralised circuits, we have collaborated with Hitoshi Okamoto's research group at the RIKEN Institute, Japan (Aizawa et al., 2005). They have determined that *laterotopic* connectivity is maintained in adult zebrafish and moreover that it is associated with an asymmetry in the subnuclear organisation of the habenulae. Their results are summarised in Figure 2.9.

As discussed above (§1.2.5 and reviewed in Concha & Wilson, 2001), the habenulae are divided into subnuclei that are frequently asymmetric between left and right sides. In adult zebrafish, morphologically discrete "medial" and "lateral" subnuclei can be identified, which differ in their target connectivity and patterns of gene expression. Neurons in the medial subnucleus are labelled in Tg(*brn3a*:GFP) transgenic fish and their axons terminate in the vIPN. By contrast, *lov* expression is largely restricted to the lateral subnucleus and these neurons innervate the dIPN. The size ratios of these subnuclei differ on left and right sides. The left habenula contains a large lateral subnucleus and relatively small medial subnucleus and so establishes connectivity predominantly with the dIPN. On the right side the size ratios are reversed such that the vast majority of neurons are located in the large medial subnucleus that innervates the vIPN.

2.6.3 IPN innervation is asymmetric from the outset and might be established by interstitial axon branching

The dye tracing patterns at early stages show habenular axons initially project well beyond their target, into the hindbrain, and only later does innervation of the IPN commence. This might occur by interstitial axon branching. In fact, many long distance axonal connections in the vertebrate brain form in this way, where axons first extend a long distance past their target and subsequently develop interstitial branches at appropriate locations along their length that innervate the target region. Later, the dis-

Figure 2.9: ***Laterotopic* connectivity in adult zebrafish.**
(A) Schematic illustrating the organisation and connectivity of the adult zebrafish habenulae. Both nuclei contain a "lateral" and "medial" subnucleus, which contain neurons that exclusively innervate either the dorsal or ventral IPN, respectively. In the left habenula, the lateral subnucleus is enlarged, resulting in greater efferent connectivity with the dIPN. By contrast, on the right the medial subnucleus is enlarged and the lateral subnucleus is very small, resulting in predominant connectivity with the vIPN. (B) Confocal projection of the adult IPN. Left-sided axons (red) terminate preferentially in the dIPN, whereas almost all right-sided axons (green) innervate the vIPN. Transverse view, adapted from Aizawa et al. (2005).

tal axonal segments degenerate (Luo & O'Leary, 2005). My results seem compatible with such a developmental mechanism: short protrusions can be seen to derive from the caudally-directed fascicles, which extend towards the IPN; at later stages, after IPN innervation, the caudally-directed fibres become progressively less visible, compatible with the notion these regions of the axons might have degenerated. Furthermore, in §3.4, I describe the morphology of an individual habenular axon that supports this hypothesis. An alternative possibility is that the early, caudally-directed fibres do not themselves develop branches that innervate the IPN, but rather they act to pioneer the fasciculus retroflexus and guide a second population of habenular axons that do innervate the target. This hypothesis is supported by the observation that most single habenular axons, which appear at early stages of IPN innervation, do not bear any caudally-directed processes that would suggest interstitial branching has occurred, but instead appear to have directly innervated the IPN (see §3.4, below). In future studies it would be informative to perform time-lapse observations of single habenular axons to help resolve this issue.

Whatever the mechanism by which habenulo-interpeduncular connectivity forms, my results reveal that the asymmetric, DV segregation of left and right terminals is established from the earliest stages of IPN innervation. This direct connectivity to the appropriate DV region of the target suggests that interactions between left and right axons are probably not important in their segregation. It seems more likely that they differ in their expression of axon guidance receptors which respond to ligands that are differentially distributed along (or around) the DV axis of the IPN. A recent report from Kuan et al. (2007b) presents evidence that Nrp1a is expressed more strongly in left habenular cells and in response to Sema3D acts to guide left-sided axons to the dIPN.

Not only are left and right axons asymmetric with respect to their targeting, but left-sided neurons also appear to start to innervate the IPN earlier than right habenular neurons. This is compatible with a recent report that showed an asymmetry in the timecourse of habenular neurogenesis (Aizawa et al., 2007). Neurons that will end up in the "lateral" subnucleus by adult stages, which are more prevalent in the left habenula, tend to be born earlier than the "medial" neurons that predominate on the right side.

2.6.4 Evolutionary conservation of *laterotopic* connectivity

My analyses of two other fish species support the idea that asymmetric habenular connectivity is evolutionarily conserved, at least in teleosts, suggesting it is functionally important.

In the closely related species *Astyanax mexicanus*, the *laterotopic* connectivity pattern was very similar indeed to that in zebrafish. In §1.1.4 I discussed the concept that a consistent direction of CNS asymmetries between individuals in a species — population laterality — may be important for mediating co-ordinated or social behaviours, such a shoaling in fish. Interestingly, whereas surface fish shoal, blind cavefish populations do not show any obvious social behaviours, at least in the laboratory. *Astyanax* therefore provides an excellent opportunity to attempt to correlate differences in the laterality of neuroanatomical asymmetries with social behaviour in recently diverged populations. As described in §1.2.4, the DDC is implicated in a number of social and emotional behaviours. In future studies, it would be interesting to determine the population laterality of habenulo-interpeduncular connectivity in larger groups of surface fish and cavefish to determine if coordinated neuroanatomical asymmetry can be correlated with social behaviour.

In the more distantly related medaka fish, I observed an even more pronounced DV segregation of habenular axon terminals. In light of the finding that *laterotopic* connectivity is accounted for by an asymmetry in subnuclear size ratios (at adult stages), one would predict that in medaka, the left–right difference in size ratios is even greater than in zebrafish. Accordingly, the left habenula would almost completely comprise a "lateral" subnucleus, whereas the vast majority (or even all) of the right-sided neurons would belong to an equivalent of the "medial" subnucleus. This illustrates that one of the advantages of specifying the same types of subnuclei on both sides of the brain is that it provides a simple way for evolutionary processes to modulate the degree of lateralisation by controlling the reciprocal expansion and contraction of the subnuclei therefore resulting in greater or lesser degrees of left–right asymmetry.

Fish are among the vertebrates that show the most pronounced asymmetries in the epithalamus (Concha & Wilson, 2001). Although a topographic

organisation of habenular inputs to the IPN has been described in mammals, where axons from the dorsal region of the medial habenula innervate the lateral IPN and axons from the lateral part of the medial habenula terminate in the dorsal IPN (see §1.2.2), no left–right differences have been described. A more recent study using lipophilic dye tracing similarly failed to observe any left–right differences in IPN innervation in either the embryonic mouse, the juvenile frog or the salamander (Kuan et al., 2007a). It is probable that in species that do not show obvious lateralisation in this circuit, there are still subnuclei with distinct connectivity preferences specified in the habenulae, but during the course of evolution their size ratios have become equivalent on the left and right sides.

Chapter 3

Analysing lateralised circuitry at single-cell resolution

In Chapter 2 we saw that the differential connectivity of the left and right habenulae of the adult zebrafish is associated with an asymmetry in subnuclear size ratios whereby both sides establish some degree of connectivity with both dorsal and ventral regions of the IPN. This suggests that lateralisation might be achieved in this circuit by specifying similar, or identical, components on the two sides of the brain, but varying their relative abundances. However, because individual neurons have not been examined, the extent of neuronal diversity within, and between, the left and right habenulae is unknown.

Moreover, to understand how information from the left and right habenulae might be processed and integrated at the IPN, it is necessary to know the connectivity patterns of single neurons within the circuit.

3.1 Focal electroporation can be used to examine the morphology of individual neurons *in vivo*

I optimised a focal electroporation technique which allowed me to express membrane-tethered fluorescent proteins in individual cells or small groups of cells, enabling visualisation of the complete morphology and axonal pro-

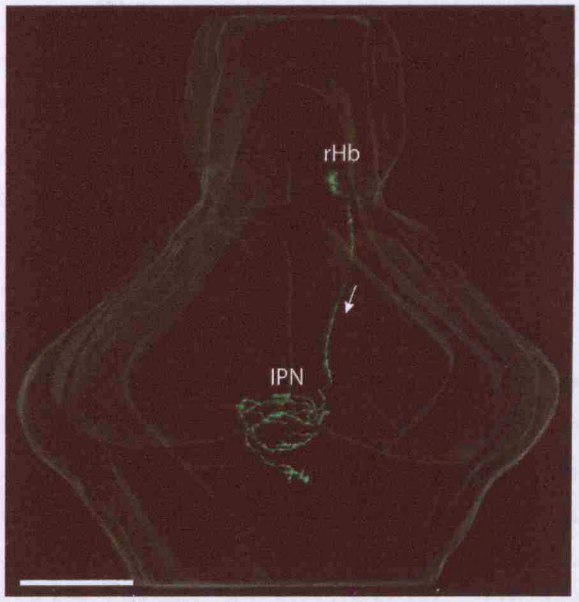

Figure 3.1: **Habenular neuron labelled by focal electroporation.** 3D isosurface reconstruction of a 4 dpf larval brain in which a single habenula neuron has been electroporated with a construct driving expression of GAP43–GFP (green). The soma is located in the right habenula and extends an axon (arrow) in the right FR that terminates within the IPN. Scale bar: 100 μm.

jections of neurons in the intact brain (Figure 3.1). In combination with high resolution confocal microscopy, this has allowed me to examine and compare the morphology of individual cells at the levels of soma, dendrites, axons and terminal arbors.

3.2 Habenular projection neurons display a stereotypical unipolar morphology

Using focal electroporation of a construct driving expression of membrane-tethered GFP, I examined the morphology of 83 habenular neurons (37 left-sided and 46 right-sided) in 3–6 dpf larvae. Given the small size of the habenulae at the stage of labelling (48–72 hpf), no attempt was made to target different positions within the nucleus and so the position of labelled neurons was essentially randomised.

The larval habenulae comprise discrete, well de-limited and coherent groups of cells. They have a glomerular organisation where neuronal somata are arranged as ovoid shells surrounding a central neuropil domain (Figure 3.2A,B). All labelled habenular neurons, wherever they were located within the shell on the left or right sides, displayed a unipolar somal morphology (Figure 3.2C–F). In all cases, neuronal somata extend a sin-

gle process, or primary neurite, directed towards the central neuropil core, where their dendritic trees are elaborated. This primary neurite was variable in length, most probably reflecting the proximity of the soma to the neuropil core. Dendritic trees showed considerable variation in size and branch complexity. However, I was unable to correlate these differences in dendritic morphology with developmental stage, molecular identity or axonal phenotype. The axon emerges from one branch of the dendritic arbor and extends, unbranched within the fasciculus retroflexus towards the ventral midbrain.

The vast majority of cells on both left and right sides were habenulo-interpeduncular projection neurons that extended long axons in the FR and innervated the IPN (95.2%). In four cases, neurons projected to a location caudal to the IPN, most likely the serotonergic raphé nucleus in the anterior hindbrain (4.8%, Figure 3.3). The axons of these neurons also coursed in the FR, but passed ipsilaterally around the vIPN before converging medially, crossing the midline and finally terminating close to it.

All of the cells labelled by focal electroporation displayed a projection neuron morphology. I did not observe any habenular interneurons, with axons confined to the habenular nucleus, nor any glial cells.

These results reveal that whilst there is clearly diversity among habenular neurons, on both left and right sides they share a common, stereotypical unipolar morphology.

3.3 Axons of habenular projection neurons cross the midline multiple times and establish bilateral connectivity

Dye tracing experiments, in which the entire population of left and right-sided projection neurons were labelled, revealed that axons from both habenulae terminate on both sides of the midline, surrounding the central "core" of IPN cell bodies. One possibility is that each habenular nucleus contains discrete ipsilaterally and contralaterally projecting neurons. Alternatively, the axons of individual habenular neurons might bifurcate so as to innervate both sides of the target.

High resolution reconstructions of the terminal arbors of habenular neu-

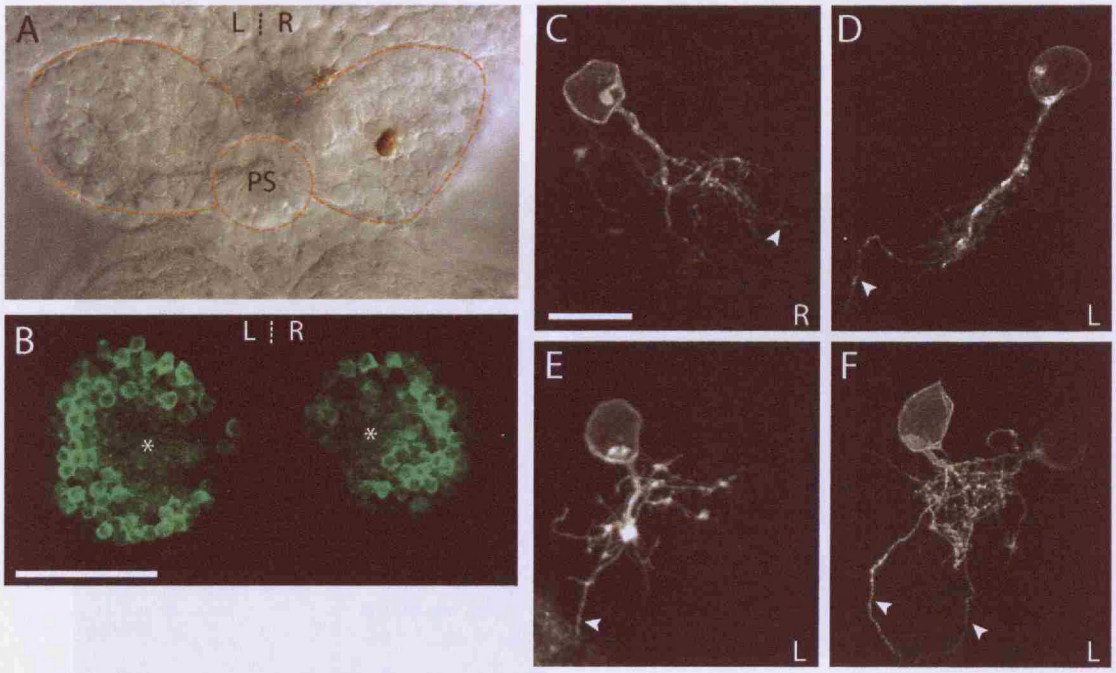

Figure 3.2: **Habenular neurons have a stereotypical unipolar morphology.** (A) A single right habenular neuron labelled by focal electroporation and visualised by anti-GFP immunostaining (brown). Image shows the dorsal diencephalon of the dissected brain of a 4 dpf larva. Dotted lines show the borders of the habenulae and the position of the pineal stalk. (B) Single-depth confocal z-slice through the habenulae of a 4 dpf Tg(ET16:GFP) transgenic larva in which a subset of habenular neurons express GFP. In each nucleus the neuronal somata are arranged as ovoid shells surrounding a central neuropil domain (asterisks). It is in this domain that neurons elaborate their dendritic arbors. (C–F) Examples of the somata, dendritic arborisations and proximal axons of habenular neurons labelled by focal electroporation of membrane-tethered GFP. (C,D) Neurons with long primary neurites that give rise to a dendritic tree and axon. (E,F) Neurons elaborating dendritic arbors close to the cell body. In (F) two neurons have been labelled with intertwined dendritic arbors located in the central neuropil of the habenula. In all panels an arrowhead marks the proximal axon and the laterality (left (L) or right (R)) of the habenular neuron(s) is indicated bottom right. Scale bars: (B) 50 μm; (C) 10 μm.

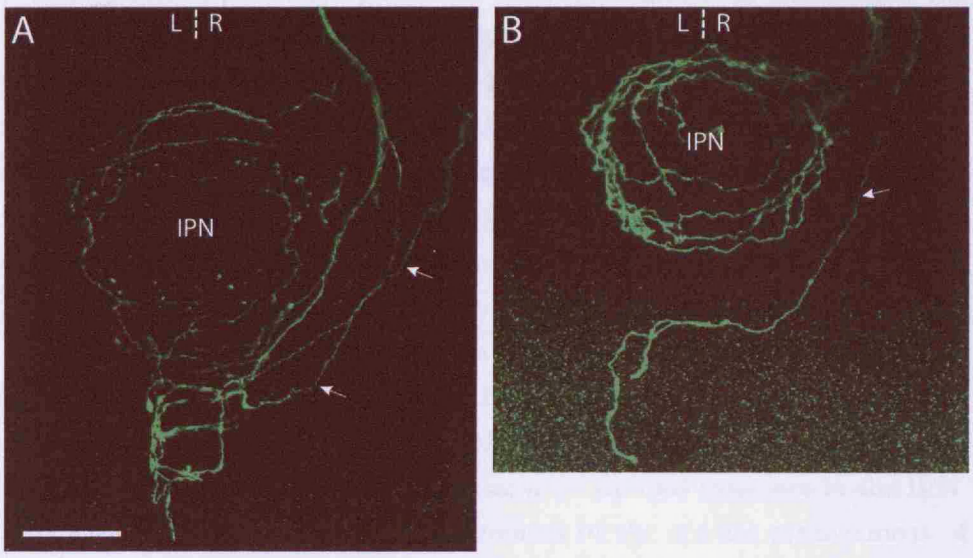

Figure 3.3: **A subset of habenular projection neurons extend axons that pass around the IPN and terminate in the anterior hindbrain.**
(A,B) Confocal maximum intensity projections of the ventral midbrain and anterior hindbrain in a 5 dpf (A) and 8 dpf (B) larva in which groups of habenular neurons have been labelled by focal electroporation. Some habenular neurons project axons that course ipsilaterally around the IPN (arrows) before converging medially to terminate on either side of the midline. These caudal terminations lie in the anterior hindbrain, most probably at the level of the serotonergic raphé nucleus (see Figure 2.2). Panels show dorsal views, anterior top. Scale bar: 25 μm.

rons revealed a striking characteristic of these cells. Axons from left or right-sided neurons cross the ventral midline multiple times, forming profusely branched "spirals" of neurites (Figure 3.4A). One hypothesis I considered was that left and right-sided axons might "spiral" in opposite senses (clockwise *versus* counter-clockwise). However, this does not appear to be the case; axons invariably branch within the IPN and branches frequently reverse sense within the arbor.

The bilateral projection pattern of individual habenular axons raises the possibility that single neurons form synaptic connections on both left and right sides of the IPN. Although the IPN is usually described as unpaired midline nucleus, both histological sections and confocal images show a left–right subdivision (Figure 2.4). To examine the synaptic connectivity of single habenular neurons I used focal electroporation to express a construct driving expression of both cytoplasmic RFP and a Synatophysin–GFP (Syp–GFP) fusion protein, which localises to presynaptic terminals in zebrafish neurons *in vivo* (Meyer & Smith, 2006). Arbors were decorated with large numbers of Syp–GFP puncta that colocalised with axonal varicosities on both left and right sides of the midline (Figure 3.4B). This suggests habenular neurons establish both ipsilateral and contralateral *en passant* synapses in the IPN. I could not observe any obvious differences in the spatial arrangement of these puncta between left and right-sided axons.

3.4 Developing arbors

It is almost universally the case that commissural axons, which cross the ventral midline (or ventral nerve cord in invertebrates), only do so once. After crossing, growth cones concomitantly lose responsiveness to midline chemoattractants and become responsive to midline repellents, preventing them from recrossing (Kaprielian et al., 2001). Why are habenular axons able to re-cross the midline multiple times to establish their "spiral-shaped" terminal arbors? Although I have not investigated this question in detail, some clues as to how the arbors develop is provided by axon arbors that appear to be at earlier stages of IPN innervation. Such "developing" arbors were most frequently seen at early stages (~60% of labelled neurons at 3–3.5 dpf) but were also quite often observed in older larvae (~30% at 4–4.5 dpf

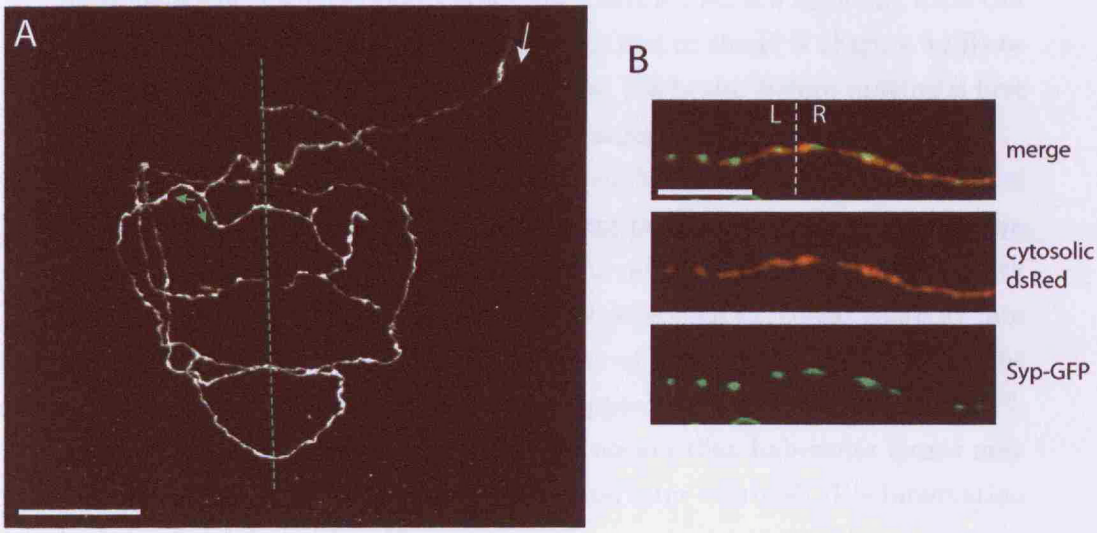

Figure 3.4: **Habenular axons elaborate "spiral-shaped" arbors and establish bilateral connectivity.**
(A) Confocal projection of the IPN showing a single axonal arbor elaborated by a right habenular projection neuron labelled by focal electroporation. The arbor crosses the ventral midline (dotted line) multiple times. Branches can also reverse direction such that they encircle the IPN in opposite senses (green arrows show examples). (B) High-magnification confocal images of a section of a habenular axon arbor crossing the ventral midline (dotted line). The neuron was electroporated with a construct driving expression of cytosolic DsRed (red, middle panel) and a Synaptophysin–GFP (Syp–GFP) fusion protein (green, lower panel). Syp–GFP puncta are present on both sides of the midline and co-localise with axonal varicosities. Scale bars: (A) 20 μm; (B) 10 μm.

and ~7% at 5-5.5 dpf), consistent with a protracted period of generation of habenular neurons (Aizawa et al., 2007).

In these cases, although the axons did not completely encircle the "core" of the IPN, they already displayed multiple branches and prominent growth cones, often on more than one branch tip (Figure 3.5). This suggests the extensive branching commences early in the development of the arbor. The morphology of the developing arbors also reveals that the incoming axon can either first cross the midline at the anterior end of the IPN (Figure 3.5B) or continue caudally, on the ipsilateral side of the brain, before making a first decussation at the posterior limit of the target (Figure 3.5C).

In one instance, I labelled a right habenular neuron that had an axonal morphology reminiscent of the dye tracing pattern seen at early developmental stages (Figure 2.5). The axon bifurcated anterior to the IPN, with one branch crossing the midline; both processes then extended caudally into the hindbrain (Figure 3.5D). Notably, one of these main processes can be seen to give rise to a small branch that appears to be innervating the IPN. This morphology appears to support the notion that habenular axons may first project a long way past their target and later establish IPN innervation by interstitial axon branching.

3.5 Two distinct sub-types of terminal arbor

Dye tracing reveals that the left and right habenulae differentially innervate the dorsal and ventral domains of the IPN. At least two hypotheses could explain this asymmetric connectivity pattern. Firstly, habenular neurons might elaborate axonal arbors which are exclusively confined to *either* the dorsal *or* ventral region of the IPN, with different proportions of dorsally and ventrally-targeting neurons on each side. Secondly, habenular neurons might form complex arbors with varying amounts of terminals branches in the dIPN and vIPN. This latter model would potentially allow for the left and right habenulae to each contain a single, distinct neuronal morphology. Left-sided neurons would elaborate arbors with more branches in the dIPN whereas the right-sided neuron morphology would involve the vast majority of branches innervating the vIPN.

To resolve this issue, which is central to determining whether similar or

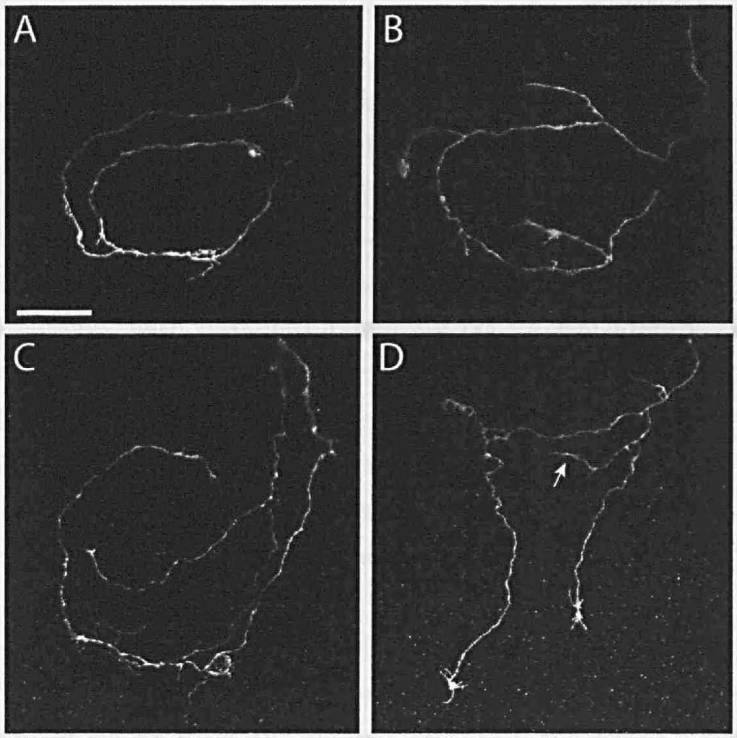

Figure 3.5: **"Developing" habenular axon arbors.**
(A-D) Confocal projections showing habenular axons, labelled by focal electroporation, that appear to be at early stages of arbor formation. Numerous growth cones can be observed on axon branches. The morphologies of these arbors demonstrate that the incoming axon may first cross the midline at the posterior limit of the IPN (C), or make a first decussation at the anterior end (B) or even bifurcate, sending branches in clockwise and counter-clockwise spiral trajectories (A). (D) shows an arbor with a morphology similar to that observed when the entire contingent of axons is labelled using lipophilic dyes at early stages (*eg* 50 hpf, see Figure 2.5). Two main branches are proceeding posteriorly and from one of these a short branch is emerging, which may be beginning to innervate the IPN (arrow). Note, however, that this is the only such example I observed. All panels show dorsal views, anterior top. Scale bar: 20 μm.

distinct circuitry components are specified on the two sides of the brain, I performed detailed morphometric analyses of terminal arbors from right and left-sided neurons, focussing on differences that might underlie lateralisation of the circuit.

I identified two very distinct arbor morphologies, which I have termed "L-typical" and "R-typical" (Figure 3.6). Both types of terminal are exhibited by left and right-sided neurons, but at very different frequencies. The vast majority (83.8%) of left-sided neurons form L-typical arbors (n=31/37; Figure 3.6A-C'; Movie 1), whereas 90.5% of right-sided neurons form R-typical arbors (n=38/42; Figure 3.6D-F'; Movie 2).

3D reconstructions of L-typical arbors reveal them to be shaped like a "domed crown", with branches extending over a considerable DV depth (31.0±1.3 μm). In contrast, R-typical arbors are significantly more flattened, reflected by a smaller average DV extent (17.7±1.2 μm; $p<0.001$; Figure 3.7B). Some R-typical arbors were remarkably flat, so much so that all of the terminal neurites were confined to a single flat plane with a depth so small that it was at the limit of what I was able to measure from my confocal dataset ($\leq$6 μm).

L-typical arbors have a circular perimeter, surrounding the central "core" of the IPN. They possess large numbers of branches which are directed dorsally and medially to form the domed crown of the arbor. In contrast, R-typical arbors appear more elongated along the anterior–posterior axis and are less highly branched. Much of the neurite length is concentrated towards the perimeter of the arbor and relatively few branches extend towards the centre of the IPN. Morphometric quantification supports these visual impressions: L-typical arbors display a significantly greater average number of branch points than R-typical arbors (L-typical=19.3±1.0; R-typical=7.6±1.2; $p<0.001$; Figure 3.7C). In addition, the width/length ratio of L-typical arbors showed a trend towards being greater than that for R-typical arbors, although this difference did not quite reach statistical significance at the 95% confidence level (L-typical=1.28±0.039; R-typical=1.13±0.070; $p=0.06$; Figure 3.7D).

I devised a morphometric method similar to Sholl analysis to quantify the distribution of neurite branches from the centre to the periphery of the arbors (described in detail in §7.7). This revealed distinct distribution

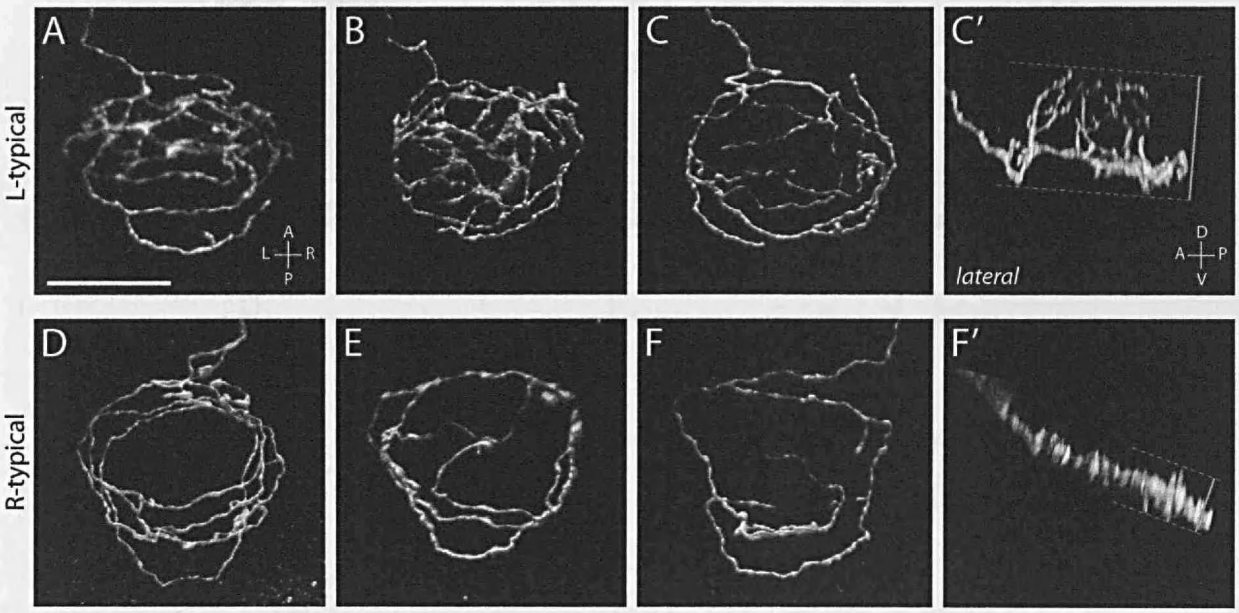

Figure 3.6: **Two distinct axon arbor morphologies formed by habenular neurons.** 3D confocal reconstructions of habenular axon arbors, labelled by focal electroporation, in the IPN. (A–C') Three examples of L-typical arbors. These arbors are shaped like a domed crown and arborise over a considerable DV extent (compare dorsal (C) and lateral (C') views of an example L-typical arbor). See also Movie 1. (D–F') Examples of R-typical arbors, which are considerably flatter. See also Movie 2. Panel (D) shows two R-typical arbors formed by two right habenular neurons. In (C') and (F'), orange dotted lines and bars indicate how DV extent was measured for L-typical and R-typical arbors (see also §7.7). Scale bar: 30 μm.

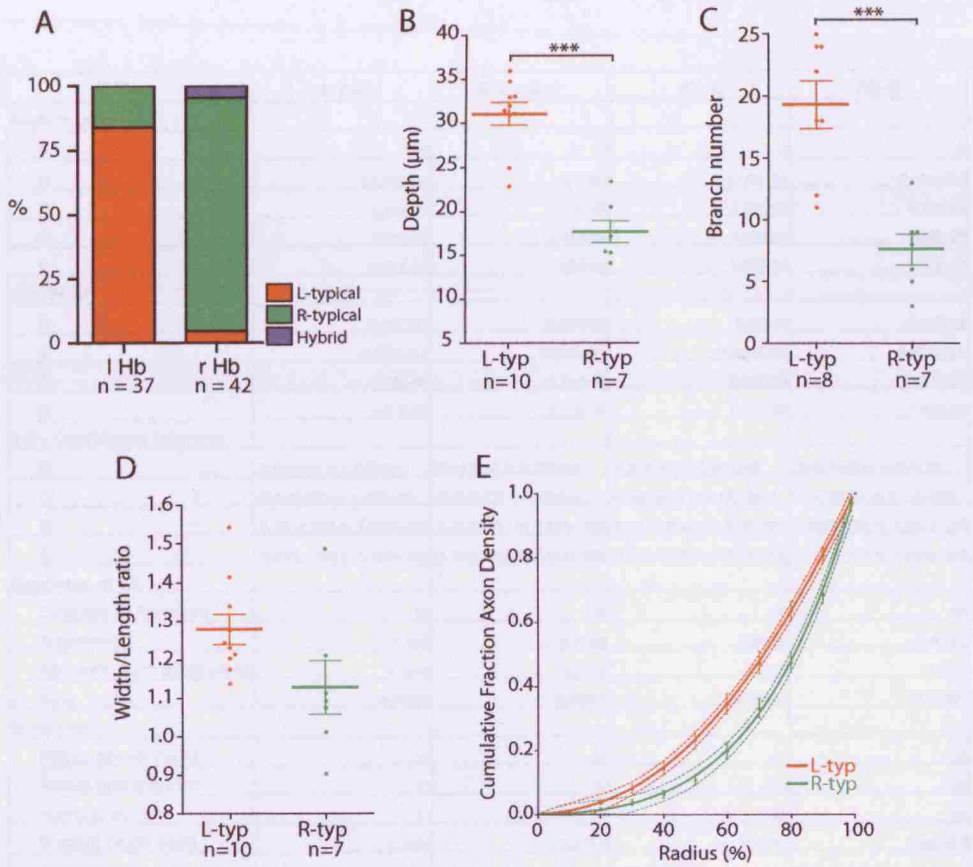

Figure 3.7: **Morphometric quantification of arbor sub-types.**
(A) Proportions of different arbor sub-types observed for left and right habenular neurons. (B) L-typical arbors extend over a greater DV extent than R-typical arbors. (C) L-typical arbors have more branch points than R-typical arbors. (D) The width/length ratio of L-typical arbors shows a trend towards higher values than for R-typical arbors. (E) Cumulative fraction of axon density plotted against radius (measured from centroid of the convex hull to the perimeter) for 10 L-typical and 7 R-typical arbors. The data are fit by fourth-order polynomial models (solid lines). Dotted lines indicate the 95% confidence band of each best-fit curve. R-typical arbors have a greater proportion of axon density localised towards the perimeter of the arbor. Horizontal lines indicate mean values and error bars show standard error of the mean (SEM). ***, $p<0.001$.

	L-typical	R-typical	Ab-L	Ab-R
Best-fit values				
A	0	0	0	0
B	0.0006474	1.44E-06	-0.001104	-0.0007964
C	4.47E-05	3.19E-05	7.12E-05	4.18E-05
D	9.30E-07	-4.47E-08	3.78E-07	-8.66E-07
E	-4.41E-09	7.20E-09	1.08E-10	1.52E-08
Std. Error				
B	0.002312	0.002001	0.00264	0.003289
C	0.0001212	0.0001049	0.0001384	0.0001724
D	1.98E-06	1.71E-06	2.26E-06	2.81E-06
E	1.01E-08	8.72E-09	1.15E-08	1.43E-08
95% Confidence Intervals				
B	-0.003949 to 0.005244	-0.003996 to 0.003999	-0.006395 to 0.004187	-0.007423 to 0.005830
C	-0.0001963 to 0.0002856	-0.0001776 to 0.0002415	-0.0002062 to 0.0003486	-0.0003057 to 0.0003892
D	-3.002e-006 to 4.861e-006	-3.463e-006 to 3.374e-006	-4.147e-006 to 4.903e-006	-6.533e-006 to 4.801e-006
E	-2.445e-008 to 1.563e-008	-1.023e-008 to 2.463e-008	-2.296e-008 to 2.318e-008	-1.373e-008 to 4.405e-008
Goodness of Fit				
Degrees of Freedom	96	66	56	46
R squared	**0.958**	**0.9768**	**0.9677**	**0.9571**
Absolute Sum of Squares	0.4659	0.1679	0.2126	0.2259
Sy.x	0.06966	0.05043	0.06161	0.07007
Runs test				
Points above curve	58	36	37	30
Points below curve	42	34	23	20
Number of runs	47	33	25	15
P value (runs test)	0.3236	0.2753	0.1442	0.002218
Deviation from Model	Not Significant	Not Significant	Not Significant	Significant
Constraints				
A	A = 0.0	A = 0.0	A = 0.0	A = 0.0

Table 3.1: **Details of non-linear regression.** For each arbor sub-type, radial distribution of axon density data was fit by non-linear regression using a fourth-order polynomial model: $Y = A + BX + CX^2 + DX^3 + EX^4$. The value of the Y-intersect was constrained to zero ($A = 0$) because no axon density can have been accumulated at 0% radius. The polynomial model produced a good fit for all four data sets (Ab-L and Ab-R arbors will be discussed in Chapter 5). R^2 values were high and 95% confidence intervals of all the parameters fit by non-linear regression were small.

profiles for the two types of arbor (Figure 3.7E). L-typical arbors show a greater proportion of axon density concentrated towards the centre of the arbor as a result of the many branches extending medially. By contrast, in R-typical arbors, over 50% of axon density is concentrated within the outer 20% of the arbor radius, reflecting the restriction of neurite branches towards the periphery of the arbor. Both average distribution profiles showed excellent fits to fourth-order polynomial models (L-typical: R^2=0.9580; R-typical: R^2=0.9768; 95% confidence intervals for all parameters fit by non-linear regression were small; Table 3.1) and comparison of the curves using Akaike's Information Criterion showed they can be considered distinct with greater than 99% probability (ΔAICc=80.39 for global *versus* individual fits).

In two cases (from a total of 79 left and right neurons), axon arbors had an "intermediate" morphology, which could not be unambiguously classified as L-typical or R-typical (*eg* Figure 3.4A).

Neurons displaying the minor arbor morphology for their respective habenula nucleus sometimes showed an unusual trajectory towards the IPN: Of the six left habenular neurons bearing R-typical arbors, three had their somata located very close to the midline and actually projected their axons across the dorsal midline of the epithalamus to enter the *right* FR. Similarly, one of the two right habenular neurons that elaborated a L-typical arbor was located at the most medial edge of the right habenula and extended its axon down the *left* FR (Figure 3.8).

3.6 L-typical and R-typical arbors display differential target localisation

Do the distinct arbor morphologies arise from axons terminating in different regions of the IPN and if so, does this account for the *laterotopic* connectivity pattern revealed by lipophilic dye tracing?

To answer this question, I performed anti-GFP immunostaining followed by histological sectioning of the brains of electroporated larvae. L-typical arbors were located surrounding the dIPN cell bodies whereas R-typical arbors were located in the vIPN (Figure 3.9A,B). Additionally, contemporaneous labelling of left *and* right neurons confirms that L-typical arbors, most likely

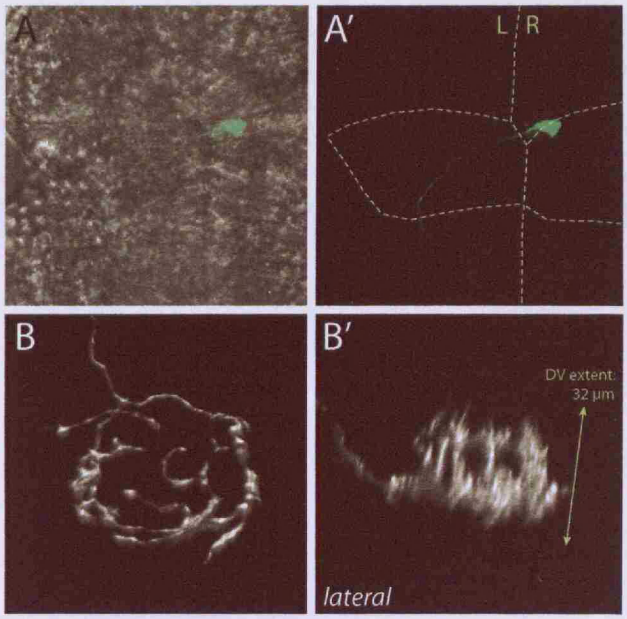

Figure 3.8: **Axonal extension in the contralateral FR.**
(A,A') Confocal projections of the epithalamus of a 4 dpf larva, where a single right habenular neuron has been labelled. (A) shows the GFP signal overlaid on a transmitted light image to show tissue organisation. (A') shows GFP fluorescence alone and the boundaries of the habenulae and location of the midline are indicated by dotted lines. The neuron is located at the most medial edge of the right habenula and extends its axon across the midline to descend in the *left* FR. (B,B') 3D confocal reconstructions of the L-typical terminal arbor formed by the same neuron. All images show dorsal views, anterior top, except (B') which is a lateral view, anterior left.

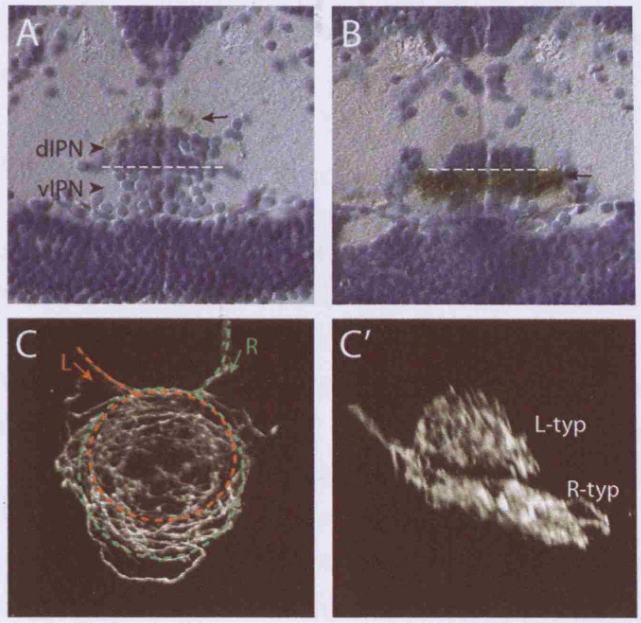

Figure 3.9: **Dorso-ventral localisation of arbor sub-types.**
(A,B) Transverse histological sections through the IPN of 10 dpf larvae in which habenular neurons were labelled by focal electroporation, followed by anti-GFP immunostaining (brown) to determine the location of axon arbors (indicated by arrows). (A) L-typical arbors are localised in the neuropil surrounding and covering the dIPN. (B) R-typical terminals are located in the vIPN. Dotted white lines indicate the boundary between the dorsal and ventral parts of the IPN. (C,C') Left and right-sided axons labelled in the same larva. L-typical arbors are located dorsal to R-typical arbors. (C) dorsal view, anterior top; (C') lateral view, anterior left.

elaborated by left-sided neurons, are located dorsal to flattened R-typical arbors, probably formed by right-sided neurons (Figure 3.9C,C'). The morphology of individual arbors also mirror the shapes of the dorsal and ventral arborisation territories: L-typical arbors, shaped like a domed crown, reflect the shape of the dorsal neuropil domain that surrounds and covers the dIPN cell bodies like a hat. In the ventral target, cells are surrounded by a dense ring of neuropil that evidently comprises R-typical arbors with peripherally localised axon branches.

These results indicate that individual habenular neurons innervate *either* the dorsal *or* ventral IPN, but not both domains. Because the majority of left-sided neurons develop L-typical arbors restricted to the dIPN, this explains the predominantly dorsal innervation pattern observed for the left habenula by dye tracing. Similarly, the predominance of ventrally-located

R-typical arbors on right-sided neurons accounts for the right habenula primarily targeting the vIPN.

3.7 IPN neuron morphology

The unique morphologies and DV segregation of habenular axon terminals raises several questions regarding the organisation of the target and the morphology of post-synaptic IPN neurons. For example, do IPN neurons, located in the central "core", radiate dendritic arbors outwards to synapse with the surrounding afferent axons? What are the consequences of the DV segregation of L-typical and R-typical inputs into the IPN? Are there IPN neurons that exclusively receive inputs from only dorsal or ventral axons or do some neurons synapse with both dorsal and ventral habenular axons, suggesting an integration of predominantly-left and predominantly-right information? Do the distinct morphologies of L-typical and R-typical axons correlate with the morphologies of post-synaptic neurons? For instance, do IPN neurons in the vIPN have flattened dendritic arbors which complement the flattened axonal arbors of R-typical neurons?

To address these and related questions, I used focal electroporation to label individual IPN neurons with membrane-localised Cherry fluorescent protein in Tg(ET16:GFP) transgenic larvae in which many habenular axons are labelled by GFP expression (the extent of habenular expression is shown in Figure 3.1B). This allowed me to examine the detailed morphology of IPN neurons whilst localising their somata and neurite arbors with respect to the dorsal and ventral interpeduncular neuropils.

In total I labelled 20 individual neurons from 14 larvae (4–6 dpf). The vast majority (18/20) were located within the central "core" of the IPN. Two neurons were located outside, but in very close apposition to, the arborisation domains which surround the core. Such "external" cells are visible in both histological sections and in the Tg(*h2afz*–GFP) transgenic line (Figure 2.4). As these neurons extend neurite arbors within the IPN neuropil, I consider them to be interpeduncular neurons.

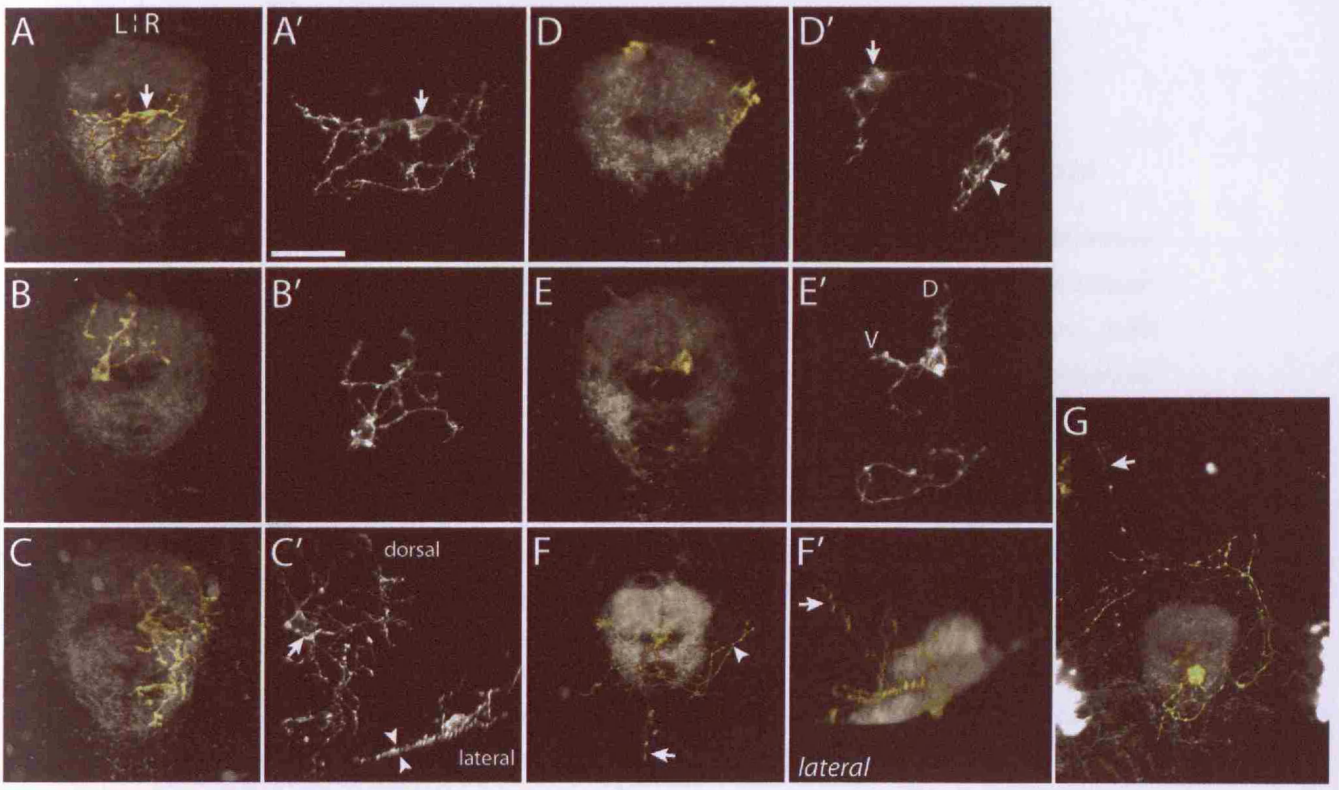

Figure 3.10: **Morphology of IPN neurons.** (A–G and F') 3D confocal projections showing electroporated IPN neurons expressing membrane-Cherry (gold) and the surrounding IPN neuropil (grey), visualised using the Tg(ET16:GFP) transgenic line. All panels are dorsal views, anterior top, except (F') which is a lateral view, anterior right. (A'-E') Maximum intensity projections of deconvolved confocal z-stacks reveal the detailed morphology of IPN neurons. (A,A') An interneuron in the vIPN that extends neurites exclusively within the vIPN neuropil. The soma (arrow) is located on the right of the midline but the neurites enter the neuropil on both left and right sides. A second, more weakly labelled neuron is also visible. (B,B') The soma of this neuron, as with most IPN neurons, occupies the central cellular core of the nucleus whilst its arbor extends radially to synapse with afferent habenular axons that encircle the core. (C,C') A vIPN neuron with a flattened dendritic arbor. In this specimen two neurons were labelled. One of these (soma marked by arrow in (C')) radiates an extensive dendritic arbor exclusively on the right of the midline within the vIPN neuropil. The lateral projection (inset in (C')) reveals the arbor is extremely flattened along the DV axis (arrowheads in (C')). (D,D') Neuron with a dorsally located soma (just outside the dIPN neuropil), which elaborates two arbors in spatially distinct regions of the IPN. The larger of these arbors (arrowhead in (D')) is connected to the cell body (arrow in (D')) by a long, unbranched process. As is also the case for some of the other interneurons, it is unclear whether these arbors are axonal, dendritic or both in nature. (E,E') A dIPN projection neuron that extends an axon just caudal to the IPN, most probably synapsing with neurons of the serotonergic raphé nucleus. This neuron has dendritic processes located both in the dorsal (D) and ventral (V) neuropils. (F,F') In this specimen, three projection neurons are labelled. Axons extend around the IPN (arrowhead in (F)) as well as caudally and dorsally (arrows in (F,F')). (G) Projection neurons extending anteriorly-directed axons which pass around the IPN, cross the midline and continue rostrally (arrow). Scale bar in (A'): 20 μm.

3.7.1 IPN neurons have radially-directed neurite arbors

One feature shared by all of the IPN neurons I labelled is that they elaborate neurite arbors within the arborisation domains of habenular axon terminals that surround and cover the IPN. For the majority of IPN neurons, with cell bodies within the central core, this means the neurons are polarised such that their neurites extend radially — from the core towards the periphery of the nucleus — to synapse with the surrounding afferent axons (Figure 3.10A,B,C,E).

3.7.2 DV localisation of arbors

I classified the IPN neurons as projection neurons (45%, 9/20), if I could observe an axonal projection extending outside the IPN, or as interneurons (55%, 11/20), if the neurites were confined to the IPN.

Both interneurons and projection neurons either extended arbors that were restricted to the dorsal *or* ventral neuropil (9/11 interneurons, Figure 3.10A,A'; 5/9 projection neurons) or innervated both dorsal *and* ventral neuropils (2/11 interneurons; 4/9 projection neurons, Figure 3.10E,E'). These results show that the IPN contains first, neurons with DV restricted arbors that could specifically relay L-typical or R-typical habenular inputs to downstream target nuclei and second, neurons that extend neurites into both dorsal *and* ventral neuropils, which consequently have the potential to integrate predominantly-left and predominantly-right information.

3.7.3 Flattened dendritic arbors

As described in §3.5, R-typical axon arbors, localised in the vIPN, are often remarkably flattened along the DV axis. In two cases I labelled vIPN neurons that also displayed remarkably flattened dendritic arbors (Figure 3.10C,C'). This suggests some habenular axon terminals might be topographically arranged within the IPN neuropil and that there might be a precise connectivity between specific pre-synaptic habenular neurons and post-synaptic IPN neurons.

3.7.4 Continuous and split arbors

IPN neurons display both "continuous" and "split" arbors: The interneurons I labelled, with somata located in the vIPN, typically extended continuous arbors, which varied in size (Figure 3.10A,A'). By contrast, two dorsal interneurons, and one dorsal projection neuron each elaborated two quite separate arbors, which were discretely localised in distinct subdomains of the IPN neuropil (Figure 3.10D,D').

3.7.5 Efferent connectivity

The projection neurons I labelled extended efferent axons to a variety of targets, compatible with reports in other species that the IPN is an integrative centre that establishes ascending and descending efferent connectivity with many CNS nuclei (Morley, 1986). It was common to observe axon terminals in a midline position just caudal to the IPN (Figure 3.10E,E'). This is the location of the serotonergic raphé nucleus, which is also innervated by the subset of habenular axons which pass around the IPN before converging to the midline (Figures 2.2 and 3.3). IPN projection neurons also extended axons caudally towards other sites in the hindbrain as well as to regions of the tegmentum surrounding the IPN (Figure 3.10F,F'). In one specimen, we observed anteriorly-directed efferent axons that passed around the IPN and crossed the ventral midline before proceeding rostrally or caudally. The lack of specific markers and anatomical data for the larval zebrafish brain mean it is difficult to determine the precise identity of these efferent target nuclei. However, in other species the IPN is known to project to midbrain and hindbrain nuclei including the raphé and dorsal tegmental nucleus as well as projecting anteriorly to diencephalic targets such as the preoptic area and dorsolateral hypothalamus. My data are compatible with the idea that similar connections may be established in larval zebrafish.

3.8 Discussion

By using focal electroporation to examine the morphology and connectivity of individual neurons, I have analysed the organisation of the lateralised habenulo-interpeduncular circuit at single-cell resolution. My principal find-

ings are:

1. All habenular neurons, on both left and right sides, display a stereotypical unipolar morphology and their axons cross the ventral midline multiple times to establish bilateral connectivity.

2. Two very distinct axon arbor morphologies are apparent, having lateralised origins and differential target connectivity; this underlies the *laterotopic* connectivity of the left and right habenulae.

3. IPN neurons have diverse morphologies that suggest lateralised inputs may either be integrated, or maintained as distinct circuits, and are relayed to diverse downstream nuclei.

3.8.1 Habenular neurons share a stereotypical unipolar morphology

Despite the fact that the habenulae display numerous asymmetries in patterns and extents of gene expression and neuropil organisation, I find that all habenular neurons share many features and possess a stereotypical morphology. The two most conspicuous aspects of this common morphology are also unusual in the vertebrate CNS: unipolar somata and axons that cross the ventral midline repeatedly.

For all the habenular neurons I labelled, the soma extends a single "primary neurite" from which both a dendritic arbor and a long axon derive. Unipolar neurons are uncommon in vertebrates where instead most neurons are bipolar or multipolar. However, unipolar habenular neurons have been described in lamprey (Yanez & Anadon, 1994), frog (Gugliemotti & Fiorino, 1998) and rat (a subset of Hb neurons, Kim & Chang, 2005), suggesting this is an evolutionarily conserved feature of the habenula.

Similar to the medial habenula of mammals (Cajal, 1995) and the dorsal habenula of frogs (Gugliemotti & Fiorino, 1998), the habenulae of larval zebrafish have a glomerular organisation wherein the unipolar neurons are arranged as ovoid shells surrounding a central neuropil domain in which they elaborate their dendritic arbors. Left and right habenulae differ in the organisation of this neuropil (Figure 2.1 and Concha et al., 2003, 2000), which

contains several different types of processes. Dendritic arbors of habenular neurons can integrate afferent inputs from the telencephalon and diencephalon (Hendricks & Jesuthasan, 2007) and, exclusively in the left habenula, parapineal axonal inputs. Given their morphology, peripheral location and the absence of associated neuropil, it seems unlikely that the somata of habenular projection neurons receive axo-somatic synapses and may therefore not play a significant role in signal transduction.

Although all habenular neurons share the same general morphological architecture, there is clearly also diversity within both left and right nuclei. Habenular neurons innervate distinct targets (dIPN, vIPN, raphé) with morphologically distinct axonal arbors and various genes are expressed in partially overlapping sub-domains of the habenulae, revealing molecular diversity (Gamse et al., 2005). Dendritic trees vary in size and morphology and although I have not investigated this possibility, it is likely that distinct sub-types of habenular neuron might elaborate their dendrites within different sub-regions of the neuropil. In support of this hypothesis, the left and right neuropil is topographically organised: parapineal axon arbors are localised to the dorsomedial aspect of the left habenular neuropil (Concha et al., 2003) and pallial afferent axons are likely to terminate in discreet mediolateral locations in a left–right asymmetric manner (Hendricks & Jesuthasan, 2007).

3.8.2 Habenular axons repeatedly cross the midline and establish bilateral connectivity

A second unusual characteristic of habenular neurons is that their axons repeatedly cross the ventral midline to establish elaborate "spiralling" terminal arbors. This feature of habenular axons has previously been described in the classical neuroanatomical studies of Cajal and Herrick (Figure 3.11 and Cajal, 1995; Herrick, 1948) and is perhaps unique to habenular neurons. Although in a few rare cases axons can cross from one side of the brain to the other and back again in two separate commissures (*eg* Fraley & Sharma, 1984), I know of no other examples, in normal development, of decussating axons that can recross the same midline structure. Indeed, there are evolutionarily conserved mechanisms, present from flies to humans, by which growth cones become repelled by midline tissue once they have crossed it

Figure 3.11: **Habenulo-interpeduncular neuroanatomy in the tiger salamander.** (A) Dorsal image showing axons from the FR spiralling back and forth across the midline of the IPN. (B) Lateral view of the IPN and surrounding regions. Urodeles possess an unusually large IPN that is elongated along the AP axis. The somata of IPN neurons are located dorsally in the grey matter of the nucleus and they extend multiple, discrete dendritic arbors ventrally into the interpeduncular neuropil, which intercept the spiralling habenular axons at successive anterior–posterior locations. The IPN neurons also extend fine axons into the tractus interpedunculo-bulbaris. These axons give rise to collaterals that also arborise ventrally within the interpeduncular neuropil and intertwine with the dendritic arbors of other interpeduncular neurons to form small glomeruli. Images adapted from Herrick (1948).

(Kaprielian et al., 2001).

In the tiger salamander (Herrick, 1948) and in mammals (Cajal, 1995), habenular axons maintain an anterior-to-posterior progression as they pass back and forth across the ventral midline. However, the habenular axons of zebrafish not only alternate between left and right sides but also oscillate along the anterior–posterior axis, as they encircle the "core" of the IPN. Because I also observe "doughnut-shaped" arborisation domains in the IPN of medaka and *Astyanax* (Figures 2.7 and 2.8), it seems likely that habenular axon "spiralling" about a dorso-ventrally orientated axis is conserved in teleosts.

How do habenular axons establish their unusual trajectories? Strictly speaking, the arbors are not true spirals but rather display profuse branching with branches reversing sense within the arbor. A relatively simple hypothesis might be that the axons arborise within a permissive territory (outward-pointing dendrites of IPN neurons) surrounding a repulsive core (IPN cell bodies). Another clue comes from *Drosophila* embryos mutant for components of Robo–Slit signalling, in which axon tracts may aberrantly recross the midline of the ventral nerve cord (Seeger et al., 1993; Kidd et al., 1998). Notably, at least one Robo receptor is expressed by habenular neurons in zebrafish embryos at a time that would be compatible with a role in axon guidance (data not shown). It will be an interesting challenge for future studies to identify the axon pathfinding mechanisms that underlie these elaborate arbors and observe how attractive and repulsive cues are arranged in and around the IPN.

3.8.3 Two arbor sub-types with left-right asymmetric origins and distinct target connectivity

Despite having a stereotypical morphology with unipolar somata and multiply-decussating axons, habenular projection neurons display one of two strikingly different axon arbor morphologies. L-typical arbors are tall and highly branched and take the form of a "domed crown". By contrast, R-typical arbors are flattened, with axon branches concentrated towards the perimeter of the arbor. Although both types of arbor are elaborated by both left and right-sided neurons, they show strongly lateralised origins, with the vast majority of left-sided neurons having L-typical arbors and most right-

sided neurons developing R-typical arbors. Because the two arbor sub-types are restricted to different regions of the IPN, their asymmetric origins underlie the *laterotopic* connectivity of the habenulae.

These results reveal, for the first time, how lateralisation of the vertebrate CNS is manifest at the level of single axon morphology and connectivity. The results support the notion that lateralisation is achieved by specifying the same types of circuitry component on both sides of the brain, but having different ratios of those common components so as to produce left–right asymmetric circuits.

Although arbors of a particular sub-type appear very similar, regardless of which habenula they derive from, I can not exclude the possibility that there might be differences between, for example, L-typical arbors from the left *versus* right side. My analysis is limited by the descriptive power of my morphometric parameters as well as by having relatively few examples of the "minority" arbor types (*eg* left-sided R-typical arbors). However, the available molecular data support the idea that similar (or even identical) neuronal types are specified on both left and right sides. As described in §2.6.2, at adult stages, equivalent medial and lateral habenular subnuclei, with distinct patterns of gene expression, can be identified on both sides of the brain. On the left side the lateral, *lov*-expressing subnucleus is enlarged, whereas in the right habenula it is the medial subnucleus, marked by *brn3a*:GFP that contains the majority of neurons. An obvious hypothesis would be that the neurons bearing L-typical arbors localise to the "lateral" subnucleus and express *lov*, regardless of which side they derive from, whilst the R-typical neurons reside in the "medial" subnucleus and express *brn3a*:GFP. Unfortunately, I have not been unable to answer this question, partly because discrete subnuclei are not easily delineated at larval stages — either molecularly or morphologically — and additionally because my confocal imaging of neuronal somata does not enable me to determine their position within the habenula with sufficient accuracy (especially along the DV axis). However, imaging of the epithalamus from the dorsal aspect showed that the neurons I labelled were distributed across the mediolateral extent of both left and right habenulae, suggesting that there is not a significant bias in my sample of left and right-sided neurons. Moreover, the relative proportions of L-typical and R-typical neurons I observed on

left and right show a good qualitative agreement with subnuclear size ratios as determined by gene/transgene expression and with the strong lateralisation evidenced from the laterotopic innervation of the IPN as assessed by lipophilic dye tracing.

Despite these limitations, one clear correlation between soma location and arbor morphology was that neurons elaborating the "minority type" of axon terminal arbor were often located at the most medial edge of the habenula and extended their axons in the contralateral FR.

Although recent studies have shown a temporal progression in the production of different neuronal types in the left and right habenulae (Aizawa et al., 2007), it is extremely unlikely that the differences I have described between L-typical and R-typical arbors can be accounted for by differences in arbor maturity. I limited my analyses to arbors that had completely encircled the IPN and did not bear any visible growth cones on axon branches. In addition, normal L-typical and R-typical morphologies are still present at 10 dpf (data not shown), which suggests the arbors I compared are representative of mature larval morphologies.

3.8.4 Morphologies of IPN neurons and processing of lateralised information

Although CNS lateralisation is manifest in the form of asymmetrical behavioural responses in several species (Vallortigara & Rogers, 2005), the lateralisation of many cognitive functions, such as language processing in the cerebral cortex, does not result in any overtly asymmetric behavioural outputs. The left and right habenulae, which are conspicuously asymmetric, establish efferent connectivity with a unilateral midline target. This potentially provides a mechanism for translating lateralised neural processing into control of bilaterally symmetric downstream circuits, enabling asymmetric circuits in the epithalamus to modulate behavioural outputs that require operation of motor circuits on both sides of the animal. Additionally, the convergence onto the same midline target potentially allows for the integration of lateralised information from the left and right sides of the brain.

Although IPN neurons displayed diverse morphologies, they also shared some common features that inform hypotheses as to how lateralised inputs might be integrated or relayed by the IPN.

A common characteristic of IPN neurons was that they extended their neurites outwards from the core of the nucleus into the surrounding domains of habenular axon terminals, presumably to establish synaptic contacts with the afferent axons. However, whilst some IPN neurons had their neurites restricted to *either* the dorsal *or* ventral arborisation domains, others extended neurites into *both* domains.

The fact that L-typical and R-typical habenular axon terminals are restricted to the dIPN and vIPN respectively, means that the post-synaptic IPN neurons with similarly restricted neurite arbors are likely to receive only one type of afferent input. Because the arbor sub-types have strongly lateralised origins, even if the IPN neurons show no selectivity for left or right-sided axons, they are likely to receive predominantly-left or predominantly-right signals. This suggests the IPN has the capacity to maintain lateralised habenular inputs as largely distinct, independent circuits. I did not have sufficient data to determine whether projection neurons with DV-restricted dendrites projected to distinct or common efferent targets.

IPN neurons with neurites in both dorsal and ventral neuropils indicate that the nucleus has the capacity to perform a balanced integration of left and right-sided signals, again without any specific recognition of the left–right origin of the axons. In this case, lateralised information from the habenulae might converge into a common output pathway. Notably, in the IPN of several mammalian species, "crest" synapses have been described wherein one left and one right habenular axon terminal establish opposing parallel synaptic contacts on either side of a dendritic process belonging to an IPN neuron (Lenn et al., 1983; Lenn, 1976), suggesting that the integration of left and right-sided signals is a conserved feature of the IPN.

The strikingly different morphologies of L-typical and R-typical arbors suggest that dorsal and ventral domains of the IPN might process information differently. Within the dIPN, the highly branched, basket-shaped L-typical arbors spread widely over the dIPN cells. This arrangement seems compatible with L-typical neurons providing widespread inputs to this region of the target rather than there being spatially localised, functionally distinct connections. Thus, the dIPN might function primarily to summate afferent inputs and deliver a uniform output, a function analogous to that originally proposed for the entire IPN by Herrick (1948).

In contradistinction, some R-typical arbors, innervating the vIPN, are remarkably flattened along the DV axis. Correspondingly, some vIPN neurons radiate similarly flattened dendritic arbors. Although I have not demonstrated a direct association between a pair of these flattened arbors, this correlation raises the exciting possibility that there might be precise mapping between the habenula and IPN, suggesting topographical patterning of these nuclei.

What is the physiological significance of the repeated midline crossing displayed by habenular axons? Although the answer to this question is far from clear, a clue might come from comparing the organisation of the zebrafish IPN to that of the tiger salamander. In the salamander, Herrick describes individual IPN neurons elaborating multiple discrete arbors, which intercept the afferent habenular axons at several locations along their length (Figure 3.11B). Because habenular axons in the zebrafish "spiral" around the core multiple times, IPN neurons might be able to intercept progressively more distal regions of the incoming axons with relatively localised dendritic arbors. I have observed some IPN neurons with multiple, discrete arbors in spatially distinct regions of the IPN neuropil (§3.7.4). One possibility is that IPN neurons receive synaptic inputs from progressively distal regions of the afferent habenular axons, perhaps to perform a temporal analysis of incoming signals.

Chapter 4

Nodal signalling specifies the laterality of *laterotopic* habenular circuitry

The Nodal signalling pathway — activated unilaterally in the epithalamus during midsomitogenesis — governs the laterality of epithalamic asymmetries (see §1.3.2 and Liang et al., 2000; Concha et al., 2000). The Nodal ligand *cyc* and the Nodal-responsive genes *lefty1* and *pitx2* are expressed in the left dorsal diencephalon from 18–22 hpf in precursors of both the left habenula and pineal complex. Experimental conditions resulting either in bilateral *or* absent Nodal signalling have the same result: Concordant randomisation of parapineal and habenular laterality. Does Nodal signalling also specifies the laterality of *laterotopic* habenulo-interpeduncular connectivity?

4.1 Disruption of asymmetric Nodal signalling results in concordant randomisation of parapineal laterality and *laterotopic* connectivity

I examined parapineal position and habenular efferent connectivity in larvae in which Nodal signalling was disrupted.

4.1.1 Loss of Nodal signalling

Late-zygotic *one-eyed pinhead* (LZ$oep^{-/-}$) larvae lack Nodal signalling in the brain (Concha et al., 2000) and in accordance with previous studies, I observed randomisation of parapineal position, which was assessed in live embryos by *foxD3*:GFP expression (50% left, 50% right, n=53, Figure 4.1). Dye tracing revealed that larvae having a left-sided parapineal showed a normal pattern of connectivity with the IPN (n=8). However, when the parapineal was positioned on the right, I found that *laterotopic* connectivity was perfectly reversed such that the right habenula predominantly innervated the dIPN and left-sided axons were confined to the ventral target (n=6).

This experiment reveals firstly that Nodal signalling is not required for the development of a left-characteristic pattern of efferent connectivity, nor for asymmetry in habenulo-interpeduncular connectivity. Secondly, the laterality of asymmetric circuitry is coupled to the laterality of epithalamic asymmetries. Thirdly, because the right habenula innervates the dIPN in larvae showing reversal of epithalamic laterality, Nodal signalling is not required for the correct development or patterning of the target IPN.

4.1.2 Bilateral Nodal signalling

In wild-type larvae, Nodal signalling is activated in the left epithalamus and subsequently the left habenula projects to the dIPN. I investigated if Nodal signalling is sufficient to impart such connectivity by examining *no tail (ntl)* morphant (*ntl*-MO) larvae in which Nodal signalling is activated bilaterally in the brain (Concha et al., 2000). In *ntl* morphants, parapineal position was randomised (56% left, 44% right, n=55, Figure 4.2) and the habenulae displayed asymmetric connectivity to the IPN. In larvae with a left-sided parapineal, habenular projections were normal (n=8) whereas the *laterotopic* connectivity pattern was reversed in larvae having a right-sided parapineal (n=7). In no instance did both habenulae make appreciable projections into the dIPN, demonstrating that Nodal signalling does not directly instruct connectivity to the dorsal target.

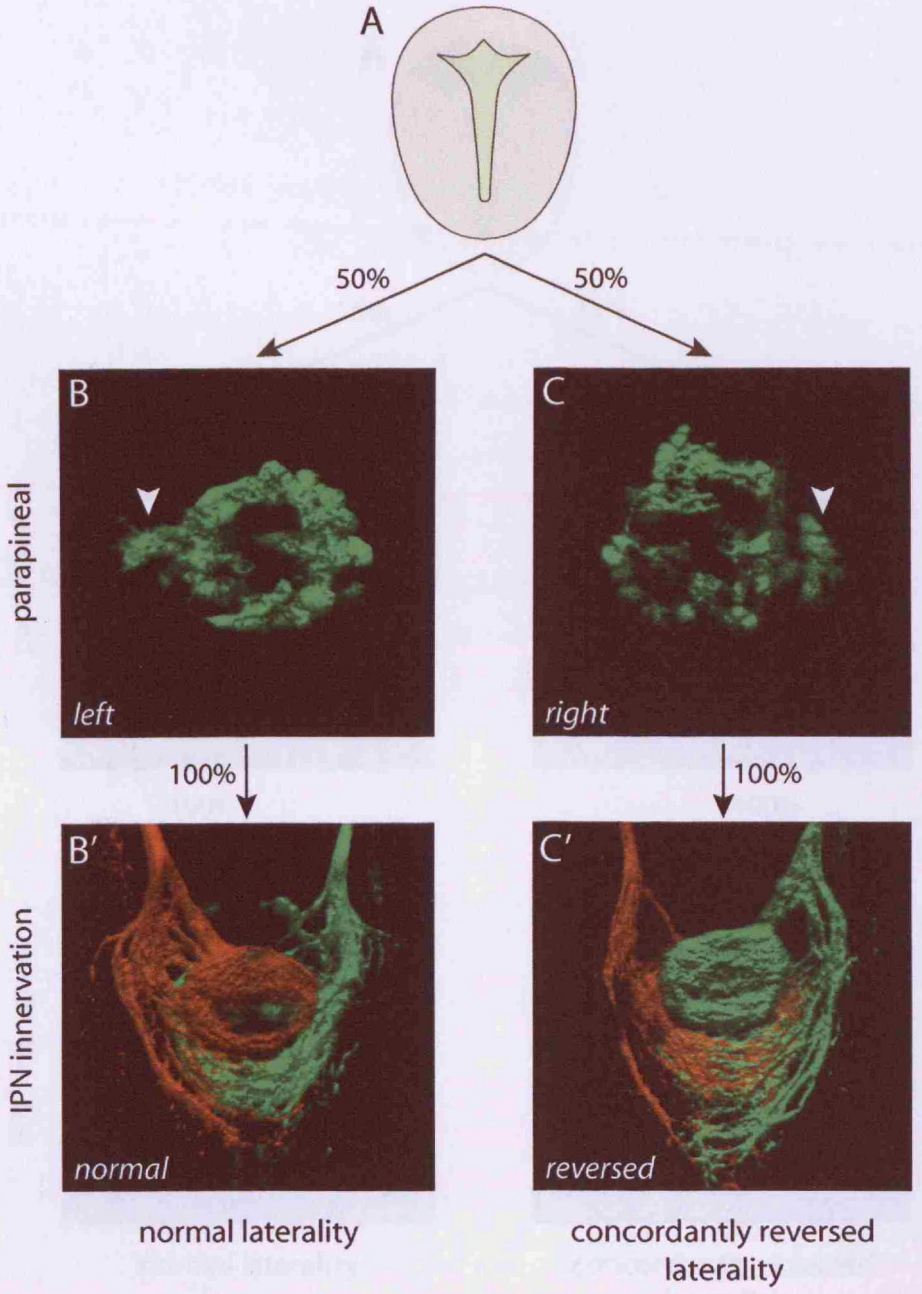

Figure 4.1: **Habenular efferent connectivity in LZ*oep*$^{-/-}$**
(A) Schematic transverse view of the neural tube during midsomitogenesis illustrating that Nodal signalling is absent from the epithalamus in LZ*oep*$^{-/-}$ embryos. (B,C) 3D confocal images of the pineal complex in LZ*oep*$^{-/-}$;Tg(*foxD3*:GFP) embryos at 2 dpf, with an arrowhead indicating the location of the parapineal. (B',C') 3D confocal images of the IPN in LZ*oep*$^{-/-}$;Tg(*foxD3*:GFP) larvae, where parapineal position was previously determined at 2 dpf and subsequently lipophilic dye tracing was used to visualise left (red) and right (green) habenular projections at 4 dpf. In the absence of Nodal signalling, half of the larvae show a normal left-sided parapineal and normal *laterotopic* innervation of the IPN (B,B'), whereas in the remaining larvae, both parapineal position and the left–right origin of axons innervating the dorsal and ventral IPN are perfectly reversed (C,C').
(B,B',C,C'): dorsal views, anterior top.

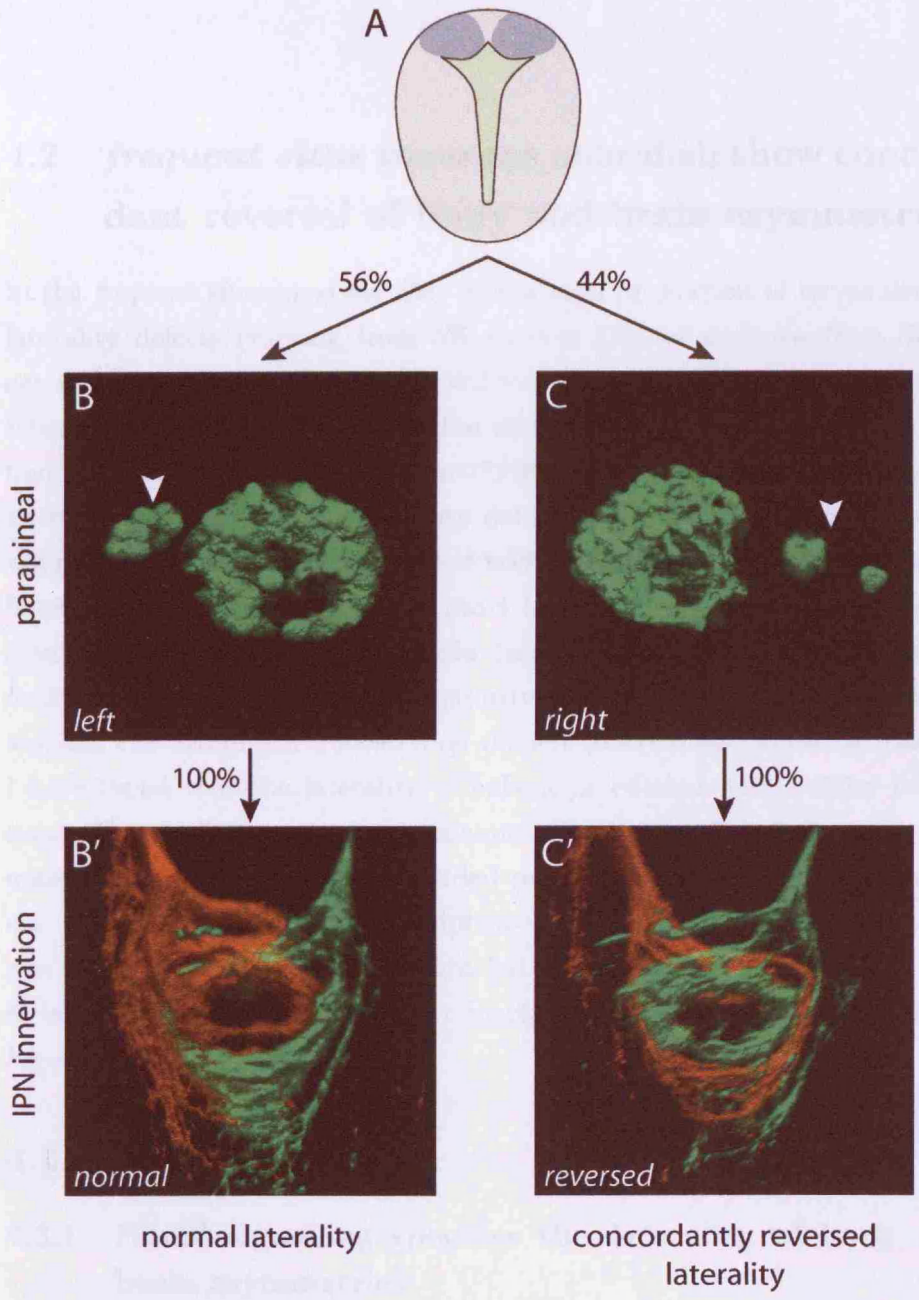

Figure 4.2: **Habenular efferent connectivity in *ntl* morphants**
(A) Schematic illustrating that Nodal signalling (blue shading) is activated bilaterally in the epithalamus of *ntl* morphant (*ntl*-MO) embryos. (B,C) 3D confocal images of the pineal complex in *ntl*-MO;Tg(*foxD3*:GFP) embryos at 2 dpf, with an arrowhead indicating the location of the parapineal. (B',C') 3D confocal images of the IPN in *ntl*-MO;Tg(*foxD3*:GFP) larvae, where parapineal position was previously determined at 2 dpf and subsequently lipophilic dye tracing was used to visualise left (red) and right (green) habenular projections at 4 dpf. When Nodal signalling is activated bilaterally, half of the larvae show normal epithalamic and connectional laterality (B,B'), whereas the other half show concordant reversals in parapineal position and habenulo-interpeduncular connectivity (C,C').

4.2 *frequent situs inversus* zebrafish show concordant reversal of body and brain asymmetries

In the *frequent situs inversus (fsi)* line, a high proportion of larvae display laterality defects (varying from 5% to over 25% of embryos from different sibling matings). The Nodal pathway genes *cyc* and *pitx2* continue to be expressed unilaterally, but on the right side of the epithalamus at high frequency (*cyc*: n=26/60; *pitx2*: n=7/18; Data: A. Barth). The vast majority of *fsi* embryos with laterality defects show complete *situs inversus*, where there is concordant reversal of body (heart, pancreas, gut) and brain laterality: When the direction of heart looping is reversed, the parapineal almost always migrates to the right (assessed by *foxD3*:GFP expression, n=216/241) whereas in the vast majority of *fsi* embryos with normal heart looping, the parapineal is located on the left (n=213/231; Data: A. Barth). I have found that the laterality of habenular efferent connectivity is also concordant with heart and epithalamic laterality in *fsi*. Larvae showing normal heart looping and a left-sided parapineal at 2.5 dpf, showed normal *laterotopic* connectivity at 4 dpf (n=4, Figure 4.3A–A") whereas there was a DV inversion of left and right habenular axon terminals in the IPN of larvae displaying reversed heart looping and parapineal position (n=8, Figure 4.3B–B").

4.3 Discussion

4.3.1 Nodal signalling specifies the *laterality* of body and brain asymmetries

My results agree with previous data showing that Nodal signalling underlies laterality decisions in the body and brain (discussed above in §1.3.2). During normal development, Nodal signalling is asymmetric, being activated unilaterally in the left lateral plate mesoderm and left epithalamus. However, in the absence of Nodal activity (for example in LZ*oep*$^{-/-}$ embryos), asymmetry still develops with apparently normal left and right-characteristic phenotypes, albeit with randomised laterality. This suggests that Nodal activity is not required for left identity, nor for asymmetry *per se*, but it is required for specifying the correct direction of asymmetry. Similarly, the bi-

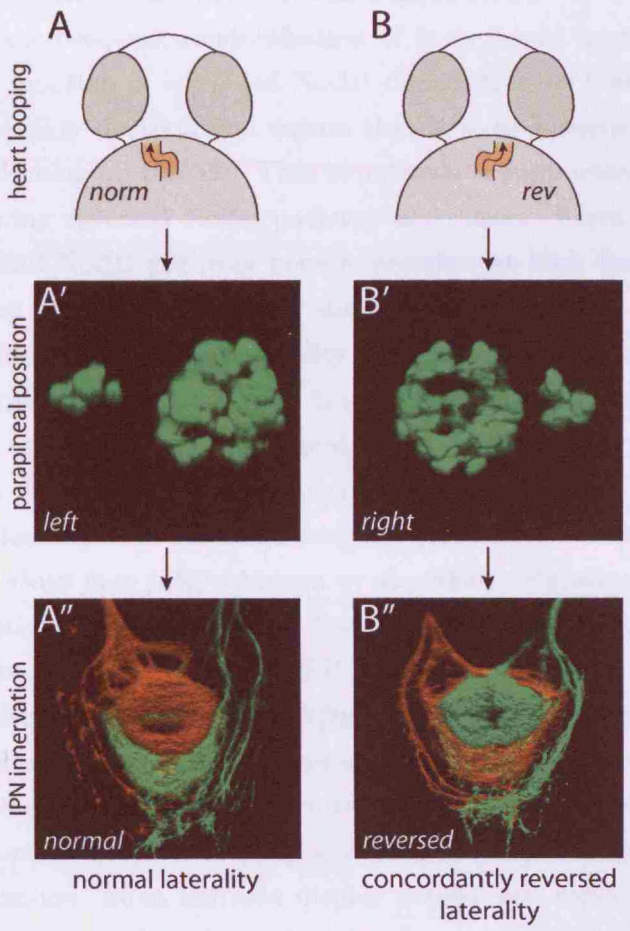

Figure 4.3: **Concordant reversals of body and brain asymmetries in *fsi*.** (A,B) Schematic frontal views, illustrating normal (A) and reversed (B) looping of the developing heart, which was assessed in live *fsi*;Tg(*foxD3*:GFP) embryos at 2.5 dpf; subsequently, parapineal position and habenular efferent connectivity were analysed. (A–A") *fsi* embryos that showed normal heart looping (A) and migration of the parapineal (A') subsequently displayed normal *laterotopic* habenular efferent connectivity (A"). (B–B") *fsi* embryos that showed reversed heart looping (B) and a right-sided parapineal (B'), displayed a perfect reversal in the pattern of IPN innervation (B").

lateral activation of epithalamic Nodal signalling in *ntl* morphant embryos reveals Nodal activity is not *sufficient* to induce left character. Again, normal asymmetries develop, but their laterality is randomised.

These experimental conditions in which asymmetric Nodal activity is lost and there is a subsequent randomisation of body/brain asymmetries, suggest that the function of left-sided Nodal signalling is to bias an otherwise stochastic laterality decision and ensure that left-characteristic phenotypes consistently develop on the left. This hypothesis is supported by data from embryos showing reversed Nodal pathway activation. Firstly, *fsi* embryos show right-sided Nodal pathway gene expression at high frequency and a high frequency of reversals in body and brain asymmetries. However, we did not directly correlate the laterality of Nodal pathway activation with subsequent body/brain asymmetries in individual embryos because gene expression was assessed by *in situ* hybridisation in fixed embryos at a stage preceding the development of asymmetric phenotypes.

Hitoshi Okamoto's lab has addressed this question in a different zebrafish mutant line, *about face (abf)* (Aizawa et al., 2005). Putative *abf* homozygotes frequently display right-sided Nodal pathway activation, which was assessed in live embryos using a GFP transgene driven by enhancer elements of the Nodal-responsive gene *lefty1*. Larvae which showed right-sided *lefty1*:GFP expression at midsomitogenesis stages always showed subsequent reversal of *laterotopic* habenular circuitry (Aizawa et al., 2005).

The concordant reversal of body and brain asymmetries observed in *fsi* embryos is unusual. Most mutants display heterotaxic randomisation (Bisgrove et al., 2000), rather than *situs inversus* and this latter phenotype suggests there is a mechanism to co-ordinate laterality decisions in the body and brain that is preserved in these larvae. In the zebrafish lateral plate mesoderm, the Nodal ligand *southpaw (spw)* is expressed unilaterally on the left side, and controls the laterality of body asymmetries (Long et al., 2003). Inhibiting the expression of *spw* results in loss of expression of *cyc* in the brain. Hence, lateralised Nodal pathway activation in the lateral plate mesoderm is somehow relayed to the brain. It follows that a likely hypothesis is that Nodal signalling is activated in the right lateral plate mesoderm at high frequency in *fsi* embryos and that this right-sided activation is subsequently relayed to the right epithalamus.

4.3.2 Concordance of brain asymmetries

A key observation is that the various asymmetries identified within the DDC of zebrafish larvae consistently display concordant laterality. In LZ*oep*$^{-/-}$ mutants and *ntl* morphants I observed 100% correspondence between parapineal position and the DV organisation of habenular axon terminals in the IPN. Although I did not directly examine habenular laterality in my experiments, previous data have shown ~100% correspondence between parapineal position and the laterality of habenular neuropil asymmetry and *lov* expression in these experimental conditions (Concha et al., 2000; Gamse et al., 2003). This concordance, along with the fact that Nodal signalling is confined to the epithalamus and acts at a much earlier stage than habenular axons start to innervate the IPN, means it is almost certain that the effect of Nodal signalling on the laterality of habenular efferent connectivity is a downstream consequence of a much earlier event in which Nodal influences the lateral identity of habenular neurons or their precursors. Indeed, the concordant laterality of all the asymmetry phenotypes seems compatible with a model where there is a single symmetry breaking event early on, which establishes left and right identities and subsequent to this the various asymmetric phenotypes develop in an invariant manner, one dependent on the other. Alternatively, concordance might be achieved by interactions between structures that, at least in part, independently make left–right identity decisions. This could apply in the case of coupling between habenular and parapineal laterality. It has been suggested that bidirectional communication between the developing parapineal and adjacent habenula functions to mediate such concordance and strengthen left-characteristic phenotypes (see §1.3.3 and Concha et al., 2003).

In summary, my results, along with previous studies, demonstrate that the role of Nodal signalling is to specify the direction of neural lateralisation, thus establishing population laterality.

Chapter 5

The role of the parapineal in the development of habenulo-interpeduncular asymmetry

The leftward migration of the parapineal represents the earliest asymmetric phenotype — subsequent to unilateral Nodal signalling — currently described in the dorsal diencephalon. As such it is a good candidate for a symmetry breaking event that might establish asymmetry in the DCC. Bilaterally located parapineal precursors condense at the rostral limit of the pineal anlage between 24 and 28 hpf and start migrating leftwards from around 30–32 hpf (Concha et al., 2003). This lateralised migration precedes the onset of *lov* expression (from 38 hpf, Gamse et al., 2003), the development of asymmetric habenular neuropil (from ~70 hpf, Concha et al., 2003) and the establishment of *laterotopic* efferent connectivity with the IPN (from ~60 hpf, see §2.4).

Two studies that have examined the development of epithalamic asymmetries following ablation of parapineal precursors have come to somewhat different conclusions regarding the role of the parapineal in establishing asymmetry. Gamse et al. (2003) state that *lov* expression and neuropil organisation become symmetric following removal of the parapineal, wherein both habenulae display a "right-sided" phenotype. These authors conclude

the parapineal is a determinant of left identity. By contrast, Concha et al. (2003) present evidence that although asymmetry of *lov* expression and neuropil density are reduced following parapineal ablation, left–right differences are still apparent. They suggest that the parapineal functions to amplify left-characteristic phenotypes but is not necessary to assign different left and right identities.

To better understand the role of the parapineal, I have analysed the development of epithalamic asymmetries, the *laterotopic* targeting of habenular axons and the lateralised morphology of individual axon terminals in larvae lacking a parapineal.

5.1 Asymmetry in the epithalamus

Using Tg(*flh*:eGFP);Tg(*foxD3*:GFP) transgenic embryos, in which the pineal anlage and mature parapineal are labelled by GFP expression, I removed parapineal precursors by laser ablation at 24–28 hpf as they condense at the dorsal midline prior to migration towards the left habenula. Successful removal of *all* parapineal cells was confirmed by confocal microscopy at 3 dpf and I subsequently examined molecular and neuroanatomical asymmetry markers at 4 dpf.

Consistent with previous data, ablation of the parapineal affected asymmetric gene expression and neuropil organisation (Table 5.1). Left-sided *lov* expression was always reduced, although a small medial domain of expression in the left habenula consistently retained asymmetry (n=20, Figure 5.1C) in a similar region to where a small tuft of neuropil also showed asymmetry (Figure 5.1G). Complementing the reduction of *lov* expression, left-sided expression of *tag1*, *ron* and *dex* were expanded to levels similar to those normally seen on the right (Figure 5.1E, Table 5.1 and data not shown).

Taken together, these results show that although the magnitude of molecular and neuroanatomical asymmetries are greatly reduced following loss of the parapineal, subtle left–right differences in *lov* expression and neuropil organisation remain, suggesting the habenulae might retain distinct characteristics.

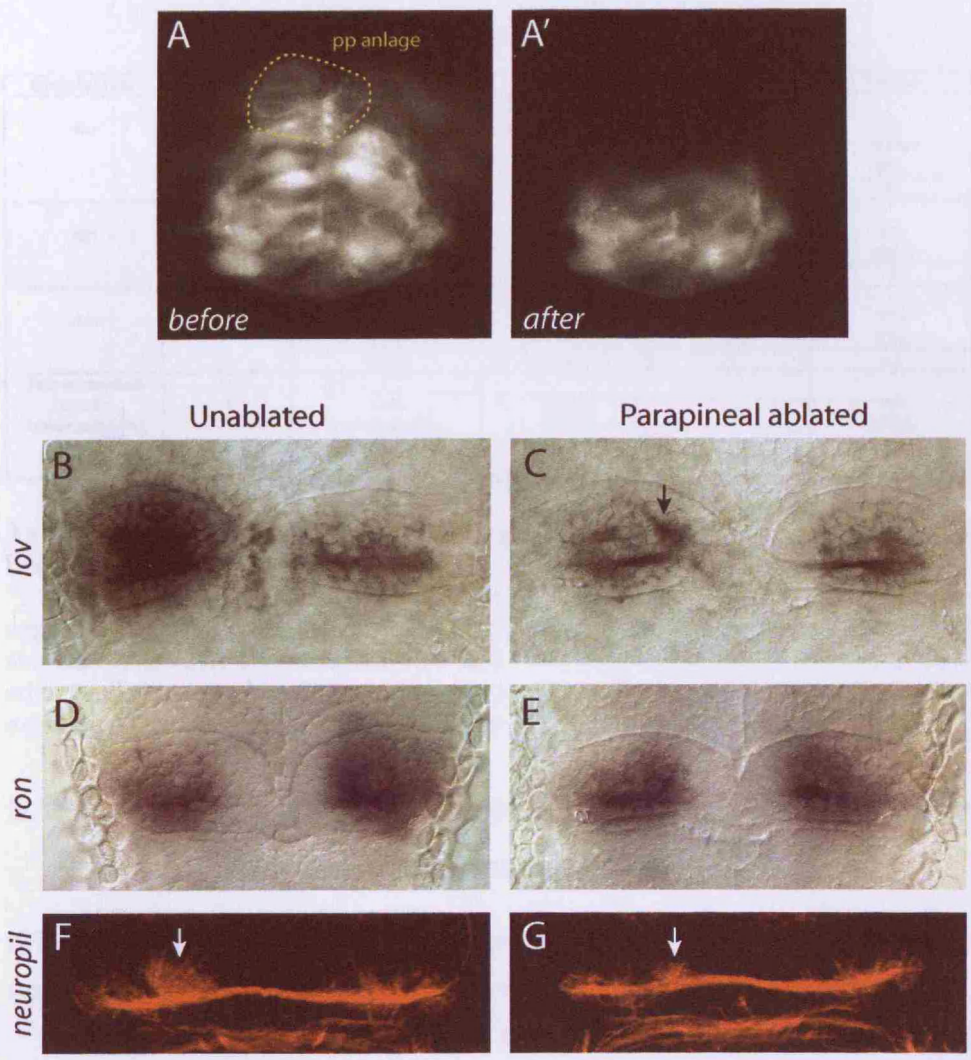

Figure 5.1: **Parapineal ablation causes a substantial reduction in epithalamic asymmetries.**
(A,A') Epifluorescence images of the pineal complex, visualised in Tg(*flh*:eGFP);Tg(*foxD3*:GFP) transgenic embryos, before (A) and after (A') laser-ablation of the parapineal anlage (indicated by orange dotted domain) at ~24 hpf. Bleaching of GFP fluorescence occurs in a broader region to that in which cells are killed during the ablation protocol. (B–G) Dorsal views of the epithalamus in unablated control larvae and larvae in which parapineal ablation was performed at 24–28 hpf and gene expression or neuropil organisation were assessed at 4 dpf. (B,C) In the parapineal-ablated larva, *lov* expression is substantially reduced in the left habenula to levels similar to the right habenula. However, a small, asymmetric, medial expression domain is retained (arrow in (C)). (D,E) *ron* expression appears bilaterally symmetric in the parapineal-ablated larva. (F,G) Anti-acetylated α tubulin immunostaining reveals a considerable reduction in the size of the asymmetric dorsomedial neuropil domain in the left habenula after parapineal ablation. However, a small medial "stump" is retained (arrows). All panels show dorsal views, anterior top.

Gene/Marker	Age (dpf)	Phenotype*	Unablated	Failed ablation	Ablated
lov	4	L>R (WT asymm) L>R (medium) L>R (weak)	100% 0% 0%	100% 0% 0%	0% 15% 85%
		n	8	8	20
ron	4	R>L R=L	83% 17%	- -	0% 100%
		n	6		7
dex	4-5	R>L R=L	90% 10%	67% 33%	27% 73%
		n	20	3	15
Anti-Acetylated tubulin immunostaining (neuropil)	4	L>R L>R (retaining truncated medial tuft)	100% 0%	- -	0% 100%
		n	7		11

Table 5.1: **Summary of effects of parapineal-ablation upon expression of habenular markers.**
*, for *lov* expression, L>R (WT asymm) indicates the wild-type pattern of *lov* expression. L>R (weak) indicates *lov* was expressed at low levels, characteristic of the wild-type right habenula, on both sides but the left habenula showed a small additional domain of medial expression. L>R (medium) clearly showed stronger expression on the left, but not to the same extent as for wild-type specimens.

5.2 The parapineal is required for *laterotopic* habenular efferent connectivity

I find that the parapineal is essential for the normal development of *laterotopic* habenulo-interpeduncular connectivity.

In unablated control larvae (n=6) and in specimens in which the ablation procedure failed to eliminate all parapineal precursors ("failed ablated", n=9), *laterotopic* connectivity was completely normal; left habenular axons show dense innervation of the dIPN and lesser innervation of the vIPN, whereas right-sided axons appear to terminate almost exclusively in the ventral target (Figure 5.2). However, in parapineal-ablated larvae, there is striking reduction in innervation of the dIPN by left habenular neurons (n=13). Moreover, I consistently observed denser innervation of the vIPN by left-sided axons, suggesting that left habenular projection neurons have re-routed to the ventral target. In parapineal-ablated specimens, we also observed two small "tufts" of neuropil at the rostral end of the dIPN, containing both left, and to a lesser extent, right-sided axons (Figure 5.2C"). Later experiments provide an explanation for this ectopic labelling (see §5.4).

In summary, this experiment suggests that at the level of resolution

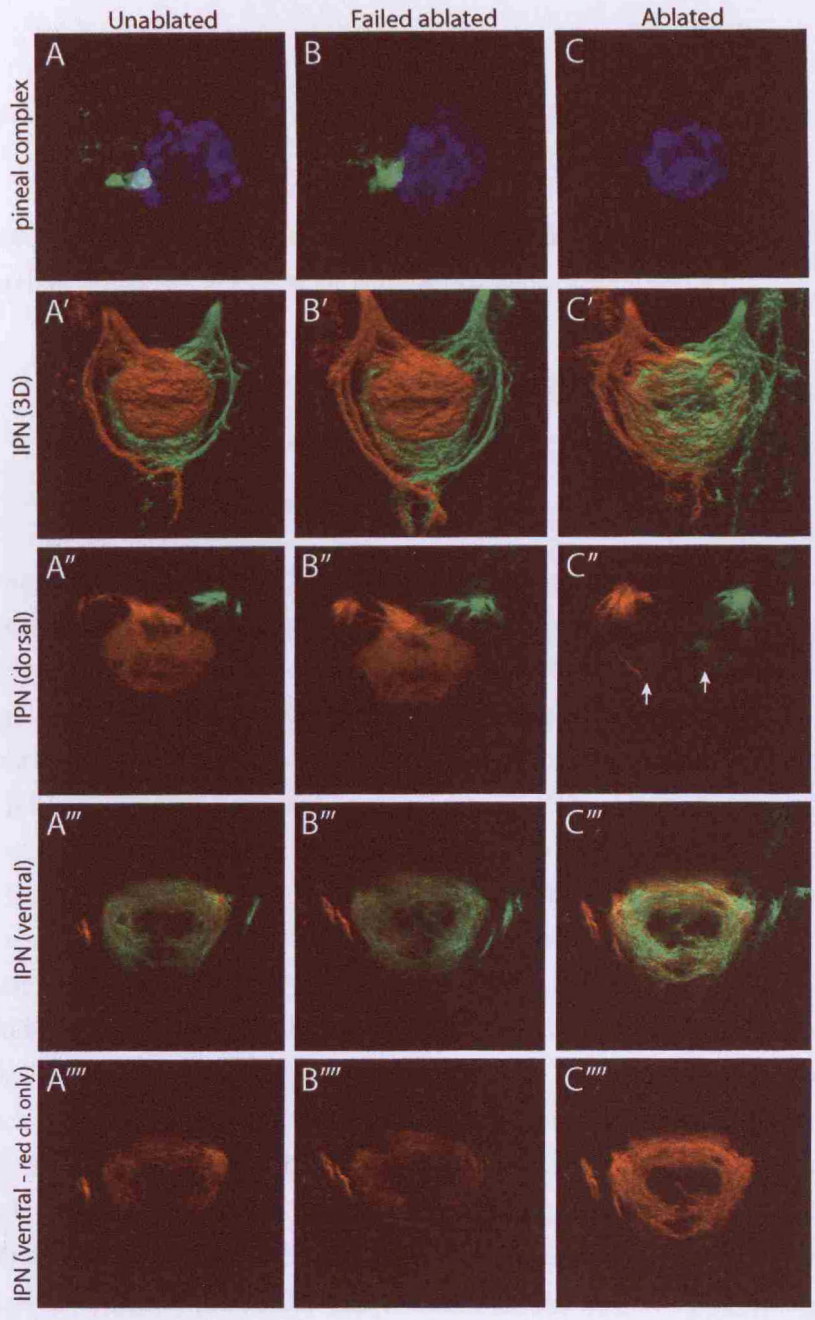

Figure 5.2: **Parapineal ablation eliminates *laterotopic* habenular efferent connectivity.** (A–C) Dorsal views of the pineal complex at 3 dpf, visualised in Tg(*flh*:eGFP);Tg(*foxD3*:GFP) transgenic larvae, following laser ablation of parapineal precursor cells at 24–28 hpf. (A) Unablated control larva. (B) "Failed ablation" larva, in which the parapineal has not been eliminated. (C) Parapineal-ablated larva, which lacks all parapineal cells. For clarity, pineal cells are pseudocoloured blue and parapineal cells pseudocoloured green. (A',B',C') 3D reconstructions of left (red) and right (green) habenular axon terminals in the IPN. (A",B",C") Single confocal *z*-slices through the dIPN. (A"', B"', C"') Single confocal *z*-slices through the vIPN. Following parapineal ablation there is an almost complete loss of left habenular innervation of the dIPN (C"). However, two small tufts of neuropil, containing both left and right-sided axons, are consistently observed in the rostral dIPN (arrows in C"). In parapineal-ablated larvae, there is an increase in the density of left-sided axon terminals in the vIPN (compare C"" to A"" and B"" — these panels show the red channel only in the vIPN *z*-slice). All panels show dorsal views, anterior top.

afforded by lipophilic dye tracing, habenular efferent connectivity becomes symmetric following ablation of the parapineal.

5.3 In the absence of the parapineal, individual left and right-sided axons retain distinct, lateralised morphologies

Although lipophilic dye tracing shows that left-habenular axons change their projection patterns following parapineal ablation, it does not reveal the underlying alterations in terminal arbor morphology responsible for this change. Two possibilities are either that left-sided axons adopt R-typical morphologies and projection patterns in the absence of the parapineal, or that left-sided axons terminate in the same vIPN region, but continue to form arbors with a distinct, lateralised morphology. To address this issue, I used focal electroporation to label individual left and right-sided projection neurons in parapineal-ablated larvae and conducted morphometric analyses of their axonal arbors.

Following parapineal-ablation, left-sided neurons elaborate arbors with a unique "Ab-L" morphology (Figure 5.3B,C). By comparing the location of such arbors to that of the oculomotor nucleus, I localised them to the vIPN. This was confirmed by anti-GFP immunostaining followed by histological sectioning (data not shown) and is in agreement with my lipophilic dye tracing results (above, §5.2). These Ab-L arbors extend over a restricted DV depth (20.1±2.9 μm), which is similar to that of R-typical arbors (17.7±1.2 μm) and significantly smaller than for L-typical axons (31.0±1.3 μm) ($p>0.05$ for Ab-L vs R-typical; $p<0.001$ for Ab-L vs L-typical; Figure 5.4A). In addition, in parapineal-ablated larvae, left-sided axons elaborate arbors with significantly fewer branch points (11.8±1.7) than wild-type L-typical arbors (19.3±1.9) ($p<0.05$ for Ab-L vs L-typical; $p>0.05$ for Ab-L vs R-typical; Figure 5.4B) and the overall width/length ratio of Ab-L arbors (1.12±0.03) is very similar to that of R-typical axons (1.13±0.07; Figure 5.4C).

Although Ab-L axons project ventrally and display several morphological features characteristic of R-typical arbors, they are not identical to the

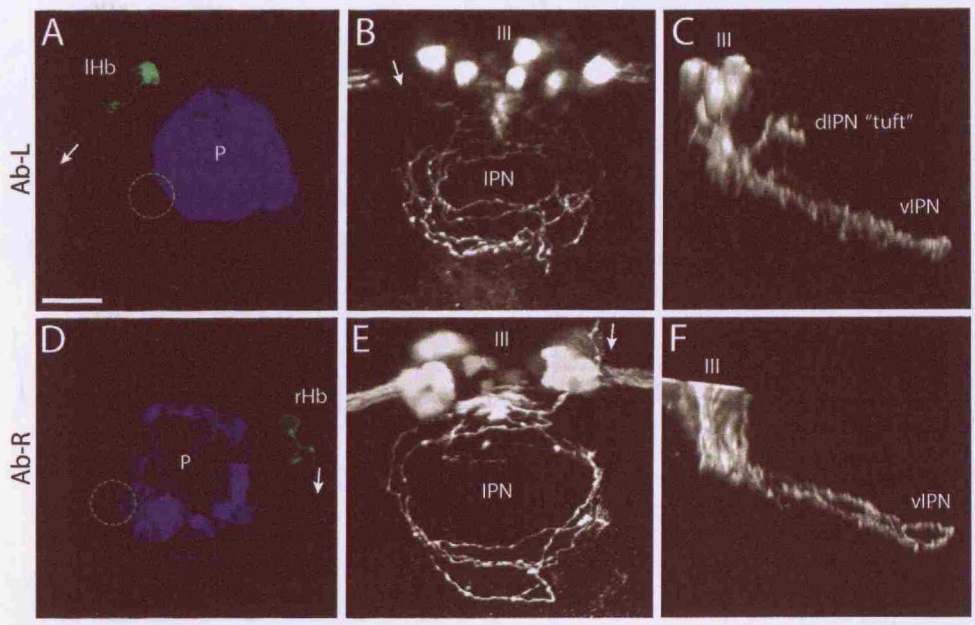

Figure 5.3: **Habenular axon arbors retain distinct morphologies in parapineal-ablated larvae.**
(A–F) Images from brains of 4 dpf Tg(*flh*:eGFP);Tg(*foxD3*:GFP) transgenic larvae in which parapineal ablation was performed at 24–28 hpf and single neurons in the left or right habenula were labelled by focal electroporation at 3 dpf. (A,D) Confocal projections of the dorsal diencephalon confirming successful ablation of the parapineal (indicated by dotted circles) and labelling of single left (A) or right (D) habenular projection neurons. (B,C) Dorsal (B) and lateral (C) views of flattened axonal arbors elaborated by single left-sided neurons in the vIPN after parapineal ablation. Axon branches frequently extend towards the centre of the vIPN in these arbors. Some left-sided axons extend collateral branches into the anterior dIPN that terminate with a unique tuft morphology (tuft in (C)). The oculomotor nucleus, which lies just anterior to the IPN, expresses GFP in these transgenic larvae and allows the DV position of the arbors to be determined. (E,F) Dorsal (E) and lateral (F) views of arbors formed by single right-sided neurons after parapineal ablation. These arbors appear as a more exaggerated form of the R-typical morphology. Axon branches are strongly localised to the perimeter of the arbor and extend over a very limited DV depth. Scale bar in (A): 20 μm. Abbreviations: III, oculomotor nucleus.

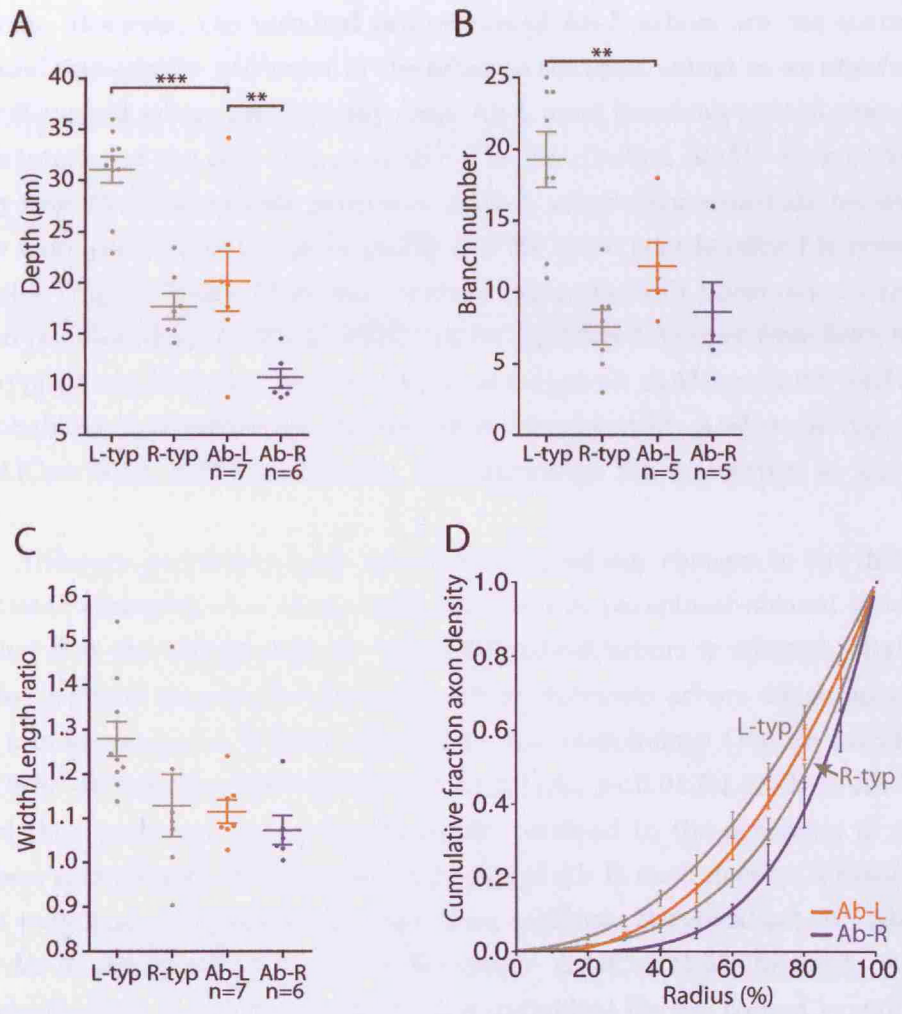

Figure 5.4: **Morphometric quantification of habenular axon arbors in parapineal ablated larvae**
(A) Both Ab-L and Ab-R arbors extend over a limited DV depth, similar to R-typical arbors. However, Ab-R arbors are significantly flatter than Ab-L arbors. (B) Ab-L arbors have a reduced number of branch points as compared to L-typical arbors. (C) The width/length ratios of Ab-L and Ab-R arbors are similar to those of R-typical arbors. (D) Radial distribution of axon density for 6 Ab-L and 5 Ab-R arbors. Details of the non-linear regression are shown in Table 3.1.
In these graphs, L-typical and R-typical data, shown in grey, is the same as presented in Figure 3.7. Horizontal lines indicate mean values and error bars show SEM. **, $p<0.01$; ***, $p<0.001$.

R-typical arbors of wild-type embryos. In Ab-L arbors, many of the terminal neurites surround the central "core" of the IPN, as is the case for R-typical axons. However, the terminal projections of Ab-L arbors are not concentrated towards the perimeter of the arbor to the same extent as we observed for R-typical arbors and in many cases Ab-L axon terminals extend towards the interior of the IPN (Figure 5.3B). The distribution profile of axon density from the centre to the perimeter of Ab-L arbors is intermediate between the more centralised L-typical profile and the more peripheralised R-typical profile (Figure 5.4D). Moreover, analysis using Akaike's Information Criterion revealed that the Ab-L profile can be considered distinct from both the L-typical and R-typical profiles (Ab-L vs L-typical: ΔAICc=12.92, 99.84% probability that individual fits are correct vs global fit; Ab-L vs R-typical: ΔAICc=19.52, >99% probability that individual fits are correct vs global fit).

Although previous studies have not reported any changes in the differentiated characteristics of the right habenula in parapineal-ablated larvae, I find that the morphology of right-sided axonal arbors is affected. Right-sided neurons in parapineal-ablated larvae elaborate arbors which appear as a more exaggerated form of the R-typical morphology (Figure 5.3E,F). "Ab-R" arbors are extremely flat (10.6$\pm$0.9 μm; $p<0.01$ for Ab-L vs Ab-R) and their processes are extremely tightly confined to the perimeter of the arbor; accordingly, the distribution profile of Ab-R axon density is distinct not only from Ab-L arbors but also from wild-type R-typical arbors (Ab-L vs Ab-R: ΔAICc=57.5; Ab-R vs R-typical: ΔAICc=21.55; for both comparisons there is >99% probability that individual fits are correct vs global fit).

In summary, these analyses reveal that in the absence of signalling from the unilateral parapineal, both left and right habenular neurons innervate the vIPN but asymmetry is retained at the level of the morphology and targeting of individual left and right-sided axon terminals.

5.4 Habenular axons form ectopic terminal tufts into the rostral dIPN in the absence of the parapineal

In parapineal-ablated specimens, I occasionally electroporated left or right-sided neurons that had "tufts" of axonal processes that innervated the dIPN (3/20 Ab-L axons; 3/32 Ab-R axons; Figure 5.3C). These arbors are highly branched, extend to both sides of the midline and are confined to the anteriormost end of the dIPN. Such tufting of axonal terminals was never observed for either left nor right habenular axons in wild-type larvae. It seems likely that these arbors constitute the small domain of neuropil density I observed in the rostral dIPN when the entire contingents of left and right-sided axons were labelled by dye tracing in laser-ablated larvae (above, §5.2).

5.5 Discussion

I have analysed the development of lateralised phenotypes in the habenulo-interpeduncular circuit in larvae in which the parapineal has been removed by laser-ablation. My results show that this unilateral nucleus is essential for the normal development of asymmetric characteristics. However, it does not seem to mediate a simple symmetry breaking mechanism that constitutes a binary choice between left and right character.

5.5.1 The parapineal is required for normal epithalamic asymmetries and *laterotopic* connectivity

In parapineal-ablated larvae, the left habenula fails to innervate the dIPN and instead left-sided axons appear to re-route to the ventral target, suggesting this is a "default" connectivity pattern. Consequently, *laterotopic* connectivity is lost and the habenulae appear to show right-isomerism in their efferent circuitry. A recent report has suggested that the mechanism by which the parapineal influences axon guidance involves upregulation of *nrp1a* expression on the left (Kuan et al., 2007b). The authors present evidence that Nrp1a is expressed by left habenular axons and acts to guide them to the dIPN in response to Sema3D. In parapineal-ablated larvae,

nrp1a expression is greatly reduced in the left habenula to levels normally seen on the right.

As discussed in §2.6.2, in adult zebrafish the *laterotopic* connectivity pattern is associated with a left–right asymmetry in the size ratios of the medial and lateral habenular subnuclei. Although at larval stages discrete subnuclei are not easily delineated, the same molecular markers that are specific for the subnuclei at adult stages are expressed asymmetrically by the left and right larval habenulae. Complementing the loss of *laterotopic* connectivity, and in agreement with previous studies (Gamse et al., 2005, 2003; Concha et al., 2003), I find that in parapineal-ablated larvae the left habenula adopts patterns of gene expression and neuropil organisation very similar to the right nucleus. The magnitude of all the molecular and neuroanatomical asymmetries is greatly reduced. However, whilst some phenotypes appear to show right-isomerism in the absence of the parapineal (*eg ron* and *dex* expression), subtle left–right differences are consistently retained in *lov* expression and anti-acetylated α tubulin immunostaining.

5.5.2 In the absence of the parapineal, both left and right-sided neurons elaborate terminate arbors with unique, lateralised morphologies.

In Chapter 3, I presented evidence that the habenulae contain two distinct sub-types of projection neuron, with either L-typical or R-typical terminal arbors and the proportions of these two neuronal sub-types is markedly different in the left and right nuclei. The epithalamic and connectional phenotypes observed in parapineal-ablated larvae seem compatible with (at least) two hypotheses. Firstly, parapineal ablation might shift the composition of the left habenula towards that observed on the right, such that both nuclei are almost entirely composed of ventrally-targeting neurons with the same molecular–genetic identity. Alternatively, there may not be a simple binary switch in neuronal fate, but rather L-typical left habenular neurons might lose a sub-set of their left-characteristics in the absence of the parapineal.

The simplest interpretation of my single-cell analyses supports the latter model. In parapineal-ablated larvae, left-sided neurons elaborate terminal arbors with a unique, Ab-L morphology. Although these terminals share features of wild-type R-typical arbors, including targeting to the vIPN and a

limited DV extent, they differ in the radial distribution of terminal neurites, showing greater branching into the interior of the IPN. These observations seem compatible with the idea that the mature L-typical phenotype is an ensemble of several sub-phenotypes and only some of these (including DV targeting, DV extent and some molecular characteristics) are under parapineal control.

Strikingly, I also observed a change in the morphology of right-sided terminals, which displayed an exaggerated Ab-R morphology following parapineal ablation. In particular, neurite branches were very strongly localised to the perimeter of the arbor. A change in the phenotype of right-sided neurons was surprising as the parapineal is exclusively associated with the left habenula in wild-type larvae. I consider the most likely explanation is that (direct or indirect) interactions between left and right axons in the vIPN are responsible for this peripheral restriction of right-sided arbors. For example, occupancy of the more medial vIPN by left-sided axons might displace the Ab-R axons towards the periphery.

In light of these observations, my data may be more compatible with the first of the hypotheses presented above, wherein identical neuronal sub-types with the same molecular–genetic identity are born in both left and right habenulae in the absence of the parapineal. Mature projection neurons could display lateralised phenotypes as a result of subsequent left–right differences in environmental interactions. One possibility as to how this might occur is suggested by a recent report that demonstrated an asymmetry in the timecourse of neurogenesis between the left and right habenulae (Aizawa et al., 2007). Neurons tend to be born earlier on the left side and these early born cells express *lov* and enter the lateral subnucleus. By contrast, neurogenesis is delayed on the right side such that few *lov*-positive cells are produced; most neurons are born at later stages when they acquire a different identity: expression of *brn3a*:GFP and incorporation into the medial subnucleus.

If such a timing difference were maintained in parapineal-ablated larvae, this could result in initially equivalent neuronal sub-types being exposed to different environmental conditions and as such, developing different mature morphologies. For example, early-born, left-sided neurons might innervate the target first and occupy the medial vIPN. Consequently, later-born right-

sided neurons would become restricted to the perimeter of the vIPN as a result of interactions with the left-sided axons already innervating the target and so consequently display the Ab-R phenotype.

In future experiments it would be interesting to examine this possibility, initially by determining whether asymmetry in the timecourse of neurogenesis and IPN innervation is preserved in parapineal-ablated embryos.

Regardless of whether neurons with equivalent, or different identities are specified in the habenulae in the absence of signalling from the parapineal, the fact that subtle asymmetries are still observed in the epithalamus, as well as at the level of terminal arbor morphology, demonstrates that the parapineal is not, by itself, a simple binary determinant of left–right identity. There must be some other developmental signal that accounts for the persistence of left–right differences in the parapineal-ablated larvae.

An obvious candidate for such a signal is unilateral Nodal pathway activity. It is very likely that Nodal signalling is activated in both parapineal and habenular precursor cells (Concha et al., 2003), suggesting that Nodal signalling could influence habenular development independently of any role in directing parapineal migration. As discussed in Chapter 4, current evidence suggests that Nodal does not directly mediate asymmetry, but rather specifies a consistent laterality, or direction, of asymmetries. However, recent unpublished results from Myriam Roussigne and Patrick Blader (personal communication) suggest that Nodal signalling might have a direct influence on very early neurogenesis in the left habenula.

In future studies, such a role for Nodal could be tested by examining the morphology of habenular axon arbors in fish that lack a parapineal *and* lateralised Nodal signalling. If Nodal is responsible for the maintenance of subtle lateralisation in parapineal-ablated larvae, left and right axons would be expected to display the same arbor morphology in conditions where Nodal is absent (*eg* parapineal-ablated LZ*oep*$^{-/-}$ embryos), or bilaterally symmetric (*eg* parapineal-ablated *ntl*-MO embryos).

5.5.3 Dorsal "tufts" observed in parapineal-ablated larvae

Although the vast majority of dIPN innervation was absent following parapineal ablation, using lipophilic dye tracing we often observed small, bilaterally paired "tufts" of neuropil from left and right-sided axons in the anterior

end of the dIPN. Two main lines of evidence suggest this neuropil represents a novel pattern of axonal termination rather than maintenance of part of the normal dIPN innervation: Firstly, the tufts contain more right-sided axon terminals than are observed in the dIPN in wild-type larvae (where right-sided innervation is on the borderline of detection by dye tracing). Secondly, my single-cell analyses reveal that the axon terminals forming these tufts have an unusual "tuft" morphology that is quite different to the L-typical morphology adopted by axons innervating the dIPN in wild-type larvae.

One explanation might be that in parapineal-ablated larvae, some vIPN targeting axons, from both sides of the brain, extend collateral branches into the vacant dIPN territory, analogous to other situations where targets have been denervated (Jain et al., 2000). The unusual morphology of the arbors might arise as a consequence of the erroneous interaction of dIPN environmental factors with the molecular characteristics of axons directed towards the ventral IPN.

In conclusion, my data demonstrate that the parapineal is important for the development of normal asymmetries in the DCC. However, subtle left–right differences are retained in the absence of this unilateral nucleus, suggesting that other developmental signals convey left–right information to this circuit.

Chapter 6

General Discussion

6.1 Summary

The aim of this thesis was to identify neural asymmetry at the level of circuit architecture and investigate the developmental mechanisms that establish circuit lateralisation. My principal findings are:

1. The habenulo-interpeduncular projection displays conspicuous asymmetry in the larval zebrafish. Left and right-sided axons are segregated along the DV axis of the IPN in a *laterotopic* manner. Most left-sided axons terminate in the dorsal IPN whereas almost all right-sided axons innervate the ventral target. Moreover, this segregation is conserved in two other teleosts species. Although differences have been described in the density/size of axon tracts or volumes of white matter on the left and right sides of the brain (see §1.1.2), this finding represents one of the first identifications, in vertebrates, of asymmetry at the level of axon targeting and neuronal connectivity.

2. Two sub-types of habenulo-interpeduncular projection neuron can be recognised with very distinct axon arbor morphologies and target connectivity. These sub-types have lateralised origins, being found in both left and right habenulae, but in very different proportions. Thus, most left-sided neurons form L-typical, crown-shaped arbors which localise to the dIPN whereas the vast majority of right-sided neurons elaborate flattened spiral-shaped R-typical arbors restricted to the vIPN.

3. The morphologies and connectivity of individual post-synaptic neurons suggest the IPN has the capacity either to integrate left-typical and right-typical inputs or to handle them independently, thus preserving left–right coding.

4. Nodal signalling controls the laterality of *laterotopic* habenular efferent connectivity. Left–right reversals in Nodal signalling correlate with reversal of epithalamic and connectional asymmetries and in cases in which unilateral Nodal signalling is lost, asymmetries still develop, but with randomised laterality. This suggests that, in the vertebrate brain, the genesis of neural asymmetry and the control of the laterality of that asymmetry are processes that can be uncoupled and that Nodal functions to ensure strong population laterality.

5. The parapineal is essential for the development of normal asymmetry phenotypes within the zebrafish DDC. However, whilst certain lateralised phenotypes are lost and the the magnitude of others is reduced in parapineal-ablated larvae, the maintenance of subtle left–right differences in single axon arbor morphology imply that other developmental signals impinge upon this circuit to mediate its lateralisation.

6.2 Models for nervous system lateralisation

It is currently unknown how lateralisation of cognitive function is manifest at the level of circuit microarchitecture. There are at least three, non-mutually exclusive ways in which neural circuits might be lateralised within the CNS (Figure 6.1).

Size In perhaps the simplest model, equivalent regions on the left and right sides would contain the same classes of neuron and patterns of circuitry but differ only in size. As a result of such "scaling", a particular cognitive function might be lateralised simply as a result of more neural substrate existing on one or other side. In support of this possibility, there are numerous reports of asymmetries in the sizes of brain regions (some are discussed in §1.1.2). Moreover, Rosen (1996) observed that in the rat somatosensory/somatomotor cortex, asymmetry in tissue volume is strongly

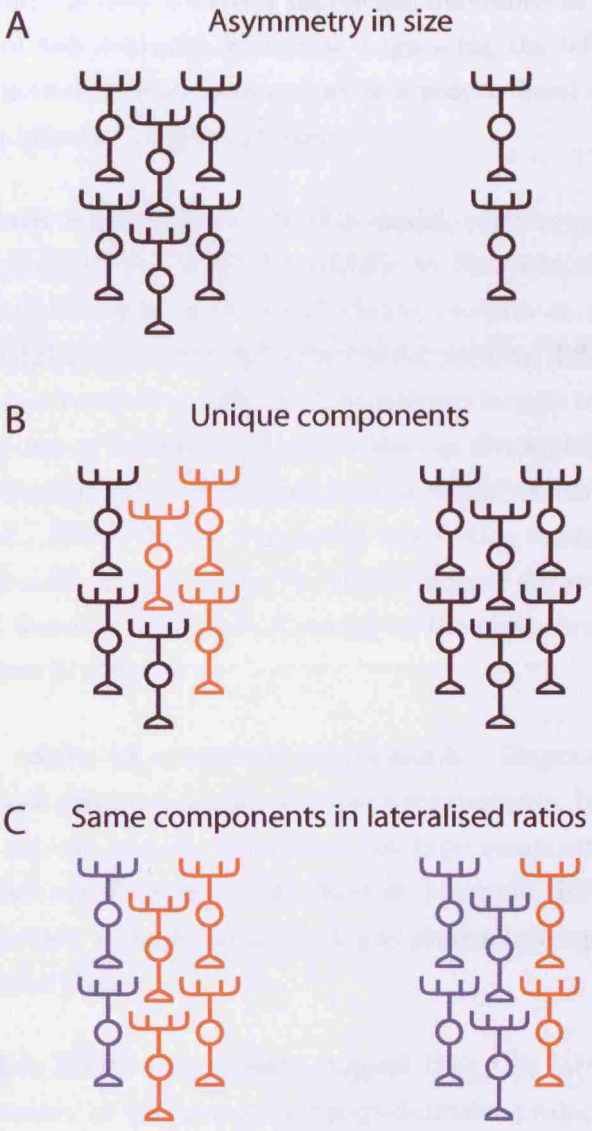

Figure 6.1: **Models for lateralisation of neural tissue.**
(A) Equivalent regions on the left and right of the CNS are identical in composition and differ only in overall size. (B) Unique types of neuron, or patterns of connectivity, may be specified on either the left or right or both sides (indicated by unique red neurons on the left in this schematic). (C) Identical circuit components might exist on both sides of the CNS, but in different ratios. Note that these models are in no way mutually exclusive. In fact, it is likely that all three strategies may be involved in lateralisation of habenulo-interpeduncular circuitry (see main text).

associated with left–right differences in the numbers of two sub-types of neuron but there is only a weakly significant difference in cell packing density for one of the neuronal sub-types, suggesting the left and right sides have similar neural architectures and show a proportional scaling to achieve differences in quantity of neural tissue.

Unique circuit components In this model, certain types of neuron, or patterns of connectivity, might be specific to one side and would not be present on the other side of the CNS. Hence, circuits on the left and right might receive different types of afferent inputs, perform different neural computations and/or connect to different downstream targets to mediate distinct types of cognition or behaviour. For instance, in *Drosophila*, an asymmetrical body, marked by fasciclin II expression, is found exclusively on the right (Pascual et al., 2004). In the vertebrate brain, this mode of lateralisation might be especially applicable to the DDC because various unilateral neuroanatomical features have been reported in the epithalamus, especially in anamniotes (see §1.2.5).

Lateralised ratios of common components Regions on the left and right might both contain the same circuitry components, but in different ratios, so as to achieve unique, lateralised, cell-type compositions. This asymmetry in circuit architecture could result in left–right differences in neural processing function without the need for any unique cell-type or connectivity pattern on either side.

The zebrafish DDC My results suggest that this latter model underlies the asymmetry of the habenulo-interpeduncular projection in zebrafish. L-typical and R-typical neurons are present on both sides, but in vastly different ratios. Because the arbor sub-types show distinct target connectivity, this lateral asymmetry in cell-type composition underlies the *laterotopic* connectivity of the habenulae. However, the models outlined above are not mutually exclusive and as I discussed in §3.8.3, it is possible that the two arbor sub-types may be further subdivided in a left–right specific manner. In other parts of the zebrafish DDC it is certainly the case that left–right specific components contribute to lateralisation: a subset of left and right-

sided pallial afferent axons terminate exclusively in a medial subdomain of the right habenula (Hendricks & Jesuthasan, 2007) and the parapineal is located on the left side and exclusively innervates the left habenula. With regard to the first model, although the habenulae display conspicuous differences in size in several species (Concha & Wilson, 2001), size differences are not substantial in larval zebrafish. Halpern et al. (2003) has reported that the left nucleus is only 15–20% larger than the right at 4 dpf; it is unclear if this is due to differences in neuronal number or size or quantity of neuropil.

6.3 Outstanding questions and future directions

The zebrafish has proved to be a valuable model in which to study the nature and development of neural lateralisation. Clearly much remains to be discovered and in this section I shall outline a few principal outstanding questions and potential areas for future research.

How is asymmetry established in the zebrafish DDC? Although laser ablation studies have provided evidence for a mutual inhibition model in which the developing left and right habenulae are proposed to compete for left character by producing signals which inhibit the contralateral side from doing so (§1.3.3 and Concha et al., 2003), the molecular/cellular mechanism of such a competition is unknown. One possibility is that the inhibitory interactions are indirect and that the habenulae compete to attract the parapineal. In support of this hypothesis, recent work in our lab has provided evidence that Fgf8, expressed bilaterally by the habenulae, acts as an attractive signal to guide parapineal migration (personal communication from Jennifer Regan). Nodal signalling might function to potentiate Fgf8-dependant signalling from the left habenula, such that it consistently wins in attracting the parapineal. Nodal might also directly promote habenular neurogenesis, such that neurons begin to be born earlier on the left side than the right (personal communication from Myriam Roussigne and Patrick Blader) and this direct effect could account for the maintenance of subtle asymmetries in parapineal-ablated larvae. An interesting experiment will be to determine whether this subtle lateralisation is retained in parapineal-ablated larvae displaying absent or bilateral Nodal signalling. Additionally, forward genetic screens for mutations resulting in symmetric development of the DDC

is a promising route to identify molecular players in the symmetry breaking process.

Whilst the parapineal is clearly essential for the generation of complete left-sided asymmetry phenotypes, the mechanism by which its acts is unknown. One hypothesis has been that parapineal innervation of the left habenula reinforces the development of left-sided character, supported by the spatial and temporal coincidence between parapineal axonal arborisation and the elaboration of left-sided neuropil density (Concha et al., 2003). However, *lov* expression begins in close proximity to the migrating parapineal at 38 hpf, well before the first axons appear (48–50 hpf). Moreover, preliminary experiments in which I eliminated parapineal axons at the time that they first emerge, using a multiphoton laser (Galbraith & Terasaki, 2003), showed that the left habenula retains laterotopic connectivity in the absence of parapineal innervation. An alternative that could be addressed in future experiments is that migrating parapineal precursors produce secreted signalling molecules that influence left-sided neurons or their precursors.

My results reveal two habenulo-interpeduncular subcircuits, one involving L-typical innervation of the dIPN and deriving mainly from the left habenula and the the other comprising R-typical connectivity to the vIPN, deriving predominantly from the right. The existence of IPN projection neurons with dendrites restricted to either dorsal or ventral neuropils suggests that left–right coding could be retained in downstream circuitry. An exciting challenge for future studies will be to resolve IPN efferent connectivity and determine if the left and right habenulae exert predominant control over distinct targets.

As discussed in the Introduction (§1.4), to understand the basis for functional lateralisation it is necessary to establish causal associations between the different levels of CNS asymmetry. Zebrafish is an excellent model in which to link particular functional circuits to behavioural outputs (*eg* Gahtan & Baier, 2004). A focus of future studies in zebrafish will be to link the asymmetries in gene expression, subnuclear organisation and neuronal morphology and connectivity to the activity of the circuit and ultimately to fish behaviour.

A first step is to directly associate molecular and morphological asymmetry within the zebrafish DDC to particular fish behaviours. Parapineal-

ablated larvae are viable and because they lack much asymmetry within this circuit they represent a useful tool to determine the function of dIPN innervation and *laterotopic* connectivity. Moreover, the function of the parapineal itself should be tested: it is a photoreceptive structure, suggesting that light-dependant sensory inputs (possibly circadian information) are processed by left DDC circuitry. LZ*oep*$^{-/-}$ larvae are likewise viable, enabling fish with normal and reversed laterality to be compared in behavioural assays. Several lateralised behaviours including eye useage for mirror viewing, direction of approach to targets to bite and direction of turn in a novel environment can be tested (Miklosi & Andrew, 1999; Barth et al., 2005). Several non-lateralised behaviours may also be modulated by asymmetric DDC circuitry. Zebrafish display quantifiable sleep-like behaviour (Prober et al., 2006), show conditional place preference in response to drugs that act on dopaminergic reward pathways (Darland & Dowling, 2001; Ninkovic & Bally-Cuif, 2006) and can be assessed for a variety of social and emotional behaviours. As discussed in §1.2.4, all of these are strong candidates for modulation by the habenulo-interpeduncular pathway.

The asymmetries within the zebrafish DDC display strong population laterality, a phenomenon that has been suggested to be important for social behaviours. The ability to manipulate Nodal signalling so as to generate normally lateralised and reversed fish and use transgenes to perform live assessment of the direction of lateralisation (*eg* using *foxD3*:GFP to assess parapineal position) provides an opportunity to investigate the consequences of a consistent direction of neural asymmetry. For instance, do fish with reversed circuitry, introduced into a population of left-lateralised fish, behave differently during a social activity such as shoaling?

Finally, it will be necessary to examine a further step in the hierarchy, namely, the activity of left and right sided neurons. *In vivo* calcium imaging has been successfully deployed in the zebrafish optic tectum to image the activity of populations of neurons (Niell & Smith, 2005). A similar approach could be used in the epithalamus to identify left–right differences in population responses. Moreover, direct modulation of neural activity, for instance using ectopically expressed proteins to excite or silence selected neurons (Knopfel, 2008), should allow lateralised neurophysiology to be directly linked to specific behaviours.

Chapter 7

Materials & Methods

7.1 Fish embryos and larvae

Zebrafish Embryos and larvae were obtained by natural spawning from wild-type, *one-eyed pinhead*^{tz57} (Gritsman et al., 1999), Tg(*foxD3*:GFP) (Gilmour et al., 2002; Concha et al., 2003), Tg(*isl1*:GFP)^{rw0}, Tg(*flh*:eGFP);Tg(*foxD3*:GFP) (Concha et al., 2003), Tg(*h2afz*–GFP) (Pauls et al., 2001), or Tg(ET16:GFP) fish (a gift from Dr. Vladimir Korzh). The ET16 enhancer trap line carries a Tol2–GFP insertion and labels a subset of habenular neurons (Choo et al., 2006; Parinov et al., 2004). For some experiments, a morpholino directed against *ntl* mRNA was used to knock-down activity of the Ntl protein in Tg(*foxD3*:GFP) embryos as described in Feldman & Stemple (2001); Nasevicius & Ekker (2000). LZ*oep*$^{-/-}$ larvae were obtained as described in Concha et al. (2000).

Embryos were reared and staged according to standard procedures (Westerfield, 1995) and occasionally 0.002% phenylthiourea was added to the fish water from 12 hpf to inhibit pigment formation.

Astyanax mexicanus Larvae were obtained by natural spawning from surface fish and Tinaja cavefish. Embryos/larvae were reared at 25°C as described previously (Yamamoto & Jeffery, 2000) and 0.002% of phenylthiourea was added to the fish water to inhibit pigment formation.

Medaka Larvae were obtained by natural spawning from the inbred Cab and Kaga strains. Embryos/larvae were reared in the same manner as ze-

brafish (Koster et al., 1997).

7.2 Lipophilic dye tracing of habenular efferent axons

Embryos or larvae were fixed at 4 or 5 dpf by overnight incubation at 4°C in 4% paraformaldehyde (PFA) in 0.1 M sodium phosphate buffer, pH 7.4 (PBS). Subsequently, the skin covering the brain was removed using a sharpened tungsten needle. Fluorescent carbocyanine dyes (1,1'-dioctadecyl-3,3,3',3'-tetramethylindocarbocyanine perchlorate, "DiI" or 1,1'-dioctadecyl-3,3,3',3'-tetramethylindodicarbocyanine, 4-chlorobenzenesulfonate salt, "DiD"; Molecular Probes) were applied to the exposed habenular nuclei using tungsten needles that were tipped with dye crystals and connected to a micromanipulator. Larvae were then incubated overnight at 4°C and axonal labelling was visualised by confocal laser-scanning microscopy. In some labelled larvae, diamino benzidine was photoconverted and brains then either processed for anti-5HT immunostaining or sectioned according to standard methods (Westerfield, 1995).

7.3 Focal electroporation

The electroporation technique was adapted from Haas et al. (2001) to enable the efficient transfer of DNA to single cells or small group of cells in the embryonic zebrafish CNS. Embryos at 48–72 hpf were mounted in 2% low melting point agarose (Sigma) and using a microsurgical blade, a small chamber of agarose was cut out to expose the dorsal diencephalon/mesencephalon. Micropipettes with a tip diameter of 1–2 μm were pulled on a P-87 micropipette puller (Sutter Instrument Company, CA) using AlSi glass capillaries containing a filament. Micropipettes were filled with a solution containing purified plasmid DNA resuspended in H_2O at a concentration of 1 $\mu g/\mu l$. For most habenular neuron electroporations, I used pCS2–GAP43–GFP (a gift from Dr. E. Amaya). GFP synthesised from this construct is localised to the cell membrane by virtue of two N-terminal palmitoylation signals from the GAP43 protein. To visualise presynaptic terminals I used a 1:1 mixture of pCS2–GAL4 plasmid DNA (a gift

from Dr. Masahiko Hibi) and pCS2–Syp:GFP–DSR (Meyer & Smith, 2006). This latter construct encodes both cytoplasmic DsRed fluorescent protein and a Synaptophysin–GFP fusion protein, driven from separate UAS elements. For IPN electroporations I used pCS2–lyn–Cherry, which encodes a membrane-targeted Cherry fluorescent protein (a kind gift from Henry Roehl). Micropipettes were guided into either the left or right habenula or the IPN using an MX3000 Huxley-style micromanipulator (Soma Scientific Instruments) under ×40 water-immersion DIC optics (Axioskop 2 FS microscope, Carl Zeiss). The following stimulation parameters were used: 1–2 s long trains of 2 ms square pulses at 200 Hz and a potential difference of 30 V. Trains were delivered 3–5 times with approximately 0.5 s interval between trains. Pulses were generated with a Grass SD9 stimulator (Grass-Telefactor, West Warwick, RI). After electroporation, embryos were cut out from the agarose and returned to embryo medium.

7.4 Laser ablation

Laser ablation of parapineal precursors was performed at 24–28 hpf in Tg(*flh*:eGFP);Tg(*foxD3*:GFP) transgenic embryos, which were anaesthetised in 0.003% tricane and mounted in a custom-made chamber for experimentation. For laser-ablation, a UV-nitrogen laser microbeam (VSL-337, Laser Sciences) tuned to 440 ηm by means of a Coumarin-440 dye (Exciton Inc.) was focussed on the selected region and laser pulses delivered at a frequency of 10 Hz for 31 s. Ablation was performed at ~10 neighbouring sites by controlling the displacement of a motorised XY stage (Ludl) using custom-made routines written in OpenLab (Improvision). Ablation was confirmed directly under DIC optics and embryos then returned to embryo medium. Larvae were subsequently examined by laser-scanning confocal microscopy at 3 or 4 dpf to determine if any parapineal cells remained. Larvae lacking *all* parapineal cells were classed as "ablated" whereas those retaining one or more parapineal cell(s) were classed as "failed ablated".

7.5 Whole-mount *in situ* hybridisation & immunohistochemistry

In situ hybridisation and immunostaining was performed according to standard methods (Shanmugalingam et al., 2000).

In situ probes for *leftover* (GenBank accession no. AY120891) , *right-on* (GenBank accession no. AY763411) and *dexter* (GenBank accession no. AY763410) were as published in Gamse et al. (2003, 2005) and the probe for *tag1* (GenBank accession no. AF064799) was a kind gift from Andrew Furley (Warren et al., 1999).

For antibody stainings, mouse anti-acetylated α tubulin (Sigma, T6793) and rabbit anti-GFP (Torrey Pines Biolabs, TP401) were used at 1:1000 dilutions, rabbit anti-DsRed (ClonTech, 632496) was used at 1:600 and anti-5HT polyclonal antibody (Diasorin) at 1:400.

7.6 Microscopy and image manipulation

Fluorescent labelling was imaged by laser-scanning confocal microscopy (Leica SP2) using $\times 40$ and $\times 63$ water-immersion objective lenses. z-stacks were typically acquired at 1–2 μm intervals for epithalamic labelling and fluorescent dye-labelling of habenular axons or 0.5–1 μm intervals for imaging axonal arbors labelled by electroporation. In some cases, z-stacks were deconvolved using Huygen's Essential software (Scientific Volume Imaging, Netherlands). 3D projections were generated from the stack of images using Volocity (Improvision) software.

In situ hybridisation staining and plastic sections were photographed using a Jentopix C14 digital camera attached to a Nikon Eclipse E1000 compound microscope. For presentation, image manipulation was performed using Photoshop CS2 (Adobe) software.

7.7 Morphometric analyses

Radial distribution of neurites To quantify the distribution of neurite branches from the centre to periphery of each terminal arbor, I developed a method similar to Sholl analysis. 3D reconstructions of each arbor were ori-

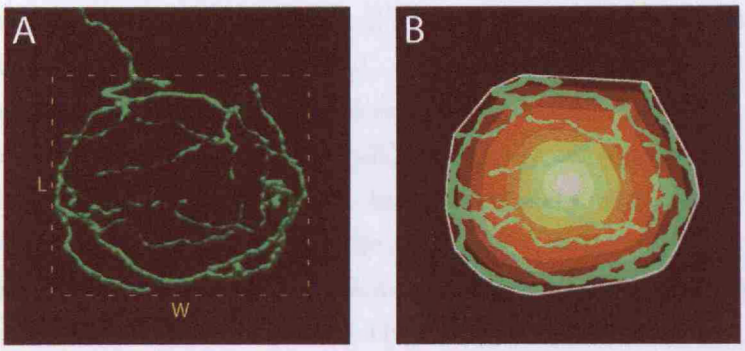

Figure 7.1: **Quantification of radial distribution of axon density and width/length ratio.**
(A) Example of a 2D image of a 3D confocal reconstruction of a habenular axon arbor in the IPN, viewed dorsally. Dotted lines indicate how width (W) and length (L) were measured and where the image was cropped for further analysis.
(B) The same arbor as in (A), after cropping and image thresholding. The convex hull method was used to define the perimeter of the arbor (white line). The area covered by the arbor was divided into 10 equally-spaced concentric shells (coloured red–white), centred on the centroid of the convex hull. The number of green pixels, representing axonal signal, was then counted in each shell to produce a plot of cumulative fraction of axon density *versus* percentage radius.

entated such that the base of the arbor lay on a flat plane and a 2D image of the reconstruction, parallel to this plane was used for further analysis. The incoming axon was cropped where it extended beyond the maximum width and length of the arbor. Next, the image was thresholded and the convex hull method was used to define the arbor perimeter (ImageJ software; Hull and Circle plug-in by A. Karperien and T. R. Roy). Using a custom-written MATLAB (Mathworks Inc.) programme (see Appendix), a series of 10 equally-spaced concentric shells were defined, centred upon the centroid of the convex hull (see Figure 7.1). The number of pixels (representing axon signal) in each shell was taken as a measure of axon density. This generated a plot of cumulative fraction of axon density *versus* radius, for each arbor. This method is resistant to differences in the absolute area covered by the arbor and the total axonal length. Because I analysed 2D images, our method will underestimate axon density where axon segments are aligned above or below one another. This occurs rarely for L-typical arbors but is more common at the perimeter of R-typical arbors. Thus, although our method detects a greater peripheral localisation of axonal length

in R-typical arbors, if anything this difference between the arbor sub-types is likely to have been underestimated.

To describe the distribution profiles for the different sub-types of arbor (L-typical, R-typical and Ab-L, Ab-R) non-linear regression was used to fit fourth order polynomial models to the raw data with the y-intersect constrained to zero (at 0% radius the cumulative fraction of axon density must be zero). To compare the curves for the different arbor sub-types I used the Akaikes Information Criterion (AIC) method (Burnham & Anderson, 2002; Motulsky & Christopoulos, 2003). Briefly, I used the AIC method to compare two models; an AICc score is computed for a "global" model that treats all the data from two arbor sub-types as a single data set and for a second model with individual curves fit to each data set. A large difference in the AICc scores, ΔAICc, indicates there is a high probability of the model with the lower AICc score being correct. If this is the model with separate fits for the two arbor sub-types it follows that the sub-types can be considered distinct. In the RESULTS text I report ΔAICc and the probability that the individual model, with separate polynomial fits for the two arbor sub-types, is correct.

Width/Length ratio The maximum length (measured along the AP axis) and maximum width (measured perpendicular to the AP and DV axes) were measured (Volocity, Improvision), as shown in Figure 7.1. Width/length ratios were compared using one-way ANOVA with Tukey's post-tests for pair-wise comparisons of arbor sub-types.

Depth The depth over which each axon elaborated its terminal arbor was measured in YZ projections made using Volocity software. For L-typical arbors located in the dIPN, depth was measured parallel to the DV axis of the brain. Because the neuropil domain of the vIPN is inclined relative to the DV axis, accurate depth measurements for ventrally-located R-typical, Ab-L and Ab-R arbors were made perpendicular to the plane of the vIPN neuropil domain. Depths were compared using one-way ANOVA with Tukey's post-tests for pair-wise comparisons of arbor sub-types.

Branching The number of branch points was counted by hand in 3D reconstructions of axonal arbors. Branch points giving rise to small filopodial extensions (less than 5 μm in length) were excluded from the analysis. Average numbers of branch points were compared by one-way ANOVA with Tukey's post-tests for pair-wise comparisons of arbor sub-types.

Statistics All statistical comparisons, non-linear regression and comparison of curves using the AIC method were performed using Prism 4 (GraphPad Software Inc., San Diego, CA).

Appendix

Instructions and MATLAB script for measuring Radial Distribution of Axon Density

1. Crop image of axon arbor to the maximum width and length of the arbor.
2. Apply thresholding in ImageJ.
3. Define the convex hull of the arbor, using the Image J Hull and Circle plug-in by A. Karperien and T.R. Roy.
4. Using Photoshop, create a TIFF with the thresholded axonal signal in the green channel and a solid polygon, derived from the convex hull, in the red channel.
5. Place all the TIFF files into a folder and name them with a common identifier, followed by a number, *eg* i1.tif, i2.tif, i3.tif ... i*n*.tif
6. Run the MATLAB script shown below.
7. The outputted data file takes the form of two columns. The first of these is the green pixel count, the second is the red pixel count (area covered by polygon at each radius). Only the green pixel count is required to determine cumulative fraction of axon density. There are 10 rows for each image/arbor, ordered from 100% to 10% radius. *The pixel count is for all pixels contained within that radius.* Hence, the first row (100% radius) gives the *total* number of green pixels, and the second row is all green pixels upto 90% radius.

MATLAB script

```
clear all
data=[];

%read image to analyze, where 'folder' is the name of the folder
containing images
%images should be labelled i1.tif, i2.tif, i3.tif ...
%set f=1:3 as per number of images

Path='/Users/isaac/Desktop/folder/';
CommonInitial='i';
```

```
CommonEnd='.tif';

for f=1:3
    f

    filenumber=mat2str(f);
    RGBstring=[Path CommonInitial filenumber CommonEnd];
    imdata=imread(RGBstring);
    imG=imdata(:,:,2); imB=imdata(:,:,1);
    imshow(imB)
    hold on
    [L, Nobjects]=bwlabel(imB);


    for c=1:Nobjects

        clear Ai areas subdata

        %select object
        [j,k]=find(L==c);
        imBW=bwselect(imB,k(1),j(1));
        objectstats=regionprops(L,'area','centroid');
        r=sqrt(objectstats(c).Area/pi);

        %calculate shell areas
        Ri=r:-r/10:r/10;
        n=1:10; Ai(n)=pi*Ri(n).*Ri(n);
        Ai(find(Ai<0))=[];

        for t=1:length(Ai)

            %get shell
            cf=sqrt(Ai(t)/objectstats(c).Area); cf=double(cf);
            imRs=imresize(imBW,cf);

            [rL, NAfterRedObj]=bwlabel(imRs);
            switch NAfterRedObj
                case 0
                    break
                case 1
                    index=find(imRs==1);
                otherwise
                    for ro=1:NAfterRedObj
```

```
                    RoAreas(ro)=length(find(rL==ro));
                end
            MaxIndx=find(RoAreas==max(RoAreas));
            index=find(rL~=MaxIndx); imRs(index)=0;
            index=find(imRs>=1);
        end

        areas(t)=length(index);

        %center shell on original image
        Ltemp=bwlabel(imRs); statstemp=regionprops(Ltemp,'area','image');
        Ltemp2=bwlabel(statstemp(1).Image); statstemp2=regionprops(Ltemp2,'centroid');
        cfX=objectstats(c).Centroid(1)-statstemp2(1).Centroid(1); cfX=round(cfX);
        cfY=objectstats(c).Centroid(2)-statstemp2(1).Centroid(2); cfY=round(cfY);
        [i,j]=find(statstemp(1).Image==1);
        i=i+cfY; j=j+cfX;
        index=sub2ind(size(imB),i, j);

        statstemp(1).Image=uint8(statstemp(1).Image);
        index2=find(imB==1); im(index2)=255;

        Garea=length(find(imG(index)>0));
        Barea=length(find(imB(index)>0));
        imB(index)=25.5*t;

        imshow(imB)
        colormap(hot)

        subdata(t,:)=[Garea Barea];
    end
    %output interpolation error
    %((Ai-areas)./Ai)*100
    if length(subdata)<10 subdata(length(subdata)+1:10,:)=0
    end
    if subdata(1,2)<10 subdata=[];
    else data=[data;subdata];
    end
  end
end

%choose destination for results file
save /Users/isaac/Desktop/results.txt data -ascii
```

Bibliography

Adamec, R. E., Blundell, J., & Burton, P. (2005). Neural circuit changes mediating lasting brain and behavioral response to predator stress. Neurosci Biobehav Rev, 29, 1225–1241.

Adrio, F., Anadon, R., & Rodriguez-Moldes, I. (2000). Distribution of choline acetyltransferase (chat) immunoreactivity in the central nervous system of a chondrostean, the siberian sturgeon (acipenser baeri). J Comp Neurol, 426, 602–21. 0021-9967 Journal Article.

Aizawa, H., Bianco, I. H., Hamaoka, T., Miyashita, T., Uemura, O., Concha, M. L., Russell, C., Wilson, S. W., & Okamoto, H. (2005). Laterotopic representation of left-right information onto the dorso-ventral axis of a zebrafish midbrain target nucleus. Curr Biol, 15, 238–43. 0960-9822 Journal Article.

Aizawa, H., Goto, M., Sato, T., & Okamoto, H. (2007). Temporally regulated asymmetric neurogenesis causes left-right difference in the zebrafish habenular structures. Dev Cell, 12, 87–98. 1534-5807 (Print) Journal Article Research Support, Non-U.S. Gov't.

Amunts, K., Schlaug, G., Schleicher, A., Steinmetz, H., Dabringhaus, A., Roland, P. E., & Zilles, K. (1996). Asymmetry in the human motor cortex and handedness. Neuroimage, 4, 216–222.

Amunts, K., Schleicher, A., Burgel, U., Mohlberg, H., Uylings, H. B., & Zilles, K. (1999). Broca's region revisited: cytoarchitecture and intersubject variability. J Comp Neurol, 412, 319–341.

Anderson, B., Southern, B. D., & Powers, R. E. (1999). Anatomic asymmetries of the posterior superior temporal lobes: a postmortem study. Neuropsychiatry Neuropsychol Behav Neurol, 12, 247–254.

Annett, M. (1972). The distribution of manual asymmetry. Br J Psychol, 63, 343–358.

Annett, M. (1998). Handedness and cerebral dominance: the right shift theory. J Neuropsychiatry Clin Neurosci, 10, 459–469.

Barneoud, P. & Van der Loos, H. (1993). Direction of handedness linked to hereditary asymmetry of a sensory system. Proc Natl Acad Sci U S A, 90, 3246–3250.

Barth, K. A., Miklosi, A., Watkins, J., Bianco, I. H., Wilson, S. W., & Andrew, R. J. (2005). fsi zebrafish show concordant reversal of laterality of viscera, neuroanatomy, and a subset of behavioral responses. Curr Biol, 15, 844–850.

Benabid, A. L. & Jeaugey, L. (1989). Cells of the rat lateral habenula respond to high-threshold somatosensory inputs. Neurosci Lett, 96, 289–294.

Biddle, F. G., Coffaro, C. M., Ziehr, J. E., & Eales, B. A. (1993). Genetic variation in paw preference (handedness) in the mouse. Genome, 36, 935–943.

Bisazza, A., Cantalupo, C., Capocchiano, M., & Vallortigara, G. (2000). Population lateralisation and social behaviour: a study with 16 species of fish. Laterality, 5, 269–284.

Bisazza, A. & Dadda, M. (2005). Enhanced schooling performance in lateralized fishes. Proc Biol Sci, 272, 1677–1681.

Bisazza, A., Dadda, M., Facchin, L., & Vigo, F. (2007). Artificial selection on laterality in the teleost fish girardinus falcatus. Behav Brain Res, 178, 29–38.

Bisgrove, B. W., Essner, J. J., & Yost, H. J. (2000). Multiple pathways in the midline regulate concordant brain, heart and gut left-right asymmetry. Development, 127, 3567–3579.

Braitenberg, V. & Kemali, M. (1970). Exceptions to bilateral symmetry in the epithalamus of lower vertebrates. J Comp Neurol, 138, 137–146.

Buijs, R. M. (1978). Intra- and extrahypothalamic vasopressin and oxytocin pathways in the rat. pathways to the limbic system, medulla oblongata and spinal cord. Cell Tissue Res, 192, 423–435.

Burnham, K. & Anderson, D. (2002). Model Selection and Multimodel Inference - A practical Information-theoretic approach. (Springer), 2nd edn.

Byrne, R., Kuba, M., & Griebel, U. (2002). Lateral asymmetry of eye use in octopus vulgaris. Animal Behaviour, 64, 461–468.

Cajal, S. R. (1995). Histology of the Nervous System of Man and Vertebrates. (Oxford University Press).

Caldecott-Hazard, S., Mazziotta, J., & Phelps, M. (1988). Cerebral correlates of depressed behavior in rats, visualized using 14c-2-deoxyglucose autoradiography. J Neurosci, 8, 1951–1961.

Caputo, A., Ghiringhelli, L., Dieci, M., Giobbio, G. M., Tenconi, F., Ferrari, L., Gimosti, E., Prato, K., & Vita, A. (1998). Epithalamus calcifications in schizophrenia. Eur Arch Psychiatry Clin Neurosci, 248, 272–276.

Catani, M., Allin, M. P. G., Husain, M., Pugliese, L., Mesulam, M. M., Murray, R. M., & Jones, D. K. (2007). Symmetries in human brain language pathways correlate with verbal recall. Proc Natl Acad Sci U S A, 104, 17163–17168.

Chastrette, N., Pfaff, D. W., & Gibbs, R. B. (1991). Effects of daytime and nighttime stress on fos-like immunoreactivity in the paraventricular nucleus of the hypothalamus, the habenula, and the posterior paraventricular nucleus of the thalamus. Brain Res, 563, 339–344.

Chi, J. G., Dooling, E. C., & Gilles, F. H. (1977). Left-right asymmetries of the temporal speech areas of the human fetus. Arch Neurol, 34, 346–348.

Choo, B. G., Kondrichin, I., Parinov, S., Emelyanov, A., Go, W., Toh, W. C., & Korzh, V. (2006). Zebrafish transgenic enhancer trap line database (zetrap). BMC Dev Biol, 6, 5. 1471-213X (Electronic) Journal Article Research Support, Non-U.S. Gov't.

Christoph, G. R., Leonzio, R. J., & Wilcox, K. S. (1986). Stimulation of the lateral habenula inhibits dopamine-containing neurons in the substantia nigra and ventral tegmental area of the rat. J Neurosci, 6, 613–619.

Cohen, S. R. & Melzack, R. (1985). Morphine injected into the habenula and dorsal posteromedial thalamus produces analgesia in the formalin test. Brain Res, 359, 131–139.

Cohen, S. R. & Melzack, R. (1986). Habenular stimulation produces analgesia in the formalin test. Neurosci Lett, 70, 165–169.

Collins, R. L. (1975). When left-handed mice live in right-handed worlds. Science, 187, 181–184.

Collins, R. L. (1991). Reimpressed selective breeding for lateralization of handedness in mice. Brain Res, 564, 194–202.

Concha, M. L. (2004). The dorsal diencephalic conduction system of zebrafish as a model of vertebrate brain lateralisation. Neuroreport, 15, 1843–6. 0959-4965 Journal Article Review Review, Tutorial.

Concha, M. L., Burdine, R. D., Russell, C., Schier, A. F., & Wilson, S. W. (2000). A nodal signaling pathway regulates the laterality of neuroanatomical asymmetries in the zebrafish forebrain. Neuron, 28, 399–409. 0896-6273 (Print) Journal Article Research Support, Non-U.S. Gov't Research Support, U.S. Gov't, P.H.S.

Concha, M. L., Russell, C., Regan, J. C., Tawk, M., Sidi, S., Gilmour, D. T., Kapsimali, M., Sumoy, L., Goldstone, K., Amaya, E., Kimelman, D., Nicolson, T., Grunder, S., Gomperts, M., Clarke, J. D., & Wilson, S. W. (2003). Local tissue interactions across the dorsal midline of the forebrain establish cns laterality. Neuron, 39, 423–38. 22778822 0896-6273 Journal Article.

Concha, M. L. & Wilson, S. W. (2001). Asymmetry in the epithalamus of vertebrates. J Anat, 199, 63–84. 0021-8782 (Print) Journal Article Research Support, Non-U.S. Gov't Review.

Contestabile, A. & Flumerfelt, B. A. (1981). Afferent connections of the interpeduncular nucleus and the topographic organization of the habenulo-interpeduncular pathway: an hrp study in the rat. J Comp Neurol, 196, 253–270.

Contestabile, A. & Fonnum, F. (1983). Cholinergic and gabaergic forebrain projections to the habenula and nucleus interpeduncularis: surgical and kainic acid lesions. Brain Res, 275, 287–297.

Contestabile, A., Villani, L., Fasolo, A., Franzoni, M. F., Gribaudo, L., Oktedalen, O., & Fonnum, F. (1987). Topography of cholinergic and substance p pathways in the habenulo-interpeduncular system of the rat. an immunocytochemical and microchemical approach. Neuroscience, 21, 253–270.

Darland, T. & Dowling, J. E. (2001). Behavioral screening for cocaine sensitivity in mutagenized zebrafish. Proc Natl Acad Sci U S A, 98, 11691–11696.

Diamond, M. C., Dowling, G. A., & Johnson, R. E. (1981). Morphologic cerebral cortical asymmetry in male and female rats. Exp Neurol, 71, 261–268.

Diaz, E., Pinto-Hamuy, T., & Fernandez, V. (1994). Interhemispheric structural asymmetry induced by a lateralized reaching task in the rat motor cortex. Eur J Neurosci, 6, 1235–1238.

Ditunno, P. L. & Mann, V. A. (1990). Right hemisphere specialization for mental rotation in normals and brain damaged subjects. Cortex, 26, 177–188.

Dorsaint-Pierre, R., Penhune, V. B., Watkins, K. E., Neelin, P., Lerch, J. P., Bouffard, M., & Zatorre, R. J. (2006). Asymmetries of the planum temporale and heschl's gyrus: relationship to language lateralization. Brain, 129, 1164–1176.

Eckenrode, T. C., Barr, G. A., Battisti, W. P., & Murray, M. (1987). Acetylcholine in the interpeduncular nucleus of the rat: normal distribution and effects of deafferentation. Brain Res, 418, 273–286.

Eckenrode, T. C., Murray, M., & Haun, F. (1992). Habenula and thalamus cell transplants mediate different specific patterns of innervation in the interpeduncular nucleus. J Neurosci, 12, 3272–3281.

Ekstrom, P. & Ebbesson, S. O. (1988). The left habenular nucleus contains a discrete serotonin-immunoreactive subnucleus in the coho salmon (oncorhynchus kisutch). Neurosci Lett, 91, 121–125.

Ellison, G. (2002). Neural degeneration following chronic stimulant abuse reveals a weak link in brain, fasciculus retroflexus, implying the loss of forebrain control circuitry. Eur Neuropsychopharmacol, 12, 287–297.

Engbretson, G. A., Reiner, A., & Brecha, N. (1981). Habenular asymmetry and the central connections of the parietal eye of the lizard. J Comp Neurol, 198, 155–165.

Fabre-Thorpe, M., Fagot, J., Lorincz, E., Levesque, F., & Vauclair, J. (1993). Laterality in cats: paw preference and performance in a visuomotor activity. Cortex, 29, 15–24.

Falcon, J. (1999). Cellular circadian clocks in the pineal. Prog Neurobiol, 58, 121–162.

Feldman, B. & Stemple, D. L. (2001). Morpholino phenocopies of sqt, oep, and ntl mutations. Genesis, 30, 175–7. 1526-954x Journal Article.

Foundas, A. L., Eure, K. F., Luevano, L. F., & Weinberger, D. R. (1998). Mri asymmetries of broca's area: the pars triangularis and pars opercularis. Brain Lang, 64, 282–296.

Foundas, A. L., Leonard, C. M., Gilmore, R., Fennell, E., & Heilman, K. M. (1994). Planum temporale asymmetry and language dominance. Neuropsychologia, 32, 1225–1231.

Foundas, A. L., Leonard, C. M., Gilmore, R. L., Fennell, E. B., & Heilman, K. M. (1996). Pars triangularis asymmetry and language dominance. Proc Natl Acad Sci U S A, 93, 719–722.

Fraley, S. M. & Sharma, S. C. (1984). Topography of retinal axons in the diencephalon of goldfish. Cell Tissue Res, 238, 529–38. 0302-766X (Print) Journal Article Research Support, U.S. Gov't, P.H.S.

Francks, C., Maegawa, S., Lauren, J., Abrahams, B. S., Velayos-Baeza, A., Medland, S. E., Colella, S., Groszer, M., McAuley, E. Z., Caffrey, T. M., Timmusk, T., Pruunsild, P., Koppel, I., Lind, P. A., Matsumoto-Itaba, N., Nicod, J., Xiong, L., Joober, R., Enard, W., Krinsky, B., Nanba, E., Richardson, A. J., Riley, B. P., Martin, N. G., Strittmatter, S. M., Moller, H.-J., Rujescu, D., St Clair, D., Muglia, P., Roos, J. L., Fisher, S. E., Wade-Martins, R., Rouleau, G. A., Stein, J. F., Karayiorgou, M., Geschwind, D. H., Ragoussis, J., Kendler, K. S., Airaksinen, M. S., Oshimura, M., DeLisi, L. E., & Monaco, A. P. (2007). Lrrtm1 on chromosome 2p12 is a maternally suppressed gene that is associated paternally with handedness and schizophrenia. Mol Psychiatry, 12, 1129–1139.

Gahtan, E. & Baier, H. (2004). Of lasers, mutants, and see-through brains: functional neuroanatomy in zebrafish. J Neurobiol, 59, 147–161.

Galaburda, A. M., Sanides, F., & Geschwind, N. (1978). Human brain. cytoarchitectonic left-right asymmetries in the temporal speech region. Arch Neurol, 35, 812–817.

Galbraith, J. A. & Terasaki, M. (2003). Controlled damage in thick specimens by multi-photon excitation. Mol Biol Cell, 14, 1808–1817.

Gamse, J. T., Kuan, Y. S., Macurak, M., Brosamle, C., Thisse, B., Thisse, C., & Halpern, M. E. (2005). Directional asymmetry of the zebrafish epithalamus guides dorsoventral innervation of the midbrain target. Development, 132, 4869–81. 0950-1991 (Print) Journal Article Research Support, N.I.H., Extramural Research Support, Non-U.S. Gov't.

Gamse, J. T., Thisse, C., Thisse, B., & Halpern, M. E. (2003). The parapineal mediates left-right asymmetry in the zebrafish diencephalon. Development, 130, 1059–68. 0950-1991 (Print) Journal Article Research Support, Non-U.S. Gov't Research Support, U.S. Gov't, P.H.S.

Gao, D. M., Hoffman, D., & Benabid, A. L. (1996). Simultaneous recording of spontaneous activities and nociceptive responses from neurons in the pars compacta of substantia nigra and in the lateral habenula. Eur J Neurosci, 8, 1474–1478.

Geschwind, D. H., Miller, B. L., DeCarli, C., & Carmelli, D. (2002). Heritability of lobar brain volumes in twins supports genetic models of cerebral laterality and handedness. Proc Natl Acad Sci U S A, 99, 3176–3181.

Geschwind, N. & Levitsky, W. (1968). Human brain: left-right asymmetries in temporal speech region. Science, 161, 186–187.

Gilmour, D. T., Maischein, H. M., & Nusslein-Volhard, C. (2002). Migration and function of a glial subtype in the vertebrate peripheral nervous system. Neuron, 34, 577–88. 0896-6273 Journal Article.

Goldstein, R. (1983). A gabaergic habenulo-raphe pathway mediation of the hypnogenic effects of vasotocin in cat. Neuroscience, 10, 941–945.

Govind, C. K. (1992). Claw asymmetry in lobsters: case study in developmental neuroethology. J Neurobiol, 23, 1423–1445.

Gritsman, K., Zhang, J., Cheng, S., Heckscher, E., Talbot, W. S., & Schier, A. F. (1999). The egf-cfc protein one-eyed pinhead is essential for nodal signaling. Cell, 97, 121–32. 0092-8674 Journal Article.

Guglielmotti, V. & Cristino, L. (2006). The interplay between the pineal complex and the habenular nuclei in lower vertebrates in the context of the evolution of cerebral asymmetry. Brain Res Bull, 69, 475–488.

Guglielmotti, V., Cristino, L., Sada, E., & Bentivoglio, M. (2004). The epithalamus of the developing and adult frog: calretinin expression and habenular asymmetry in rana esculenta. Brain Res, 999, 9–19.

Guglielmotti, V. & Fiorino, L. (1999). Nitric oxide synthase activity reveals an asymmetrical organization of the frog habenulae during development: A histochemical and cytoarchitectonic study from tadpoles to the mature rana esculenta, with notes on the pineal complex. J Comp Neurol, 411, 441–454.

Gugliemotti, V. & Fiorino, L. (1998). Asymmetry in the left and right habenulo-interpeduncular tracts in the frog. Brain Res Bull, 45, 105–110.

Haas, K., Sin, W. C., Javaherian, A., Li, Z., & Cline, H. T. (2001). Single-cell electroporation for gene transfer in vivo. Neuron, 29, 583–91. 0896-6273 Journal Article.

Hagmann, P., Cammoun, L., Martuzzi, R., Maeder, P., Clarke, S., Thiran, J.-P., & Meuli, R. (2006). Hand preference and sex shape the architecture of language networks. Hum Brain Mapp, 27, 828–835.

Halpern, M. E., Gunturkun, O., Hopkins, W. D., & Rogers, L. J. (2005). Lateralization of the vertebrate brain: taking the side of model systems. J Neurosci, 25, 10351–7. 1529-2401 (Electronic) Journal Article Research Support, N.I.H., Extramural Research Support, Non-U.S. Gov't Research Support, U.S. Gov't, P.H.S. Review.

Halpern, M. E., Liang, J. O., & Gamse, J. T. (2003). Leaning to the left: laterality in the zebrafish forebrain. Trends Neurosci, 26, 308–13. 0166-2236 (Print) Journal Article Research Support, Non-U.S. Gov't Research Support, U.S. Gov't, Non-P.H.S. Review.

Harris, J. A., Guglielmotti, V., & Bentivoglio, M. (1996). Diencephalic asymmetries. Neurosci Biobehav Rev, 20, 637–643.

Hattar, S., Kumar, M., Park, A., Tong, P., Tung, J., Yau, K.-W., & Berson, D. M. (2006). Central projections of melanopsin-expressing retinal ganglion cells in the mouse. J Comp Neurol, 497, 326–349.

Haun, F., Eckenrode, T. C., & Murray, M. (1992). Habenula and thalamus cell transplants restore normal sleep behaviors disrupted by denervation of the interpeduncular nucleus. J Neurosci, 12, 3282–3290.

Hayes, T. L. & Lewis, D. A. (1995). Anatomical specialization of the anterior motor speech area: hemispheric differences in magnopyramidal neurons. Brain Lang, 49, 289–308.

Heldt, S. A. & Ressler, K. J. (2006). Lesions of the habenula produce stress- and dopamine-dependent alterations in prepulse inhibition and locomotion. Brain Res, 1073-1074, 229–239.

Hendricks, M. & Jesuthasan, S. (2007). Asymmetric innervation of the habenula in zebrafish. J Comp Neurol, 502, 611–9. 0021-9967 (Print) Journal Article Research Support, Non-U.S. Gov't.

Hepper, P. G., Shahidullah, S., & White, R. (1991). Handedness in the human fetus. Neuropsychologia, 29, 1107–1111.

Herkenham, M. & Nauta, W. J. (1977). Afferent connections of the habenular nuclei in the rat. a horseradish peroxidase study, with a note on the fiber-of-passage problem. J Comp Neurol, 173, 123–146.

Herkenham, M. & Nauta, W. J. (1979). Efferent connections of the habenular nuclei in the rat. J Comp Neurol, 187, 19–47. 0021-9967 Journal Article.

Herrick, C. J. (1948). The Brain of the Tiger Salamander. (The University of Chicago Press).

Highley, J. R., Walker, M. A., Esiri, M. M., Crow, T. J., & Harrison, P. J. (2002). Asymmetry of the uncinate fasciculus: a post-mortem study of normal subjects and patients with schizophrenia. Cereb Cortex, 12, 1218–1224.

Hochberg, F. H. & Le May, M. (1975). Arteriographic correlates of handedness. Neurology, 25, 218–222.

Hope, B. T., Michael, G. J., Knigge, K. M., & Vincent, S. R. (1991). Neuronal nadph diaphorase is a nitric oxide synthase. Proc Natl Acad Sci U S A, 88, 2811–2814.

Hori, M. (1993). Frequency-dependent natural selection in the handedness of scale-eating cichlid fish. Science, 260, 216–219.

Hutsler, J. & Galuske, R. A. W. (2003). Hemispheric asymmetries in cerebral cortical networks. Trends Neurosci, 26, 429–435.

Jain, N., Florence, S. L., Qi, H. X., & Kaas, J. H. (2000). Growth of new brainstem connections in adult monkeys with massive sensory loss. Proc Natl Acad Sci U S A, 97, 5546–50. 0027-8424 (Print) Journal Article Research Support, Non-U.S. Gov't Research Support, U.S. Gov't, P.H.S.

Jeffery, W. R. (2001). Cavefish as a model system in evolutionary developmental biology. Dev Biol, 231, 1–12.

Jung-Beeman, M. (2005). Bilateral brain processes for comprehending natural language. Trends Cogn Sci, 9, 512–518.

Kaprielian, Z., Runko, E., & Imondi, R. (2001). Axon guidance at the midline choice point. Dev Dyn, 221, 154–181.

Kawakami, R., Shinohara, Y., Kato, Y., Sugiyama, H., Shigemoto, R., & Ito, I. (2003). Asymmetrical allocation of nmda receptor epsilon2 subunits in hippocampal circuitry. Science, 300, 990–4. 1095-9203 (Electronic) In Vitro Journal Article Research Support, Non-U.S. Gov't.

Kemali, M., Guglielmotti, V., & Fiorino, L. (1990). The asymmetry of the habenular nuclei of female and male frogs in spring and in winter. Brain Res, 517, 251–255.

Kemali, M., Miralto, A., & Sada, E. (1980). Asymmetry of the habenulae in the elasmobranch "scyllium stellare". i. light microscopy. Z Mikrosk Anat Forsch, 94, 794–800. 0044-3107 Journal Article.

Kennedy, D. N., O'Craven, K. M., Ticho, B. S., Goldstein, A. M., Makris, N., & Henson, J. W. (1999). Structural and functional brain asymmetries in human situs inversus totalis. Neurology, 53, 1260–1265.

Kidd, T., Brose, K., Mitchell, K. J., Fetter, R. D., Tessier-Lavigne, M., Goodman, C. S., & Tear, G. (1998). Roundabout controls axon crossing of the cns midline and defines a novel subfamily of evolutionarily conserved guidance receptors. Cell, 92, 205–215.

Kim, U. & Chang, S.-Y. (2005). Dendritic morphology, local circuitry, and intrinsic electrophysiology of neurons in the rat medial and lateral habenular nuclei of the epithalamus. J Comp Neurol, 483, 236–250.

Klein, D. C. & Moore, R. Y. (1979). Pineal n-acetyltransferase and hydroxyindole-o-methyltransferase: control by the retinohypothalamic tract and the suprachiasmatic nucleus. Brain Res, 174, 245–262.

Knecht, S., Drager, B., Floel, A., Lohmann, H., Breitenstein, C., Deppe, M., Henningsen, H., & Ringelstein, E. B. (2001). Behavioural relevance of atypical language lateralization in healthy subjects. Brain, 124, 1657–1665.

Knopfel, T. (2008). Expanding the toolbox for remote control of neuronal circuits. Nat Methods, 5, 293–295.

Koster, R., Stick, R., Loosli, F., & Wittbrodt, J. (1997). Medaka spalt acts as a target gene of hedgehog signaling. Development, 124, 3147–3156.

Kuan, Y., Gamse, J., Schreiber, A., & Halpern, M. (2007a). Selective asymmetry in a conserved forebrain to midbrain projection. J Exp Zoolog B Mol Dev Evol.

Kuan, Y. S., Yu, H. H., Moens, C. B., & Halpern, M. E. (2007b). Neuropilin asymmetry mediates a left-right difference in habenular connectivity. Development. 0950-1991 (Print) Journal article.

Laland, K. N., Kumm, J., Van Horn, J. D., & Feldman, M. W. (1995). A gene-culture model of human handedness. Behav Genet, 25, 433–445.

Lecourtier, L., Deschaux, O., Arnaud, C., Chessel, A., Kelly, P. H., & Garcia, R. (2006). Habenula lesions alter synaptic plasticity within the fimbria-accumbens pathway in the rat. Neuroscience, 141, 1025–1032.

Lecourtier, L. & Kelly, P. H. (2005). Bilateral lesions of the habenula induce attentional disturbances in rats. Neuropsychopharmacology, 30, 484–496.

Lecourtier, L. & Kelly, P. H. (2007). A conductor hidden in the orchestra? role of the habenular complex in monoamine transmission and cognition. Neurosci Biobehav Rev, 31, 658–672.

Lecourtier, L., Neijt, H. C., & Kelly, P. H. (2004). Habenula lesions cause impaired cognitive performance in rats: implications for schizophrenia. Eur J Neurosci, 19, 2551–2560.

Lee, E. H. & Huang, S. L. (1988). Role of lateral habenula in the regulation of exploratory behavior and its relationship to stress in rats. Behav Brain Res, 30, 265–271.

Lenn, N. J. (1976). Synapses in the interpeduncular nucleus: electron microscopy of normal and habenula lesioned rats. J Comp Neurol, 166, 77–99. 0021-9967 (Print) Journal Article Research Support, U.S. Gov't, P.H.S.

Lenn, N. J. & Hamill, G. S. (1984). Subdivisions of the interpeduncular nucleus: a proposed nomenclature. Brain Res Bull, 13, 203–204.

Lenn, N. J., Wong, V., & Hamill, G. S. (1983). Left-right pairing at the crest synapses of rat interpeduncular nucleus. Neuroscience, 9, 383–9. 0306-4522 (Print) Journal Article Research Support, Non-U.S. Gov't Research Support, U.S. Gov't, P.H.S.

Liang, J. O., Etheridge, A., Hantsoo, L., Rubinstein, A. L., Nowak, S. J., Izpisua Belmonte, J. C., & Halpern, M. E. (2000). Asymmetric nodal signaling in the zebrafish diencephalon positions the pineal organ. Development, 127, 5101–12. 0950-1991 Journal Article.

Lisoprawski, A., Herve, D., Blanc, G., Glowinski, J., & Tassin, J. P. (1980). Selective activation of the mesocortico-frontal dopaminergic neurons induced by lesion of the habenula in the rat. Brain Res, 183, 229–234.

Long, S., Ahmad, N., & Rebagliati, M. (2003). The zebrafish nodal-related gene southpaw is required for visceral and diencephalic left-right asymmetry. Development, 130, 2303–2316.

Luo, L. & O'Leary, D. D. M. (2005). Axon retraction and degeneration in development and disease. Annu Rev Neurosci, 28, 127–156.

Lydic, R., Baghdoyan, H. A., Hibbard, L., Bonyak, E. V., DeJoseph, M. R., & Hawkins, R. A. (1991). Regional brain glucose metabolism is altered during rapid eye movement sleep in the cat: a preliminary study. J Comp Neurol, 304, 517–529.

Matsumoto, M. & Hikosaka, O. (2007). Lateral habenula as a source of negative reward signals in dopamine neurons. Nature, 447, 1111–1115.

Matthews-Felton, T., Corodimas, K. P., Rosenblatt, J. S., & Morrell, J. I. (1995). Lateral habenula neurons are necessary for the hormonal onset of maternal behavior and for the display of postpartum estrus in naturally parturient female rats. Behav Neurosci, 109, 1172–1188.

McGrew, W. C., Marchant, L. F., Wrangham, R. W., & Klein, H. (1999). Manual laterality in anvil use: wild chimpanzees cracking strychnos fruits. Laterality, 4, 79–87.

McManus, I. C. (1985). Handedness, language dominance and aphasia: a genetic model. Psychol Med Monogr Suppl, 8, 1–40.

Medland, S. E., Wright, M. J., Geffen, G. M., Hay, D. A., Levy, F., Martin, N. G., & Duffy, D. L. (2003). Special twin environments, genetic influences and their effects on the handedness of twins and their siblings. Twin Res, 6, 119–130.

Mench, J. A. & Andrew, R. J. (1986). Lateralization of a food search task in the domestic chick. Behav Neural Biol, 46, 107–114.

Meyer, M. P. & Smith, S. J. (2006). Evidence from in vivo imaging that synaptogenesis guides the growth and branching of axonal arbors by two distinct mechanisms. J Neurosci, 26, 3604–14. 1529-2401 (Electronic) Journal Article Research Support, N.I.H., Extramural Research Support, Non-U.S. Gov't.

Miklosi, A. & Andrew, R. J. (1999). Right eye use associated with decision to bite in zebrafish. Behav Brain Res, 105, 199–205.

Miklosi, A., Andrew, R. J., & Savage, H. (1997). Behavioural lateralisation of the tetrapod type in the zebrafish (brachydanio rerio). Physiol Behav, 63, 127–135.

Miralto, A. & Kemali, M. (1980). Asymmetry of the habenulae in the elasmobranch "scyllium stellare". ii. electron microscopy. Z Mikrosk Anat Forsch, 94, 801–13. 0044-3107 Journal Article.

Modianos, D. T., Hitt, J. C., & Flexman, J. (1974). Habenular lesions produce decrements in feminine, but not masculine, sexual behavior in rats. Behav Biol, 10, 75–87.

Moffat, S. D., Hampson, E., & Lee, D. H. (1998). Morphology of the planum temporale and corpus callosum in left handers with evidence of left and right hemisphere speech representation. Brain, 121 (Pt 12), 2369–2379.

Mori, I., Diehl, A. D., Chauhan, A., Ljunggren, H. G., & Kristensson, K. (1999). Selective targeting of habenular, thalamic midline and monoaminergic brainstem neurons by neurotropic influenza a virus in mice. J Neurovirol, 5, 355–362.

Morley, B. J. (1986). The interpeduncular nucleus. Int Rev Neurobiol, 28, 157–82. 0074-7742 Journal Article Review.

Morris, J. S., Smith, K. A., Cowen, P. J., Friston, K. J., & Dolan, R. J. (1999). Covariation of activity in habenula and dorsal raphe nuclei following tryptophan depletion. Neuroimage, 10, 163–172.

Motulsky, H. & Christopoulos, A. (2003). Fitting models to biological data using linear and nonlinear regression. A practical guide to curve fitting. (San Diego CA: GraphPad Software Inc.).

Murphy, C. A., DiCamillo, A. M., Haun, F., & Murray, M. (1996). Lesion of the habenular efferent pathway produces anxiety and locomotor hyperactivity in rats: a comparison of the effects of neonatal and adult lesions. Behav Brain Res, 81, 43–52.

Nasevicius, A. & Ekker, S. C. (2000). Effective targeted gene 'knockdown' in zebrafish. Nat Genet, 26, 216–20. 1061-4036 Journal Article.

Niell, C. M. & Smith, S. J. (2005). Functional imaging reveals rapid development of visual response properties in the zebrafish tectum. Neuron, 45, 941–951.

Ninkovic, J. & Bally-Cuif, L. (2006). The zebrafish as a model system for assessing the reinforcing properties of drugs of abuse. Methods, 39, 262–274.

Nishikawa, T., Fage, D., & Scatton, B. (1986). Evidence for, and nature of, the tonic inhibitory influence of habenulointerpeduncular pathways upon cerebral dopaminergic transmission in the rat. Brain Res, 373, 324–336.

Nucifora, P. G. P., Verma, R., Melhem, E. R., Gur, R. E., & Gur, R. C. (2005). Leftward asymmetry in relative fiber density of the arcuate fasciculus. Neuroreport, 16, 791–794.

Parent, M., Levesque, M., & Parent, A. (2001). Two types of projection neurons in the internal pallidum of primates: single-axon tracing and three-dimensional reconstruction. J Comp Neurol, 439, 162–175.

Parinov, S., Kondrichin, I., Korzh, V., & Emelyanov, A. (2004). Tol2 transposon-mediated enhancer trap to identify developmentally regulated zebrafish genes in vivo. Dev Dyn, 231, 449–59. 1058-8388 (Print) Journal Article Research Support, Non-U.S. Gov't.

Pascual, A., Huang, K.-L., Neveu, J., & Preat, T. (2004). Neuroanatomy: brain asymmetry and long-term memory. Nature, 427, 605–606.

Pauls, S., Geldmacher-Voss, B., & Campos-Ortega, J. A. (2001). A zebrafish histone variant h2a.f/z and a transgenic h2a.f/z:gfp fusion protein for in vivo studies of embryonic development. Dev Genes Evol, 211, 603–10. 0949-944X (Print) Journal Article Research Support, Non-U.S. Gov't.

Petersen, M. R., Beecher, M. D., Zoloth, S. R., Moody, D. B., & Stebbins, W. C. (1978). Neural lateralization of species-specific vocalizations by japanese macaques (macaca fuscata). Science, 202, 324–327.

Poole, R. J. & Hobert, O. (2006). Early embryonic programming of neuronal left/right asymmetry in c. elegans. Curr Biol, 16, 2279–2292.

Previc, F. H. (1991). A general theory concerning the prenatal origins of cerebral lateralization in humans. Psychol Rev, 98, 299–334.

Prober, D. A., Rihel, J., Onah, A. A., Sung, R.-J., & Schier, A. F. (2006). Hypocretin/orexin overexpression induces an insomnia-like phenotype in zebrafish. J Neurosci, 26, 13400–13410.

Provins, K. A. (1997). Handedness and speech: a critical reappraisal of the role of genetic and environmental factors in the cerebral lateralization of function. Psychol Rev, 104, 554–571.

Pujol, J., Deus, J., Losilla, J. M., & Capdevila, A. (1999). Cerebral lateralization of language in normal left-handed people studied by functional mri. Neurology, 52, 1038–1043.

Raya, A. & Belmonte, J. C. I. (2006). Left-right asymmetry in the vertebrate embryo: from early information to higher-level integration. Nat Rev Genet, 7, 283–293.

Ringo, J. L., Doty, R. W., Demeter, S., & Simard, P. Y. (1994). Time is of the essence: a conjecture that hemispheric specialization arises from interhemispheric conduction delay. Cereb Cortex, 4, 331–343.

Rogers, L. J. (1990). Light input and the reversal of functional lateralization in the chicken brain. Behav Brain Res, 38, 211–221.

Rogers, L. J. & Deng, C. (1999). Light experience and lateralization of the two visual pathways in the chick. Behav Brain Res, 98, 277–287.

Rogers, L. J. & Sink, H. S. (1988). Transient asymmetry in the projections of the rostral thalamus to the visual hyperstriatum of the chicken, and reversal of its direction by light exposure. Exp Brain Res, 70, 378–384.

Rogers, L. J. & Workman, L. (1989). Light exposure during incubation affects competitive behaviour in domestic chicks. App Anim Behav Sci, 23, 187—198.

Rogers, L. J., Zucca, P., & Vallortigara, G. (2004). Advantages of having a lateralized brain. Proc Biol Sci, 271 Suppl 6, S420–2.

Rosen, G. D. (1996). Cellular, morphometric, ontogenetic and connectional substrates of anatomical asymmetry. Neurosci Biobehav Rev, 20, 607–615.

Sagasti, A. (2007). Three ways to make two sides: genetic models of asymmetric nervous system development. Neuron, 55, 345–351.

Sampath, K., Rubinstein, A. L., Cheng, A. M., Liang, J. O., Fekany, K., Solnica-Krezel, L., Korzh, V., Halpern, M. E., & Wright, C. V. (1998). Induction of the zebrafish ventral brain and floorplate requires cyclops/nodal signalling. Nature, 395, 185–189.

Sandyk, R. (1992). Pineal and habenula calcification in schizophrenia. Int J Neurosci, 67, 19–30.

Sasaki, K., Suda, H., Watanabe, H., & Yagi, H. (1990). Involvement of the entopeduncular nucleus and the habenula in methamphetamine-induced inhibition of dopamine neurons in the substantia nigra of rats. Brain Res Bull, 25, 121–127.

Sato, T., Deguchi, T., Ichikawa, T., Fujieda, H., & Wake, K. (1991). Localization of hydroxyindole o-methyltransferase-synthesizing cells in bovine epithalamus: immunocytochemistry and in-situ hybridization. Cell Tissue Res, 263, 413–418.

Scheibel, A. B., Paul, L. A., Fried, I., Forsythe, A. B., Tomiyasu, U., Wechsler, A., Kao, A., & Slotnick, J. (1985). Dendritic organization of the anterior speech area. Exp Neurol, 87, 109–117.

Schier, A. F. & Shen, M. M. (2000). Nodal signalling in vertebrate development. Nature, 403, 385–389.

Schulte-Merker, S., van Eeden, F. J., Halpern, M. E., Kimmel, C. B., & Nusslein-Volhard, C. (1994). no tail (ntl) is the zebrafish homologue of the mouse t (brachyury) gene. Development, 120, 1009–1015.

Seeger, M., Tear, G., Ferres-Marco, D., & Goodman, C. S. (1993). Mutations affecting growth cone guidance in drosophila: genes necessary for guidance toward or away from the midline. Neuron, 10, 409–426.

Shanmugalingam, S., Houart, C., Picker, A., Reifers, F., Macdonald, R., Barth, A., Griffin, K., Brand, M., & Wilson, S. W. (2000). Ace/fgf8 is required for forebrain commissure formation and patterning of the telencephalon. Development, 127, 2549–61. 0950-1991 (Print) Journal Article Research Support, Non-U.S. Gov't.

Shaywitz, B. A., Shaywitz, S. E., Pugh, K. R., Constable, R. T., Skudlarski, P., Fulbright, R. K., Bronen, R. A., Fletcher, J. M., Shankweiler, D. P., & Katz, L. (1995). Sex differences in the functional organization of the brain for language. Nature, 373, 607–609.

Shepard, P. D., Holcomb, H. H., & Gold, J. M. (2006). Schizophrenia in translation: the presence of absence: habenular regulation of dopamine neurons and the encoding of negative outcomes. Schizophr Bull, 32, 417–421.

Shibata, H. & Suzuki, T. (1984). Efferent projections of the interpeduncular complex in the rat, with special reference to its subnuclei: a retrograde horseradish peroxidase study. Brain Res, 296, 345–349.

Shibata, H., Suzuki, T., & Matsushita, M. (1986). Afferent projections to the interpeduncular nucleus in the rat, as studied by retrograde and anterograde transport of wheat germ agglutinin conjugated to horseradish peroxidase. J Comp Neurol, 248, 272–284.

Smith, W. J., Stewart, J., & Pfaus, J. G. (1997). Tail pinch induces fos immunoreactivity within several regions of the male rat brain: effects of age. Physiol Behav, 61, 717–723.

Sorvano, V. A., Rainoldi, C., Bisazza, A., & Vallortigara, G. (1999). Roots of brain specializations: preferential left-eye use during mirror-image inspection in six species of teleost fish. Behav Brain Res, 106, 175–180.

Sovrano, V. A., Dadda, M., & Bisazza, A. (2005). Lateralized fish perform better than nonlateralized fish in spatial reorientation tasks. Behav Brain Res, 163, 122–127.

Steinmetz, H. (1996). Structure, functional and cerebral asymmetry: in vivo morphometry of the planum temporale. Neurosci Biobehav Rev, 20, 587–591.

Su, C.-H., Kuo, P.-H., Lin, C. C. H., & Chen, W. J. (2005). A school-based twin study of handedness among adolescents in taiwan. Behav Genet, 35, 723–733.

Sun, T., Patoine, C., Abu-Khalil, A., Visvader, J., Sum, E., Cherry, T. J., Orkin, S. H., Geschwind, D. H., & Walsh, C. A. (2005). Early asymmetry of gene transcription in embryonic human left and right cerebral cortex. Science, 308, 1794–1798.

Sun, T. & Walsh, C. A. (2006). Molecular approaches to brain asymmetry and handedness. Nat Rev Neurosci, 7, 655–662.

Sutherland, R. J. (1982). The dorsal diencephalic conduction system: a review of the anatomy and functions of the habenular complex. Neurosci Biobehav Rev, 6, 1–13. 0149-7634 Journal Article Review.

Tabin, C. J. (2006). The key to left-right asymmetry. Cell, 127, 27–32.

Teraoka, H., Russell, C., Regan, J., Chandrasekhar, A., Concha, M. L., Yokoyama, R., Higashi, K., Take-Uchi, M., Dong, W., Hiraga, T., Holder, N., & Wilson, S. W. (2004). Hedgehog and fgf signaling pathways regulate the development of tphr-expressing serotonergic raphe neurons in zebrafish embryos. J Neurobiol, 60, 275–288.

Thompson, P. M., Cannon, T. D., Narr, K. L., van Erp, T., Poutanen, V. P., Huttunen, M., Lonnqvist, J., Standertskjold-Nordenstam, C. G., Kaprio, J., Khaledy, M., Dail, R., Zoumalan, C. I., & Toga, A. W. (2001). Genetic influences on brain structure. Nat Neurosci, 4, 1253–1258.

Thornton, E. W. & Bradbury, G. E. (1989). Effort and stress influence the effect of lesion of the habenula complex in one-way active avoidance learning. Physiol Behav, 45, 929–935.

Thornton, E. W., Evans, J. A., & Harris, C. (1985). Attenuated response to nomifensine in rats during a swim test following lesion of the habenula complex. Psychopharmacology (Berl), 87, 81–85.

Toga, A. W. & Thompson, P. M. (2003). Mapping brain asymmetry. Nat Rev Neurosci, 4, 37–48. 1471-003X (Print) Journal Article Research Support, U.S. Gov't, P.H.S. Review.

Tzourio, N., Nkanga-Ngila, B., & Mazoyer, B. (1998). Left planum temporale surface correlates with functional dominance during story listening. Neuroreport, 9, 829–833.

Tzourio-Mazoyer, N., Josse, G., Crivello, F., & Mazoyer, B. (2004). Interindividual variability in the hemispheric organization for speech. Neuroimage, 21, 422–435.

Valjakka, A., Vartiainen, J., Tuomisto, L., Tuomisto, J. T., Olkkonen, H., & Airaksinen, M. M. (1998). The fasciculus retroflexus controls the integrity of rem sleep by supporting the generation of hippocampal theta rhythm and rapid eye movements in rats. Brain Res Bull, 47, 171–184.

Vallortigara, G. & Rogers, L. J. (2005). Survival with an asymmetrical brain: advantages and disadvantages of cerebral lateralization. Behav Brain Sci, 28, 575–89; discussion 589–633. 0140-525X (Print) Journal Article Review.

Vernooij, M. W., Smits, M., Wielopolski, P. A., Houston, G. C., Krestin, G. P., & van der Lugt, A. (2007). Fiber density asymmetry of the arcuate fasciculus in relation to functional hemispheric language lateralization in both right- and left-handed healthy subjects: a combined fmri and dti study. Neuroimage, 35, 1064–1076.

Villarreal, J. S., Gonzalez-Lima, F., Berndt, J., & Barea-Rodriguez, E. J. (2002). Water maze training in aged rats: effects on brain metabolic capacity and behavior. Brain Res, 939, 43–51.

Wang, R. Y. & Aghajanian, G. K. (1977). Physiological evidence for habenula as major link between forebrain and midbrain raphe. Science, 197, 89–91.

Warren, J. T. J., Chandrasekhar, A., Kanki, J. P., Rangarajan, R., Furley, A. J., & Kuwada, J. Y. (1999). Molecular cloning and developmental expression of a zebrafish axonal glycoprotein similar to tag-1. Mech Dev, 80, 197–201.

Watkins, J., Miklosi, A., & Andrew, R. J. (2004). Early asymmetries in the behaviour of zebrafish larvae. Behav Brain Res, 151, 177–183.

Watkins, K. E., Paus, T., Lerch, J. P., Zijdenbos, A., Collins, D. L., Neelin, P., Taylor, J., Worsley, K. J., & Evans, A. C. (2001). Structural asymmetries in the human brain: a voxel-based statistical analysis of 142 mri scans. Cereb Cortex, 11, 868–877.

Weaver, D. R., Rivkees, S. A., & Reppert, S. M. (1989). Localization and characterization of melatonin receptors in rodent brain by in vitro autoradiography. J Neurosci, 9, 2581–2590.

Wes, P. D. & Bargmann, C. I. (2001). C. elegans odour discrimination requires asymmetric diversity in olfactory neurons. Nature, 410, 698–701.

Westerfield, M. (1995). The zebrafish book. (Eugene, OR: University of Oregon).

Wiechmann, A. F. & Wirsig-Wiechmann, C. R. (1993). Distribution of melatonin receptors in the brain of the frog rana pipiens as revealed by in vitro autoradiography. Neuroscience, 52, 469–480.

Williams, H., Crane, L. A., Hale, T. K., Esposito, M. A., & Nottebohm, F. (1992). Right-side dominance for song control in the zebra finch. J Neurobiol, 23, 1006–1020.

Witelson, S. F. (1985). The brain connection: the corpus callosum is larger in left-handers. Science, 229, 665–668.

Wittbrodt, J., Shima, A., & Schartl, M. (2002). Medaka–a model organism from the far east. Nat Rev Genet, 3, 53–64.

Woolf, N. J. & Butcher, L. L. (1985). Cholinergic systems in the rat brain: Ii. projections to the interpeduncular nucleus. Brain Res Bull, 14, 63–83.

Wree, A., Zilles, K., & Schleicher, A. (1981). Growth of fresh volumes and spontaneous cell death in the nuclei habenulae of albino rats during ontogenesis. Anat Embryol (Berl), 161, 419–431.

Yamamoto, Y. & Jeffery, W. R. (2000). Central role for the lens in cave fish eye degeneration. Science, 289, 631–3. 0036-8075 Journal Article.

Yanez, J. & Anadon, R. (1994). Afferent and efferent connections of the habenula in the larval sea lamprey (petromyzon marinus l.): an experimental study. J Comp Neurol, 345, 148–160.

Yang, L.-M., Hu, B., Xia, Y.-H., Zhang, B.-L., & Zhao, H. (2008). Lateral habenula lesions improve the behavioral response in depressed rats via increasing the serotonin level in dorsal raphe nucleus. Behav Brain Res, 188, 84–90.

Zhao, H. & Rusak, B. (2005). Circadian firing-rate rhythms and light responses of rat habenular nucleus neurons in vivo and in vitro. Neuroscience, 132, 519–528.

Zilles, K., Schleicher, A., & Wingert, F. (1976). [quantitative growth analysis of limbic nuclei areas fresh volume in diencephalon and mesencephalon of an albino mouse ontogenic series. i. nucleus habenulare]. J Hirnforsch, 17, 1–10.

Produced with LaTeX